

AD-A074 420

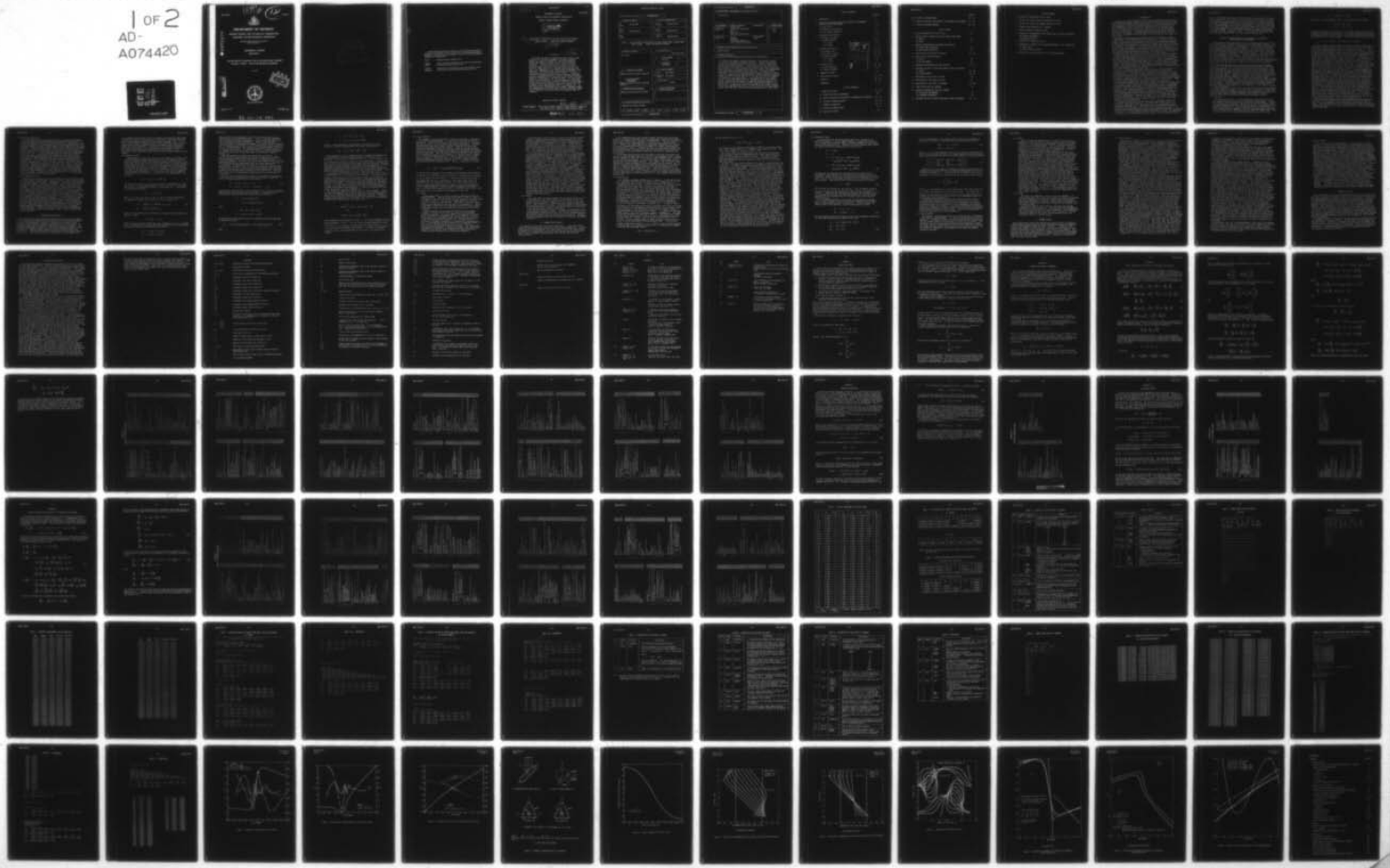
WEAPONS SYSTEMS RESEARCH LAB ADELAIDE (AUSTRALIA)  
THE ANALYSIS OF TRAJECTORY AND SOLAR ASPECT ANGLE RECORDS OF SH--ETC(U)  
SEP 78 R L POPE  
WSRL-0039-TR

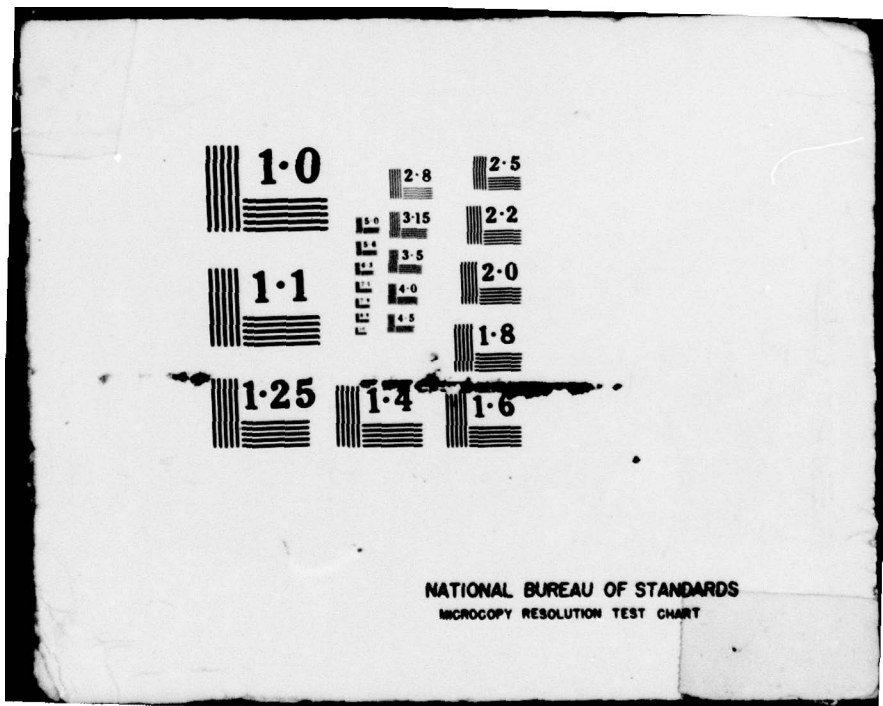
F/G 19/4

UNCLASSIFIED

1 OF 2  
AD-  
A074420

NL





WSRL-0039-TR

LEVEL  
2



AR-001-389



DA074420

DEPARTMENT OF DEFENCE  
DEFENCE SCIENCE AND TECHNOLOGY ORGANISATION  
WEAPONS SYSTEMS RESEARCH LABORATORY

DEFENCE RESEARCH CENTRE SALISBURY  
SOUTH AUSTRALIA

TECHNICAL REPORT

WSRL-0039-TR

THE ANALYSIS OF TRAJECTORY AND SOLAR ASPECT ANGLE RECORDS  
OF SHELL FLIGHTS. THEORY AND COMPUTER PROGRAMS.

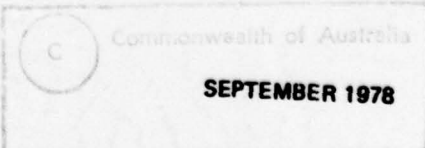
R.L. POPE

DRG FILE COPY



Approved for Public Release

COPY No. 50



79 09 26 062

THE UNITED STATES NATIONAL  
TECHNICAL INFORMATION SERVICE  
IS AUTHORIZED TO  
REPRODUCE AND SELL THIS REPORT

APPROVED  
FOR PUBLIC RELEASE

The official documents produced by the Laboratories of the Defence Research Centre Salisbury are issued in one of five categories: Reports, Technical Reports, Technical Memoranda, Manuals and Specifications. The purpose of the latter two categories is self-evident, with the other three categories being used for the following purposes:

- Reports : documents prepared for managerial purposes.
- Technical Reports : records of scientific and technical work of a permanent value intended for other scientists and technologists working in the field.
- Technical Memoranda : intended primarily for disseminating information within the DSTO. They are usually tentative in nature and reflect the personal views of the author.

(11) Sep 78

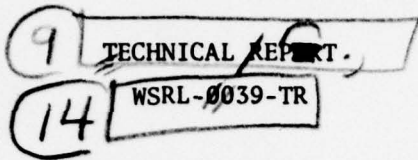
UNCLASSIFIED

DEPARTMENT OF DEFENCE

AR-001-389

DEFENCE SCIENCE AND TECHNOLOGY ORGANISATION

WEAPONS SYSTEMS RESEARCH LABORATORY



(6) THE ANALYSIS OF TRAJECTORY AND SOLAR ASPECT ANGLE RECORDS  
OF SHELL FLIGHTS. THEORY AND COMPUTER PROGRAMS.

(10) R.L. Pope

SUMMARY

(12) 96p.

The theory and computer programs described in this report form part of a research programme in nonlinear dynamics. Methods and computer programs for obtaining aerodynamic coefficients from free flight trials of shells have been developed. The data from the trials consists of both trajectory data from either radar tracking of the shell or ballistic camera records of a flashing light carried in the shell, and complementary solar aspect angle measurements from yawsondes. The data analysis techniques will be used to investigate the exterior ballistics of shells. As well as a tool for investigating dynamic stability problems concerning standard or modified shells they offer a new and more efficient approach to developing a Fire Control Model. An interesting facet of the data analysis is the representation of the aerodynamic force coefficients as analytic functions of Mach number, an approach which has potential for greater accuracy than the piecewise linear representation which is in general use. To facilitate use of the programs by the reader, program listings are supplemented by tables of input variables and sample output. Results from test runs using artificially generated data are discussed.

Approved for Public Release

410 719

LW

POSTAL ADDRESS: Chief Superintendent, Weapons Systems Research Laboratory,  
Box 2151, G.P.O., Adelaide, South Australia, 5001.

UNCLASSIFIED 7909 26 062

## DOCUMENT CONTROL DATA SHEET

Security classification of this page

UNCLASSIFIED

## 1 DOCUMENT NUMBERS

AR Number: AR-001-389

Report Number: WSRL-0039-TR

Other Numbers:

## 2 SECURITY CLASSIFICATION

a. Complete Document: UNCLASSIFIED

b. Title in Isolation: UNCLASSIFIED

c. Summary in Isolation: UNCLASSIFIED

## 3 TITLE

THE ANALYSIS OF TRAJECTORY AND SOLAR ASPECT ANGLE RECORDS FROM SHELL FLIGHTS. THEORY AND COMPUTER PROGRAMS.

## 4 PERSONAL AUTHOR(S):

R.L. Pope

## 5 DOCUMENT DATE:

September 1978

6 6.1 TOTAL NUMBER OF PAGES 81

6.2 NUMBER OF REFERENCES: 18

## 7 7.1 CORPORATE AUTHOR(S):

Weapons Systems Research Laboratory

## 7.2 DOCUMENT SERIES AND NUMBER

Weapons Systems Research Laboratory  
0039-TR

## 8 REFERENCE NUMBERS

a. Task: DST 76/011

b. Sponsoring Agency: DST 76/011

## 9 COST CODE:

331251

## 10 IMPRINT (Publishing organisation)

Defence Research Centre Salisbury

11 COMPUTER PROGRAM(S)  
(Title(s) and language(s))

## 12 RELEASE LIMITATIONS (of the document):

Approved for Public Release

12.0 OVERSEAS

NO

P.R. 1

A

B

C

D

E

Security classification of this page:

UNCLASSIFIED

## 13 ANNOUNCEMENT LIMITATIONS (of the information on these pages):

No limitation.

14 DESCRIPTORS:		Computer programs Projectiles Projectile trajectories Yaw Ballistics Ballistic trajectories	Trajectories	15 COSATI CODES:
a. EJC Thesaurus Terms				1904 2011
b. Non-Thesaurus Terms		Shells Yawsonges Parameter estimation Free flight data analysis	Solar aspect angle	

## 16 LIBRARY LOCATION CODES (for libraries listed in the distribution):

SW SR SD AACA

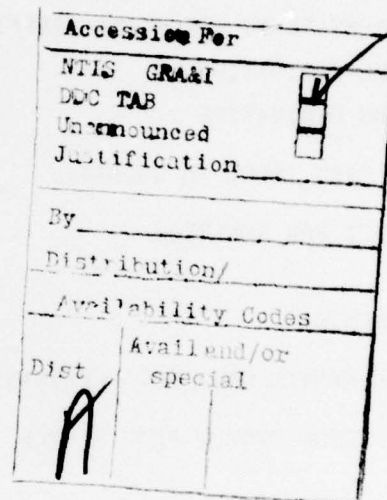
## 17 SUMMARY OR ABSTRACT:

(if this is security classified, the announcement of this report will be similarly classified)

The theory and computer programs described in this report form part of a research programme in nonlinear dynamics. Methods and computer programs for obtaining aerodynamic coefficients from free flight trials of shells have been developed. The data from the trials consists of both trajectory data from either radar tracking of the shell or ballistic camera records of a flashing light carried in the shell, and complementary solar aspect angle measurements from yawsonges. The data analysis techniques will be used to investigate the exterior ballistics of shells. As well as a tool for investigating dynamic stability problems concerning standard or modified shells they offer a new and more efficient approach to developing a Fire Control Model. An interesting facet of the data analysis is the representation of the aerodynamic force coefficients as analytic functions of Mach number, an approach which has potential for greater accuracy than the piecewise linear representation which is in general use. To facilitate use of the programs by the reader, program listings are supplemented by tables of input variables and sample output. Results from test runs using artificially generated data are discussed.

## TABLE OF CONTENTS

	Page No.
1. INTRODUCTION	1 - 2
2. ANALYTICAL REPRESENTATION OF THE VARIATION OF AERODYNAMIC COEFFICIENTS WITH MACH NUMBER	2 - 4
2.1 Axial force	2 - 3
2.2 Normal force derivative	4
2.3 Roll damping derivative	4
3. TRAJECTORY DATA ANALYSIS	4 - 9
3.1 Mathematical model	5 - 7
3.2 Program SHELTRAJ	7 - 9
3.2.1 Input	8 - 9
3.2.2 Output	9
4. YAWSONDE DATA ANALYSIS	9 - 14
4.1 Yawsonde usage	10 - 11
4.2 Mathematical model	12 - 13
4.3 Program YAWSONDE	13 - 14
4.3.1 Input	14
4.3.2 Output	14
5. PROGRAM TESTING	14 - 17
5.1 Program SHELTRAJ	15 - 16
5.2 Program YAWSONDE	17
6. SUMMARY OF RESULTS	17
7. APPLICATION OF RESULTS	18 - 19
NOTATION	20 - 23
REFERENCES	24 - 25



## LIST OF APPENDICES

I NR3634 DRAG CURVE	26 - 27
II CORIOLIS AND GRAVITY COMPONENTS	28
III PARTIAL DERIVATIVES WITH RESPECT TO PARAMETERS FOR SHELTRAJ	29 - 32
IV LISTING OF PROGRAM SHELTRAJ	33 - 39
V YAWSONDE CALIBRATION	40 - 41
VI LISTING OF PROGRAM YAWCAL	42
VII SOLAR ASPECT ANGLE	43

	Page No.
VIII LISTING OF PROGRAM ASPECT	44 - 45
IX PARTIAL DERIVATIVES WITH RESPECT TO PARAMETERS FOR YAWSONDE	46 - 47
X LISTING OF PROGRAM YAWSONDE	48 - 53

## LIST OF TABLES

1. TYPICAL AERODYNAMIC DATA FOR A SHELL	54
2. FITTING ANALYTIC CURVES TO THE AXIAL FORCE COEFFICIENT	
(A) NR3634	55
(B) GAVRE	55
3. ANALYTIC REPRESENTATIONS FOR OTHER COEFFICIENTS	
(A) NORMAL FORCE DERIVATIVE	55
(B) ROLL DAMPING DERIVATIVE	55
4. DESCRIPTION OF CARD INPUT TO SHELTRAJ	56 - 57
5. SAMPLE INPUT DECK FOR SHELTRAJ	
(A) FORCES	58
(B) ROLLING MOMENTS	59
6. SIMULATED EXPERIMENTAL DATA FOR SHELTRAJ	60 - 61
7. BEGINNING AND END OF OUTPUT FROM SAMPLE INPUT FOR SHELTRAJ	
(A) FORCES	62 - 63
(B) ROLLING MOMENTS	64 - 65
8. DESCRIPTION OF CARD INPUT TO YAWCAL	66
9. DESCRIPTION OF CARD INPUT TO ASPECT	67
10. DESCRIPTION OF CARD INPUT TO YAWSONDE	68 - 69
11. SAMPLE INPUT DECK FOR YAWSONDE	70
12. SIMULATED EXPERIMENTAL DATA FOR YAWSONDE	
(A) TRAJECTORY MEASUREMENTS	71
(B) YAWSONDE MEASUREMENTS	72
13. BEGINNING AND END OF OUTPUT FROM SAMPLE INPUT TO YAWSONDE	73 - 75

## LIST OF FIGURES

1. Residues for fitted axial force curves
2. Residues for fitted normal force derivative curves
3. Residues for fitted roll damping derivative curves
4. Schematic representation of a yawsonde
5. Typical yawsonde calibration curve
6. Variation of complementary solar aspect angle with shell elevation
  - (a) heading 300 degrees T
  - (b) heading due north
7. Conditions for detecting the sun
8. Comparison of methods for estimating aerodynamic force coefficients
  - (a) axial force
  - (b) normal force derivative
9. Effects of noise on estimation of roll damping moments

## 1. INTRODUCTION

In recent years the development of new flight instrumentation for shells and new sophisticated methods of analysing free flight data has resulted in a substantial increase in the possible applications of artillery shell flight trials. The developments which have resulted in important gains in the study of the flight behaviour of shells include the invention of the solar aspect angle sensor or yawsonde(ref.1) and the many improvements to it, some of which are described in reference 2. Other developments of note include the modified point mass or four degree of freedom shell trajectory model(ref.3), and the application of parameter estimation methods to the analysis of free flight data (ref.4,5,6).

One potential application of parameter estimation techniques is in the preparation of a Fire Control Model for a shell(ref.7). Currently, the model is made as accurate as possible using wind tunnel data, then modifications to produce a final version of the model are made, using scaling factors obtained by calibrating the four degree of freedom model against impact point data from test firings. The method is costly because the number of firings is very large and the calibration complex. By using parameter estimation techniques to analyse trajectory data derived from radar or other projectile tracking systems such as the flashing light methods described in reference 8, it is possible to substantially reduce the cost of developing a Fire Control Model.

Another major area of application for the yawsonde and associated parameter estimation algorithms is investigation of shell stability. There are many occasions in the development and testing of shells when there is a requirement for free flight investigation of dynamic stability. Such a requirement may result from changes to the external appearance of the shell to meet the need for a long range, low drag shell or from the need for terminal guidance by canard control. In addition, there are often unexpected problems with shells which cannot be explained without using yawsondes to gather further information on the free flight behaviour of such "rogue" shells.

The U.K. is currently developing a method which uses radar tracking data to produce the Fire Control Model from which aiming tables for shells are constructed(ref.7). The USA has been using yawsonde and radar data for some time now to study dynamic stability and anomalous flight behaviour of shells. The potential savings of these techniques in all areas of research, development and usage of artillery shells are so large that Defence Research Centre Salisbury has begun a program which will lead to the development of these skills. Such skills can then be applied with substantial benefits in many areas.

The present report describes the analysis methods and computer programs which will be used to process the data from the preliminary trials. The parameter estimation algorithm used presently is a simple minimum variance application (ref.4,5). This could be improved considerably by using maximum likelihood estimators(ref.7) and Bayesian methods. However, the minimum variance estimator should work satisfactorily in preliminary trials. The first major use of these programs will be a study to quantify the advantages of using parameter identification techniques to construct a Fire Control Model from trajectory measurements. Such an assessment will also involve estimating the accuracy of various alternative tracking techniques and the effect of such accuracies on the data analysis.

An analytic representation of the variation of aerodynamic coefficients, particularly axial force coefficient, with Mach number should result in a substantial improvement in the speed and accuracy of the algorithm for processing the trajectory data. The results of an investigation of analytic functions used to represent such variations are discussed in Section 2. The results of testing the programs for analysing yawsonde and radar data are discussed in Section 5. The two principal points of interest are firstly, the advantages of using an analytic representation of Mach number variation compared with the

commonly used method of analysing a section of data restricted so that the Mach number variation over that section is not significant, and secondly, the effect on the parameter estimation process of noise in the data. Section 3 discusses the method for analysing the trajectory data and gives details of the operation of the program SHELTRAJ, which is used to implement it. The factors affecting the design of experiments involving yawsondes are summarised in Section 4, which also describes the method of analysing the yawsonde data, and the operation of the program YAWSONDE. The final section discusses the design of experiments using radar tracking, yawsondes, or both. It also looks at the present state of progress and considers which direction future work should take.

## 2. ANALYTICAL REPRESENTATION OF THE VARIATION OF AERODYNAMIC COEFFICIENTS WITH MACH NUMBER

In analysing data from free flight trials, the methods generally used involve the assumption that aerodynamic coefficients are not Mach number dependent. In a few cases a linear variation is allowed(ref.9). The variation of aerodynamic force and moment coefficients with Mach number is taken into account in using these methods by restricting the data analysed in any one pass to a section in which the Mach number variation is so small that there will not be a significant variation in any of the aerodynamic coefficients extracted. There are several obvious disadvantages of this system. The major drawback is the difficulty of obtaining information in the transonic region where the axial force in particular is changing rapidly. Thus in the transonic range it is difficult if not impossible to find a sufficient length of trajectory over which drag coefficient can be adequately represented by a constant or a linear variation with Mach number.

The slowly varying nature of the tracking data from which the aerodynamic forces are derived and the roll rate data from which roll damping is obtained, necessitates using as long a section of the trajectory data as possible. The rapid oscillatory nature of the angular data means that the aerodynamic moments can be determined from much shorter sections of the trajectory so that it is not necessary to use a sophisticated representation of the variation of aerodynamic moments with Mach number. Therefore an analytic form for the variation of axial force coefficient with Mach number will be used, and in addition analytic representations will be used for other slowly varying quantities, namely, average normal force and roll damping. Then the data analysis method will make optimum use of the data, and much more accurate estimates of the aerodynamic parameters will be obtained. In particular, the best estimates of axial force will be obtained, and this is most important if the technique is to be useful in setting up a Fire Control Model.

In order to choose an analytic form to describe the variation with Mach number of the three coefficients, that is, the axial force coefficient, the normal force coefficient and the roll damping coefficient, some experiments were conducted in fitting analytic forms to typical aerodynamic coefficients for a shell. Tabulated values which were used in this exercise are shown in Table 1.

### 2.1 Axial force

The transonic drag rise is such that polynomial representations of the Mach number variation of axial force coefficient are always poor. Criteria for choosing a suitable analytic function can be found in reference 10 and have been repeated in Appendix I, which gives details of the functional form proposed in reference 10. The principal advantage of this function lies with the small number of parameters necessary to provide adequate representation of the axial force coefficient, over the whole Mach number range. The function, which will be called the NR3634 drag function, has the form

$$C_x = (1+s)A(r) + (1-s)B(r)$$

where  $A(r)$ ,  $B(r)$  are polynomials and  $r$ ,  $s$  are functions of Mach number,

$$r = (M^2 - K^2) / (M^2 + K^2),$$

$$s = r / [(1 - L^2) r^2 + L^2]^{1/2}.$$

A detailed discussion of the function, its properties and the values of the constants can be found in reference 10. A possible alternative is the Gavre drag function(ref.11), which is slightly more complex than the NR3634 function but otherwise has the same advantages. The Gavre drag function has the form

$$C_x = a + [1 + b(M-c)^2] \tan^{-1} \{ d(M-c) / [e + f(M-c)^2] \} .$$

In order to choose the more appropriate analytic form for incorporation into the data analysis a short study of the goodness of fit of each form was carried out for the tabulated axial force coefficient in Table 1. A non-linear least squares method was used to fit the curves to the data. The sum of squares of the differences between the tabulated values and those derived from the analytical representation was minimised, using the subroutine given in reference 13, which implements the method described in reference 12. The results of the study are given in Table 2 and figure 1. The fitting was carried out over the Mach number range from 0.65 to 1.4 since this particular shell will not be subject to Mach numbers outside that range except in exceptional circumstances. From part (a) of Table 2 it is clear that the optimum fit is obtained using linear polynomials in  $r$  to represent both supersonic and subsonic parts of the curve. This result is optimum in the sense that it involves using the least number of adjustable parameters and yet results in a very small r.m.s. error for the fit. If more parameters are used the root mean square error of the fit does not decrease substantially. Coincidentally the number of parameters for optimum use of the NR3634 drag function is the same as the number of parameters used with the Gavre drag function, namely, six. However, the root mean square error attained with the NR3634 drag function is less than one fifth of that obtained with the Gavre drag function, so that the choice is quite clear cut. Since all drag functions have basically the same shape, which includes in particular a rapid rise in the transonic region, this preference can be expected to hold generally. Figure 1, which shows the drag variation with Mach number and the residues obtained with the various fitted curves supports this choice. It is particularly noticeable that the Gavre drag function has difficulty coping with the transonic drag rise. The error peaks at  $M = 0.93$  and  $M = 1.02$  show an inability to cope with the high curvatures at these points which are a feature of the transonic drag rise. These results contrast with the residues shown for the NR3634 drag curves, of which one uses a constant and the other uses a linear representation to describe the subsonic part of the curve. Both are linear supersonically.

It was concluded from this study that the NR3634 drag curve using linear functions of  $r$  both subsonically and supersonically would represent the axial force curve adequately over the Mach number range used by shells in flight. However provision was made in the parameter estimation program for analysing the radar data to use up to quadratic terms to cope with exceptional cases if they arise.

## 2.2 Normal force derivative

Since the NR3634 drag function provides such an excellent representation of the axial force and since the normal force coefficient derivative has similar characteristics to the axial force coefficient, in particular a rapid increase in magnitude in the transonic region, then the NR3634 function is an appropriate choice for analytic representation of the normal force coefficient derivative. Details of the results of fitting such a function to the values of normal force coefficient derivative given in Table 1 are presented in figure 2 and Table 3. Again fitting has only been tried for the Mach number range 0.65 to 1.4. It is clear from the table and figure that an NR3634 curve using linear representations both subsonically and supersonically provides quite adequate representation of the normal force while using only six parameters. The deviation of the analytic representation from the tabulated curve will be less than half a per cent at its maximum value and generally very much less. Since the effect of normal force on the shell is principally involved with the drift of the shell, such accuracy is more than sufficient. Therefore an NR3634 curve can provide an adequate representation of the normal force coefficient derivative, using a linear form both subsonically and supersonically. Again provision is made in the parameter estimation program SHELTRAJ to use up to quadratic terms if necessary, but such a requirement is unlikely and it would be difficult, if not impossible, to determine values for the extra parameters.

## 2.3 Roll damping derivative

Unlike the force coefficient, the roll damping coefficient derivative does not change rapidly in the transonic region, but shows a small steady variation over the whole Mach number range. Consequently, a polynomial representation is perfectly adequate. Table 3(b) and figure 3 show the results of fitting polynomials to the tabulated values in Table 1, using a linear regression technique. Figure 3 shows the magnitude of the residuals obtained, using both linear and quadratic variations and Table 3(b) shows the r.m.s. errors for polynomials up to and including the fourth degree. The fitting was done over a Mach number range from 0 to 2.5 using all the points tabulated in Table 1. The decrease in the sum of squares of the residuals as the degree of the polynomial increases is a useful measure of the improvement in fitting to the data of the higher degree polynomial. It follows that the results in Table 3(b) show that no significant improvement can be achieved with polynomials of degree higher than four and that a quadratic representation is quite adequate, since the residuals of the quadratic form are less than one per cent. Hence provision is made in program SHELTRAJ to use up to third degree polynomial representations of the derivative of the roll damping moment coefficient. However, a quadratic will generally be adequate, and in many cases with a restricted Mach number range, a linear representation will be sufficient.

## 3. TRAJECTORY DATA ANALYSIS

The trajectory data analysis and the yawsonde data analysis can be viewed as entirely separate and unconnected processes and both can be undertaken together or each can be undertaken in isolation. Analysis of the trajectory data obtained by radar tracking or flashing light measurement will be the basis of any method, which might be developed for producing a Fire Control Model. The mathematical model which is used as a basis for the parameter estimation is the four degree of freedom or modified point mass model proposed by Lieske and Rieter(ref.3). The algorithm is similar in many ways to the methods already in use(refs.7,9). The basic difference is that both of the above methods treat

only a length of the trajectory which is limited so that the Mach number range is sufficiently small for the variation of aerodynamic coefficients with Mach number to be adequately represented by constants or straight lines. On the other hand the method described below will process the whole trajectory in one sweep using the analytic representations of aerodynamic forces and rolling moments described in Section 2. In addition to describing the mathematical model used in the program, this section outlines the parameter estimation algorithm, describes the program SHELTRAJ itself and provides a brief description of the method for using it and the input to and the output from the program.

### 3.1 Mathematical model

The mathematical model allows for motion with respect to the three translational degrees of freedom and the axial spin or roll degree of freedom, and so is generally called a four degree of freedom trajectory model. The model relies on the fact that for a well behaved shell, an accurate prediction of the shell drift, that is, the lateral displacement of the shell's impact position from that given by a point mass trajectory model, can be made by assuming that the shell flies at the yaw of response. The yaw of response of a shell is the equilibrium value of incidence when transient yawing and pitching moments are damped out. For most shells the yaw of response is close to the horizontal plane and its magnitude can be approximated by the expression

$$\xi_R = p_s I_x v_1 g_3 / QSDV^2 C_m \xi \quad (1)$$

The axes system in which the equations of motion are formulated is a range axes system. It has OX downrange along the line of fire, OY to the right and OZ vertically downwards to complete a right handed set. The velocity in the range axes system is

$$\underline{U} = \dot{x}\underline{i} + \dot{y}\underline{j} + \dot{z}\underline{k},$$

where  $\underline{i}$ ,  $\underline{j}$ ,  $\underline{k}$  are unit vectors in the X, Y and Z directions respectively. The equations of motion for the shell at the yaw of repose, are

$$\dot{\underline{U}} = -(QSC_x/m) \underline{v} + (QSC_L/m) \underline{j} + \underline{g} - \underline{\Delta} \quad (2)$$

$$\dot{p}_s = (QSD/I_x) (p_s d/2V) C_t p$$

where  $\underline{v}$  is a unit vector in the direction of the shell velocity relative to the air, so that

$$\underline{v} = |v| \underline{v} = \underline{U} - \underline{W}$$

where  $\underline{W}$  is the local wind velocity and  $V$  has components ( $v_1$ ,  $v_2$ ,  $v_3$ ) in range axes. The drag and lift coefficients shown in equation (2) can be expressed in terms of axial force and normal force as follows,

$$C_D = -C_x \cos \xi - C_z \sin \xi, \quad (3)$$

$$C_L = C_x \sin \xi - C_z \cos \xi.$$

The resolution of the aerodynamic forces of lift and drag into axial and normal force is not generally necessary. In fact, if the sole purpose of the data analysis were the development of a Fire Control Model the use of lift and drag forces would be preferable. However, since the more significant aspect of the present development is a general study of stability and the program is intended for use in the yawsonde data analysis program as well, it is advantageous at this stage to use a formulation which is in terms of axial and normal force. The remaining symbols in the above equations are standard and are defined in the list of notation at the end of the text. The gravity and Coriolis acceleration terms are discussed at length in Appendix II.

Small approximations have been used in equations (1) and (2). In equation (1) the vertical component of the yaw of repose has been ignored and an approximate expression has been used for the magnitude of the horizontal component. The errors arising from both approximations will have maximum values of only one or two per cent of the total yaw of repose and so it is expected that this approximation will not affect the results significantly. In equation (2), the direction of the lift force has been taken along the vector  $j$ . This is true at the beginning of the trajectory if there is no wind, but the direction will alter slightly with cross wind present and as the shell drifts slightly from the line of fire. Once again the overall errors arising from this approximation will not generally be significant.

The final part of the mathematical model is the parametric representation which enables the implementation of the parameter estimation algorithm. Firstly, we consider initial values of the variables

$$\begin{aligned} P_1 &= x_0, \quad P_2 = y_0, \quad P_3 = z_0 \\ P_4 &= \dot{x}_0, \quad P_5 = \dot{y}_0, \quad P_6 = \dot{z}_0 \quad \text{and} \quad P_{27} = P_{so}. \end{aligned} \quad (4)$$

The parametric representations of the aerodynamic forces and the roll damping moment include the axial force coefficient which is represented in the following way, using the functional form presented in Section 2,

$$\begin{aligned} C_x &= (1+s) (P_9 + P_{10} r + P_{11} r^2) \\ &\quad + (1-s) (P_{12} + P_{13} r + P_{14} r^2) \end{aligned} \quad (5)$$

where

$$\begin{aligned} r &= (M^2 - P_7^2) / (M^2 + P_7^2), \\ s &= r / [(1 - P_8^2) r^2 + P_8^2]^{1/2}. \end{aligned}$$

The normal force coefficient derivative is represented using the same type of function as follows,

$$C_{Zf} = (1+f) (P_{17} + P_{18} g + P_{19} g^2) + (1-f) (P_{20} + P_{21} g + P_{22} g^2) \quad (6)$$

where

$$g = (M^2 - P_{15}^2) / (M^2 + P_{15}^2),$$

$$f = g / [(1 - P_{16}^2) g^2 + P_{16}^2]^{1/2}$$

Finally, a simple polynomial representation is satisfactory for the derivative of the roll damping moment coefficient, having the form

$$C_{\ell p} = P_{23} + P_{24}M + P_{25}M^2 + P_{26}M^3 \quad (7)$$

Thus equations (1) to (7) completely define a mathematical model describing a four degree of freedom or modified point mass model of a shell trajectory in terms of the 27 unknown parameters  $P_i$ . In most cases it will not be necessary to determine values for all the parameters. Firstly, some or all of the initial conditions may be sufficiently well determined by other means and so they can be kept fixed throughout the data analysis. Secondly, the variation of the aerodynamic coefficients with Mach number may be adequately represented by fewer parameters than are available, particularly when the available data covers only a restricted range of Mach number. Then the less significant parameters can be set to zero and held constant.

The parameter estimation process which is used to assign values to the unknown parameters  $P_i$  is a minimum variance technique. The minimum variance estimator aims to find values of the parameters which will minimise the weighted sum of the squares of the residuals, of the measured values of the three position coordinates and the roll rate when compared with the values predicted by the model. The method is described in detail in references 4, 5 and 8. It is basically a modified Newton-Raphson algorithm and as such it needs an estimate of the partial derivatives of each of the measured variables with respect to the parameters. A means of derivation for these partial derivatives is given in Appendix III.

The interaction between position and roll rate data is minimal. Since the only connecting variable is yaw of repose it is very difficult and often impossible to determine simultaneously, parameters affecting aerodynamic forces directly and those affecting rolling moments directly. In order to determine them separately, use can be made of the fact that in determining minimum variance the residuals are weighted, that is,

$$\sigma^2 = (1/4N) \sum_{j=1}^N [w_1 (\hat{x}_j - x_j)^2 + w_2 (\hat{y}_j - y_j)^2 + w_3 (\hat{z}_j - z_j)^2 + w_4 (\hat{p}_j - p_j)^2]$$

Then aerodynamic force parameters,  $P_i$  for  $i = 1$  to 22 and aerodynamic rolling moment parameters,  $P_i$  for  $i = 23$  to 27 can be determined separately, using  $w_k \neq 0$  for  $k = 1, 2, 3$  and  $w_4 = 0$ , when forces are required and  $w_1 = w_2 = w_3 = 0$ ,  $w_4 \neq 0$  when rolling moments are required. The choice of appropriate values for the  $w_i$  is discussed further in Section 3.2.1 on input to the program.

### 3.2 Program SHELTRAJ

The mathematical model and parameter estimation algorithm are implemented by the computer program SHELTRAJ. A listing of the program is given in Appendix IV. This section discusses input, output and usage of the program. The program consists of a main program and thirteen subroutines. The main program controls the input, output, solution of equations of motion and adjustment of parameter values by iteration. There are sets of routines controlling input/output, setting up and integrating the mathematical model equations by a fourth order Runge Kutta method, and implementing the parameter estimation algorithm. Function routines define the Kronecker delta and the pitching moment derivative at zero incidence, for the shell under consideration. The pitching moment derivative is used in equation (1) to estimate the yaw of repose. The need for this can be avoided by formulating the parameterised mathematical model equations (2) to (7) in terms of drag and lift rather than axial and normal force. Then  $C_L$  in equation (2) is given by

$$C_L = C_{L\zeta} \xi = (p_s I_x V_1 g_3 / Q S d V^2) (C_{L\zeta} / C_{M\zeta}) \quad (8)$$

so that the ratio  $(C_{L\zeta} / C_{M\zeta})$  can be included in the parametric representation in equation (6) in place of  $C_{Z\zeta}$  and the parametric representation in equation (5) can be used for  $C_D$  rather than  $C_X$ . This course would be preferable if the program were for use in constructing a Fire Control Model, where the separation of  $C_X$ ,  $C_{Z\zeta}$ ,  $C_{M\zeta}$  is not necessary, since shell trajectories are calculated simply using the mathematical model and the estimated parameter values. When yawsonde data, which will provide independent estimates of  $C_{M\zeta}$ , is available then the approach employed in SHELTRAJ is more useful, since it provides a better description of the behaviour of the shell.

#### 3.2.1 Input

Three logical units, 3, 5 and 8 are used to input all the data to program SHELTRAJ. The input required from unit 5 either as cards or card images is described in Table 4, and two examples of such input decks are shown in Table 5. The variables LENTER and LCASE are used to control a facility for multiple runs. When LCASE is non-zero control returns to the beginning of the card input on run completion. Then by using LENTER, control can be transferred to any one of several points in the input stream and the run repeated with new values for selected variables.

Several facilities are available in choosing values for input variables to provide the user with fine control on the parameter estimation algorithm. The array JORDER, allows the user to set the order of priority of the parameters so that if  $JORDER(i)=j$  then the  $i$ th parameter in the mathematical model defined above will be placed in the  $j$ th position in the reordered set. The most reliable strategy for obtaining convergence is to approach the solution piece-meal. The technique involves allowing only a few parameter values to vary initially and then repeating the run several times with a gradually increasing number of parameters varying. This is achieved by arranging the parameters in order of importance using JORDER, then gradually increasing the value of NPARAM with repeated runs until values have been estimated for all the desired parameters.

During execution, after the first iteration, the measured variable values are compared with the mathematical model outputs and if the differences between the two are greater than four standard deviations for any element of the measurement vector then that measurement is rejected because it is considered to be a rogue. During the first iteration no estimate of the standard deviation is available and so a value for the data rejection level, REJECT, must be supplied by the user. It is generally good policy to choose a large value so that few, if any, points will be rejected on the first iteration.

As we will discover below it is often difficult, if not impossible, to determine parameters defining aerodynamic forces and those defining rolling moments simultaneously. Separating the two problems can be achieved by means of the weighting factors XS. To estimate force parameters we set XS(1), XS(2), XS(3) at non-zero values and XS(4) = 0, while to estimate the rolling moment parameters we set XS (1) = XS (2) = XS (3) = 0 and XS (4) = 1. Tables 5(a) and 5(b) show data decks designed to implement the two types of calculation. In general values of the weighting factors XS(I) are chosen in proportion to the relative accuracies of each component of the measurement vector.

In addition to the input from unit 5, the program uses experimental data from unit 3 and meteorological data from unit 8. The experimental measurements should be in 5E16.8 format and each record should contain one value of each of time, x, y and z coordinates in range axes, and roll rate. Input begins at the first data point with time greater than T0 and every ISKIP th point is read until a total of NPTS points is reached. Finally meteorological data is input as described by the control variable IND. There are two types of table for the meteorological data and they use a 3F10.0 format. Each record contains only one table entry consisting of three items and each table may have up to 150 entries. Each entry in the wind table contains altitude above range origin, range wind, which is positive downrange and crosswind, which is positive to the right, while each entry in the pressure temperature table contains altitude, pressure in pascals and temperature in degrees Kelvin.

### 3.2.2 Output

The output from the program SHELTRAJ consists basically of a record of the input data, successive values of the parameters as they are adjusted at each iteration, together with r.m.s. errors in each parameter. When convergence is achieved the final parameter values and the covariance matrix are printed. The model outputs and the residuals of the measured values can be both printed and plotted if requested by using a non-zero value of NPLOT in the input.

Artificially produced data from a six degree of freedom model of the shell behaviour is shown in Table 6. This data has been used in conjunction with the data decks in Table 5 to test the program extensively. The results of these tests will be discussed in Section 5. Excerpts from the beginning and the end of the outputs for each data deck appear in Table 7.

## 4. YAWSONDE DATA ANALYSIS

The yawsonde was developed in the early 1960s(ref.1). Since then several significant improvements have been made to the original design(ref.2). The yawsonde measures the complementary solar aspect angle, which is the angle between the normal to the longitudinal axis of the shell and the direction of the sun. Figure 4 shows a schematic representation of the yawsonde and the angles associated with it.

As the yawsonde measures only the angle between the shell axis and the sun direction it provides essentially only a one-dimensional picture of the angular motion of the shell, which is basically two-dimensional. For this reason the use of yawsondes to study flight behaviour of shells was quite limited for many years. However, the recent application of parameter estimation to the problem has greatly increased the potential of yawsondes with regard to analysing the flight behaviour of shells. Provided that there is a significant component of the angular motion in the plane defined by the instantaneous velocity vector and the direction of the sun, parameter estimation can be used to reconstruct the total motion.

The following subsections deal with the factors which need to be taken into account in designing experiments with yawsondes, the mathematical model on which the data analysis is based, and the use of the program YAWSONDE which is designed to carry out that data analysis. An important aspect of the analysis of the yawsonde data is the piecemeal approach. This change is due to the much higher frequencies of those components of the motion measured by the yawsonde, that is, nutation and precession, compared with the components discussed in the previous section. Because of the higher frequencies the required parameters can be determined from much shorter lengths of data. Hence the restriction of data analysis runs to sections of the trajectory over which variations in Mach number are not significant, is no longer a problem so that the piecemeal approach, which severely limits analysis of the trajectory data, is quite adequate for analysing yawsonde data.

#### 4.1 Yawsonde usage

The yawsonde is depicted schematically in figure 4. It consists of two slits containing sun sensors at two points on the circumference of the shell. The longitudinal plane of each slit makes a specified angle with the longitudinal axis of the shell. As the shell rotates, the yawsonde produces a pulse train of the type shown in figure 4, with pulses of different polarity from each sensor. The relationship between the pulse train and the angle between the direction of the sun and the normal to the longitudinal axis of the shell, that is, the complementary solar aspect angle, is derived in Appendix V. Since the angles  $\gamma_1$ ,  $\gamma_2$  and  $\beta$  are nominal values only and cannot be reproduced exactly in the real yawsonde, and since the theoretical relationship derived in Appendix V does not take account of the finite displacement of the slits from the origin of the axes system, the yawsonde must be calibrated. One method of calibration is described in reference 2. Any such method involves a series of measurements of the corresponding values of  $\tau/T$  and  $\sigma_N$  as they appear in equation (22). In order to smooth

measurement errors and obtain an analytic calibration curve which can be used later to process the experimentally measured values of  $\tau/T$ , we obtain values of the parameters  $\gamma_1$ ,  $\gamma_2$  and  $\beta$  using a nonlinear least squares fitting technique similar to that described in Section 2. A listing of the program YAWCAL, which is used to do the fitting, appears in Appendix VI. The input required by the program is described in Table 8. The program uses a minimisation routine from reference 13 which is based on the method of Fletcher and Powell (ref.12). Figure 5 shows a typical calibration curve for a yawsonde. The main features which are worth noticing are the sensitivity at  $\sigma_N = 0$  and the limitations on the measurement range. If we use the

commonly chosen nominal values  $\gamma_1 = -\gamma_2 = \gamma$  and  $\beta = \pi$  for the angles defined in figure 4 where  $\gamma$  is usually chosen near  $\pi/4$ , the expressions in Appendix V show that the measurement range is

$$-(\pi/2 - \gamma) < \sigma_N < \pi/2 - \gamma$$

and the sensitivity at  $\sigma_N = 0$  is

$$\frac{d \sigma_N}{d (\tau/T)} \Big|_{\tau/T=1/2} = \pi / \tan \gamma .$$

This means that the sensitivity deteriorates rapidly as  $\gamma$  increases beyond  $\pi/4$  so that a useful value of  $\gamma$  is somewhere in the range  $\pi/6$  to  $\pi/4$ . The value in the examples in figures 5, 6 and 7 is  $\pi/4$ .

The limited range of measurement means that care must be exercised in trials planning to keep the complementary solar aspect angle within the range that the yawsonde can measure accurately. Care should be taken to avoid approaching the limits  $+\pi/2 - \gamma$  too closely because the finite physical dimensions of the slits render the calibration curves unreliable near those limits.

In order to use the yawsonde effectively we need to estimate the position of the sun. The method for estimating the azimuth and elevation of the sun in earth axes is given in Appendix VII together with an expression for the complementary solar aspect angle. For trials planning purposes we assume that the azimuth of the shell is the same as the bearing of the line of fire, since the difference between the two is generally quite small. The program ASPECT uses the results quoted in Appendix VII to estimate the complementary solar aspect angles at a range of times and elevation angles of the shell for a given day, place and line of fire. A listing of the program ASPECT may be found in Appendix VIII. Details of the input required by the program are given in Table 9. Two sets of results are given in figure 6 for this type of calculation for a shell fired at the Woomera Range on the 15th of March 1978. The results are given for directions of firing with bearings of 300 degrees and 0 degrees from true north. The range of angle which can be measured with the yawsonde,  $-\pi/4$  to  $\pi/4$  in this example, is shown by the dashed line. It is clear from these two figures that in order to obtain complete coverage of the trajectory, particularly for high elevations, it is necessary to fire nearly due north or nearly due south early in the day. In order to get a clearer picture of the optimum firing conditions the results have been presented slightly differently in figure 7. This figure shows an example of the range of elevation angles of the shell for which the yawsonde can detect the sun, as a function of time of day and bearing of the line of fire. The elevation angles on the shaded side of the curve are outside the range. It is apparent from the figure that the whole range of elevation angles can only be covered by firing sufficiently close to due north before 0930 or near enough to due south before 1100. Only the morning hours are covered in this figure, but similar conditions prevail in the late afternoon, when the whole range of elevation angles can be covered again by firing sufficiently near due north or due south. If we are prepared to sacrifice most of the downward leg of the trajectory, that is, negative elevation angles, and the firing elevation is not too high, then there is a much wider choice of firing conditions. For example, if a shell is fired at an elevation of 40 degrees and the trajectory is only required down to -10 degrees, then the firing can take place any time between 1100 hours and 1300 hours on a bearing between 110 degrees and 280 degrees. Alternatively, if the line of fire is fixed and some part of the trajectory can be sacrificed, there is generally a period during the day when the firing can be carried out and a satisfactory coverage of the trajectory obtained.

#### 4.2 Mathematical model

In analysing the data from measurements made with a yawsonde we are interested primarily in the two angular degrees of freedom, pitch and yaw, which are neglected in the four degree of freedom mathematical model used in analysing the trajectory data. The four first order equations which define the angular pitching and yawing motion of the shell are

$$\begin{aligned}\dot{\psi} &= r \sec\theta, \\ \dot{\theta} &= q, \\ \dot{q} &= pr - (I_x/I) p_s r + (QSD/I) [C_m \cos\phi \\ &\quad - C_{np} (p_s d/2V) \sin\phi + C_{mq} (qd/2V)], \\ \dot{r} &= -pq + (I_x/I) p_s q + (QSD/I) [C_m \sin\phi \\ &\quad + C_{np} (p_s d/2V) \cos\phi + C_{mq} (rd/2V)].\end{aligned}\tag{9}$$

The equations are formulated in an aeroballistic axes system, which is constrained to pitch and yaw with the vehicle and to maintain the GY' axis horizontal. Hence the GX' axis is forward along the horizontal axis of the shell; the GY' axis is horizontal and the GZ' axis is such that GX'Z' is a vertical plane. Then the roll rate of the axes system must be given by

$$p = -r \tan\theta\tag{10}$$

The roll rate of the shell,  $p_s$ , the velocity,  $V$ , and the dynamic pressure,  $Q$ , can all be obtained from the trajectory data analysis, discussed in Section 3. Apart from the aerodynamic coefficients and the angle  $\phi$ , which are discussed further below, the remaining parameters in equation (9) all represent physical characteristics of the vehicle which can be measured before the trial.

If this mathematical model is to be used in the parameter estimation process, then a parametric representation of the unknown quantities which appear in these equations has to be formulated. Firstly, consider the initial values of the variables; they are represented as follows,

$$\begin{aligned}\psi_0 &= P_1, \theta = P_2, \\ q_0 &= P_3 \text{ and } r_0 = P_4.\end{aligned}\tag{11}$$

The other unknown quantities in equation (9) are the aerodynamic coefficients. The following representation has been used for them

$$\begin{aligned}C_m &= (P_5 + P_{12}M)\xi + P_6\xi^3 + P_7\xi^5, \\ C_{np} &= P_8\xi + P_9\xi^3, \\ C_{mq} &= P_{10} + P_{11}\xi^2.\end{aligned}\tag{12}$$

If,  $\xi$  is the magnitude of the angle of attack and  $\phi$  is the orientation of the plane of the angle of attack then they are defined by the relations

$$\tan \xi = (v + w)^{1/2} / |u| , \quad (13)$$

$$\tan \phi = (-v) / w ,$$

where  $(u, v, w)$  are the components of the true air velocity in aeroballistic axes. They are defined in terms of the range components of vehicle velocity which are obtained from analysis of the trajectory data, by the transformation

$$\begin{bmatrix} u \\ v \\ w \end{bmatrix} = \begin{bmatrix} \cos\theta \cos\psi & \cos\theta \sin\psi & -\sin\theta \\ -\sin\psi & \cos\psi & 0 \\ \sin\theta \cos\psi & \sin\theta \sin\psi & \cos\theta \end{bmatrix} \begin{bmatrix} v_1 \\ v_2 \\ v_3 \end{bmatrix} \quad (14)$$

Equations (9) to (12) comprise a mathematical model of the portion of the behaviour of the shell which affects the yawsonde measurements, in terms of the unknown parameters,  $P_i$ . The criterion used to estimate values for the parameters is to minimise the average of the sum of squares of the residuals

$$\sigma^2 = \frac{1}{N} \sum_{j=1}^N (\hat{\sigma}_{Nj} - \sigma_{Nj})^2$$

where  $\hat{\sigma}_{Nj}$  is the measured value of the complementary solar aspect angle and  $\sigma_{Nj}$  is the value predicted by the mathematical model. The value of  $\sigma_{Nj}$  is estimated by substituting the value of the local time at which the trial occurred and the values of  $\psi$  and  $\theta$  predicted by the mathematical model into the relations given in Appendix VI.

The parameter estimation algorithm is the same as that used in the trajectory analysis and described in detail in references 4, 5, 8 and 9. The algorithm uses partial derivatives of the complementary solar aspect angles with respect to the parameters to obtain adjustments for each parameter value during each iteration. These partial derivatives are obtained by numerical integration of equations which are derived from the mathematical model equations by partial differentiation. Details of the derivation of the partial derivatives are given in Appendix IX.

#### 4.3 Program YAWSONDE

The parameter estimation processing for the yawsonde data is implemented in the computer program YAWSONDE. A listing of the program may be found in Appendix X. The program consists of a main program and eleven subroutines. The main program controls the processing of the data by the routines. The subroutines fall into three categories which serve the functions of input and output, numerical integration of the differential equations to simulate shell behaviour and estimate values of partial derivatives and finally, the calculation of adjustments to the parameter values using the parameter estimation algorithm.

#### 4.3.1 Input

Details of the input needed from unit 5 either as cards or card images are provided in Table 10, and an example of such a deck appears in Table 11. The controls for the parameter estimation process are the same as those used by SHELTRAJ. They are discussed in detail in Section 3.2.1, and therefore will not be discussed here. The meteorological data is also the same as that for SHELTRAJ and a detailed description of this also may be found in Section 3.2.1.

The major differences from the input requirements of the program SHELTRAJ are the specification of sun position and trajectory data and the experimental measurements. There is provision to tabulate variation of the direction cosines of the sun as a function of time along the trajectory. If this is not deemed necessary constant average values can be entered with times corresponding to the beginning and end of the trajectory as has been done in the example in Table 11. The trajectory data which is needed to estimate such things as dynamic pressure, velocity and so on, in the mathematical model equations must be supplied in a separate input dataset on unit 4. The data will usually be obtained from the smoothed trajectory produced by the analysis described in Section 3. The program will read from the dataset a total of NTRAJ points on the trajectory, using only every ISKIP th point in the dataset, where NTRAJ and ISKIP are input from unit 5. The records in the dataset should have 8F10.0 format and each record should contain values of time, range velocity, drift velocity, which is positive to the right, vertical velocity, which is positive downwards, altitude and roll rate. Finally the experimental data is input from a dataset attached as unit 3. The first data point is that for the first time greater than T0. Every ISKIP th point is input until a total of NPTS points is reached. Values for T0, ISKIP and NPTS are all read from the cards described in Table 10. Each experimental record is in 2E16.7 format and contains a value of time and the complementary solar aspect angle in radians.

#### 4.3.2 Output

The output from YAWSONDE is similar to that from SHELTRAJ. It consists principally of a record of the input data, values of parameters and their estimated errors after each iteration and the covariance matrix when convergence is achieved. Model outputs and residuals of the measured values can be both printed and plotted by assigning a non-zero value to N PLOT.

Artificially produced data relating to trajectory and yawsonde measurements is given in Table 12. This has been used in conjunction with the card deck in Table 11 to test the program. The beginning and end of the output from this test run is given in Table 13. The more significant aspects of the results from the program testing are discussed in detail in the next section.

### 5. PROGRAM TESTING

Both programs were tested using simulated data obtained from a six degree of freedom trajectory model which used linear interpolation amongst the tabulated values of the aerodynamic coefficient given in Table 1. Listings of the simulated data appear in Tables 6 and 12. Test cases were run both with and without Gaussian white noise superimposed on the data for each program. Tests were also run with the trajectory data to compare the efficiency of the program SHELTRAJ with a method which allowed only a linear variation of drag with Mach number and kept all other coefficients constant. Details of the results of these test runs are given below.

### 5.1 Program SHELTRAJ

The testing of SHELTRAJ fell naturally into two areas, one involving the aerodynamic forces and the other involving the aerodynamic moments, specifically the roll damping moment. The determination of aerodynamic forces will be discussed first. It proved impossible to determine all the parameters defining the forces even using the clean data. However, only the subsonic part of the curve for the normal force derivative was troublesome. The initial conditions, the drag force coefficient and the supersonic part of the normal force derivative, a total of 16 parameters in all, were well determined. These parameters were the first 16 defined by the data deck in Table 5(a). The whole run occupied some 10 minutes of CPU time on the IBM 370/168 computer. However, it should be remembered that the whole trajectory was processed in that one run, whereas other methods would require at least 25 runs to process the same data.

The same test case was rerun with Gaussian white noise superimposed on each component of the data. The noise had a standard deviation of 5 m. The information extracted from this case was very limited. Only the axial force was obtained with any reliability at all, and the error in that approached 10 per cent in many places. This means that the r.m.s. noise level in each position coordinate would need to be much lower than 5 m if the application of parameter estimation methods to the analysis of trajectory data were to be used in constructing a Fire Control Model.

In order to gauge the improvement in the data analysis which was achieved by using analytic functions of Mach number to represent aerodynamic forces, tests were run allowing only linear variation of axial force and keeping the normal force derivative constant, an approach similar to that used in reference 9. The results of the testing of capabilities of the two methods are shown in figure 8. Figure 8(a) shows the results for the axial force, comparing results obtained from the parameter estimation methods, using both noisy and clean data, with the curve used to generate the data from the six degree of freedom model. From analysis of uncontaminated data, the method proposed in Section 2 produced an analytic axial force curve which followed the original except at very low Mach numbers where there was no data because the section of trajectory which was analysed only covered Mach numbers from 1.37 down to 0.57. When the method was applied to noisy data the result contained errors as high as 8 per cent but generally followed the original fairly well. It should be noted that the noise model used represents an extremely noisy data collection method and modern tracking radars would produce a very much better signal. The tests with such poor data were aimed at determining the advantages of analytic representations of Mach number, and also the general capabilities of the method when radar data is poor. This aspect of the problem is discussed further in the next section.

By comparing the results from the present approach with those of the method of reference 9 one can elicit very definite conclusions. As far as the axial force is concerned the method of reference 9 produced reasonable results when the data was uncontaminated, although it was unable to represent the high curvatures near Mach numbers of 0.9 and 1.1. However, the results using noisy data were quite hopeless, except around Mach 0.7 where the very large number of data points in a small Mach number range was sufficient to compensate for the effects of noise. Figure 8(b) shows the corresponding results for normal force derivative. Both methods gave reasonable results from uncontaminated data but were completely hopeless when noisy data was used. An interesting feature of the results shown in figure 8(b) is that the normal force derivative was consistently underestimated. The error ranges from two to five per cent and arises because data generated by a six degree of freedom model has been fitted by an approximate four degree of freedom model. It is not apparent whether the principal source of the

discrepancy is the approximate form used for the four degree of freedom model, or whether the discrepancy is mainly due to the use of the four degree of freedom model itself. This aspect of the problem is discussed further in Section 7, in connection with the possible use of program SHELTRAJ in constructing or improving a Fire Control Model.

Finally it should be noted that the average CPU time used in the computer runs implementing the method of reference 9 was 10 s so that if the axial force coefficient can be adequately represented over the range of Mach number covered by the whole trajectory with about thirty straight lines, then one might achieve a fifty percent saving in CPU time compared with the analytic functions method. However, the results for axial force coefficient, derived by the piecemeal approach are less accurate and the method is less robust in the presence of noise. Also, if more runs are needed, the CPU time advantage will rapidly disappear.

Now let us consider the roll damping moments. Experiments with the program rapidly showed that aerodynamic force coefficients and aerodynamic roll damping coefficients could not be satisfactorily determined simultaneously and the method outlined in Section 3.2.1 was used to separate the two processes. Figure 9 shows the results of some test runs to gauge the effect of noisy data on the results obtained for the roll damping moment. The Mach number range covered by the data is from 0.63 to 1.37 and it is apparent from figure 9 that if a cubic expression is used to represent the variation of the roll damping moment coefficient with Mach number there is considerable deviation from the true results near the limits of the range. This deviation increases dramatically as the noise level in the data increases. The examples shown in figure 9 include a quadratic curve obtained by least squares fitting to the original data given in Table 1. This curve, for which coefficients are given in Table 3, is a base against which we can evaluate the other results. Also shown are four curves obtained from applying parameter estimation to artificially generated data from a six degree of freedom model, one obtained using uncontaminated data and the other three using noisy data. The noisy data was obtained from the uncontaminated data by adding Gaussian white noise with r.m.s. levels of 1 and 10 radians respectively. For the data with the higher noise level, results are shown for both cubic and linear variations with Mach number. It is clear from the figure that high noise levels will result in large deviations near the ends of the Mach number range unless the degree of the polynomial is severely restricted. Thus the linear representation results in much lower overall errors when there are high noise levels in the data. It is generally true in all parameter estimation problems, that there exists a critical number of parameters for given noise levels in the data, such that increasing the parameters past that number introduces spurious trends into the results. This applies to most curve fitting problems and is particularly evident here because of the relative simplicity of the problem. Figure 9 shows that the derivation of roll damping moments will be quite accurate despite high noise levels in the data, provided that the degree of polynomial representation is appropriately restricted. The rolling moment is estimated to better than five per cent accuracy when there is a r.m.s. noise level of 10 radians in the data, if a linear representation is used for variation of the moment coefficient with Mach number.

The determination of the roll damping moment is still part of the program SHELTRAJ at this stage, and in this form it takes about 6 minutes of CPU time on an IBM 370/168 to determine one of the cubic curves shown in figure 9. However, it would be a relatively simple undertaking to separate out the portion of the program which deals with rolling motion and this should reduce the computing time to less than a minute.

### 5.2 Program YAWSONDE

The testing of the program YAWSONDE was rather unrealistic in some respects. The data used, shown in Table 11, was generated from a simple undisturbed trajectory and so represented a very low amplitude oscillation. Hence even the results for uncontaminated data show errors of several per cent in the restoring moment. However, the parameter estimation algorithm converged, even when all twelve parameters were allowed to vary (Table 13). When noise was added to the data with a root mean square amplitude about twice that of the oscillation, the algorithm converged with five parameters varying, although the actual results obtained were meaningless. Therefore two important conclusions can be drawn from the testing of program YAWSONDE. Firstly, in designing experiments to obtain aerodynamic moments from yawsonde measurements, care should be taken to produce an oscillation of several degrees amplitude if the moments are to be determined accurately. Secondly the parameter estimation is remarkably robust in this case since it was possible to get convergence with extremely high noise levels in the data.

The program YAWSONDE is restricted to ranges of data where changes in Mach number do not significantly affect aerodynamic coefficients. However, as a result of the high frequencies present in angular oscillations, particularly nutation which can show frequencies around 20 Hz, much shorter ranges of data are needed to determine aerodynamic moment coefficients reliably. As a general rule the amount of data necessary to determine a value for a given parameter is of a length representing about two or three cycles of the component of the motion which is most affected by that parameter. Therefore this restriction will not generally present any problems. In addition, each test run took only about twenty seconds of CPU time. Hence the analysis will be economical of computing time even though many runs will be needed to cover the complete range of Mach number.

## 6. SUMMARY OF RESULTS

The program SHELTRAJ, which was developed to analyse radar tracking and roll rate data is based on the concept of using analytic functions to represent the Mach number dependence of aerodynamic forces and rolling moments. Testing of the program demonstrated that this approach has potential for providing more accurate estimates of the relevant aerodynamic coefficients than a piecewise approach to the data analysis especially when there is a significant noise component in the data(ref.9). This result is particularly important in the context of using the technique to develop a Fire Control Model because highly accurate estimates of the axial force coefficient of a shell are needed in such a situation. The difficulties with estimating roll damping moments indicate that roll rate data should be analysed independently of the shell position data. This could be accomplished most efficiently using a completely separate computer program and removing altogether the facility for analysing roll rate measurements from SHELTRAJ.

The program YAWSONDE is very similar to other programs for analysing data on the complementary solar aspect angle. This particular version appears to be extremely stable. However, it is important to realise that the program will only provide an accurate estimate of the aerodynamic moments if the data being analysed covers a trajectory segment in which there is a pronounced incidence oscillation. Possible methods for generating the appropriate incidence oscillations are discussed in Section 7.

## 7. APPLICATION OF RESULTS

Many avenues for further investigation arose during the course of the work which has been reported here. Of these three particular areas are most likely to yield useful results. First let us consider improvements or changes to the programs developed to analyse both trajectory and yawsonde data. It is apparent from the work reported here that two improvements are particularly important. They are the development of a completely separate program to analyse roll rate data, and the formulation of the four degree of freedom model, which is used in the analysis of radar tracking data, in terms of the ratio of lift force derivative to pitching moment derivative. The idea of a separate program to analyse roll rate data was discussed at length in Section 5 where it was indicated that the CPU time used to process roll data could be substantially reduced by this means. Initial trials indicate that the reduction is substantial and that less than ten seconds of CPU time will be needed, rather than several minutes. The use of the ratio of the derivatives of normal force and restoring moment was discussed in detail in Section 3.2 and the key equation (8) given. This formulation of the problem is such that analysis of the trajectory data is completely self contained. Thus a Fire Control Model could be constructed from measurement of several trajectories without the need for wind tunnel data or a large number of range and accuracy firings.

A second avenue which needs further investigation is the connection between the amplitude of angular motions of the shell, accuracy capabilities of the yawsonde, and accuracy requirements for the aerodynamic coefficients which are derived from the measurements. Apart from studies applying the program to artificially manufactured data containing noise of known characteristics, studies will need to be made of methods for exciting angular motion in shells. Application of such methods would need to provide sufficient amplitude of shell yaw to satisfy accuracy requirements for the aerodynamic moment derivatives. Two methods which have been suggested are the introduction of an asymmetric mass distribution(ref.7) and the use of an asymmetrical muzzle brake(ref.18).

Finally, the data analysis method developed in Section 3 could be used extensively in the construction of a Fire Control Model. An investigation of the benefits of introducing parameter estimation techniques into the methodology for constructing a Fire Control Model should elicit many useful results. Several factors would need to be considered, such as the number of firings which would be necessary, the accuracy with which shell position would have to be measured, the possibility of using flashing lights rather than radar to measure position, how accurate the meteorological data would have to be and so on. One aspect of the method of Section 3 which would definitely require further investigation is the use of the four degree of freedom model and the approximations which were used in equations (1) and (2) to make them tractable in the above application. In fact further study of these approximations may be worthwhile in its own right, particularly since they are suspected of causing errors in the estimates of the lift force. The question of the four degree of freedom or modified point mass model is different altogether and it may be a definite advantage of the technique. In general, the Fire Control Model uses a four degree of freedom representation to calculate aiming data, because a more complex model is too difficult to implement on a field computer and too expensive of computing time. The four degree of freedom trajectory model is used in the reverse mode in the Model, from its application in the parameter estimation algorithm. Hence, while parameter estimates, obtained by fitting to several sets of trajectory data, may contain significant errors compared with wind tunnel measurements of the aerodynamic forces represented by them, the overall Model which is derived by this means is likely to be better than one which uses exact wind tunnel data. This follows because the parameter estimation process for construction of the Model would involve fitting the Model to

data from a wide range of trajectories, and so one would expect the Model to be extremely accurate when it is used in reverse to generate trajectories. Using such a method the development of a Fire Control Model would be faster and cheaper than at present, mainly because the number of range and accuracy firings would be substantially reduced. Hence, this is potentially the most useful application of the methods developed in this report, and therefore the most likely to repay further study.

## NOTATION

$A(r), B(r)$	Polynomial functions in the NR3634 drag function
$a$	local speed of sound
$a, b, c, d, e, f$	coefficients of the Gavre drag function
$a_n, b_n$	coefficients of polynomials in the NR3634 drag function
$C_D$	aerodynamic drag force coefficient
$C_L$	aerodynamic lift force coefficient
$C_X$	aerodynamic axial force coefficient
$C_{Yps}$	aerodynamic Magnus force derivative
$C_Z$	aerodynamic normal force coefficient, generally negative
$C_{L\zeta}$	aerodynamic lift force derivative
$C_{M\zeta}$	aerodynamic normal force derivative
$C_{\ell_p}$	aerodynamic roll damping moment derivative
$C_{mq}$	aerodynamic pitch damping moment derivative
$C_{np}$	aerodynamic Magnus moment derivative
$d$	maximum body diameter
$f, g$	variables used in NR3634 curve, representing normal force derivative, corresponding to the variables $r, s$ used in representing axial force
$\underline{g} = \begin{bmatrix} g_1 \\ g_2 \\ g_3 \end{bmatrix}$	acceleration due to gravity in range axes
$g_0$	acceleration due to gravity at sea level
$H$	hour angle of the sun
$h$	height of range origin, 0, above mean sea level
$I_x$	moment of inertia about the longitudinal axis
$I$	moment of inertia about the lateral axis
$\underline{i}, \underline{j}, \underline{k}$	unit vectors in the range axes system
$K$	Mach number centred on the transonic drag rise for the NR3634 drag curve
$L$	width of the transonic drag rise for the NR3634 drag curve
$M$	free stream Mach number

m	mass of shell
N	number of data points
$N_a$	degree of the polynomial used in the supersonic region of the NR3634 function
$N_b$	degree of the polynomial used in the subsonic region of the NR3634 function
$p_i$	unknown parameters in mathematical model
$p_s$	roll rate of shell
$\begin{bmatrix} p \\ q \\ r \end{bmatrix}$	angular rates describing motion of the aeroballistic axes. Pitch and yaw rates are the same as those for the shell. Roll rate is such that the GY' axis remains horizontal.
$Q = \frac{1}{2} \rho V^2$	dynamic pressure
r	variable used in the NR3634 drag curve, $(M^2 - K^2)/(M^2 + K^2)$ .
$r_o$	radius of the earth
r	distance of the shell from the centre of the earth
S	maximum cross-sectional area of the shell
s	variable used in the NR3634 drag curve, $r/[ (1-L^2) r^2 + L^2 ]^{1/2}$
T	period between pulses of like sign from the yawsonde, that is, roll period
t	time from the beginning of the shell flight
$\underline{U}$	velocity of the shell relative to range axes. It has components ( $\dot{x}$ , $\dot{y}$ , $\dot{z}$ ) in range axes.
$\underline{V}$	true air velocity of the shell. It has components ( $V_1$ , $V_2$ , $V_3$ ) in range axes and (u, v, w) in aeroballistic axes. Magnitude is denoted by V.
$\underline{\underline{v}}$	a unit vector in the direction of $\underline{V}$ .
$\underline{\underline{w}}$	wind vector, with components ( $w_1$ , $w_2$ , 0) in range axes.
$w_i$	weights used in forming the sum of squares of the residues of the data variables.
$\begin{bmatrix} x \\ y \\ z \end{bmatrix}$	denotes position in range axes, where OX is downrange, OY is horizontal to the right and OZ is vertically downwards. The origin 0 is generally at the gun

$$\begin{bmatrix} x' \\ y' \\ z' \end{bmatrix}$$

denotes position in aeroballistic body axes, where  $Gx'$  is forward along the longitudinal axis,  $Gy'$  is horizontal to the right, and  $Gz'$  completes a right handed axes system. The origin G is at the centre of gravity of the shell.

$$\begin{bmatrix} x'' \\ y'' \\ z'' \end{bmatrix}$$

Denotes position in rolling body axes with the origin S on the longitudinal axis of the shell at the location of the centre of the sun slits.  $Sx''$  is forward along the longitudinal axis,  $Sz''$  is outwards through the centre of sensor 1 in the yawsonde and  $Sy''$  completes a right handed set as shown in figure 4.

 $\beta$ 

the circumferential angle between the two sensors in the yawsonde (see figure 4)

 $\gamma_1, \gamma_2$ 

the angles which the respective sensors in the yawsonde make with the longitudinal axis of the shell (see figure 4).

 $\delta$ 

declination of the sun

 $\delta_{ij}$ 

Kronecker delta, = 1 when  $i = j$  and 0 otherwise

 $\xi$ 

total angle of attack

 $\xi_R$ 

yaw of repose

 $\Theta$ 

latitude of shell

 $\theta$ 

elevation of the longitudinal axis of the shell

 $\theta_s$ 

elevation of the sun

 $\Lambda$ 

vector defining Coriolis force, with components  $(\Lambda_1, \Lambda_2, \Lambda_3)$  in range axes

 $\rho$ 

local air density

 $\sigma$ 

root mean square error in fitting the parametric model to the data

 $\sigma_N$ 

complementary solar aspect angle, that is, the complement of the angle between the longitudinal axis of the shell and the direction of the sun.

 $\tau$ 

time between positive and negative pulses from the yawsondes (see figure 4)

 $\Phi$ 

longitude of the shell.

 $\phi$ 

orientation of the incidence of the shell relative to a vertical plane containing the longitudinal axis of the body. It is positive clockwise and is zero when the shell is nose up.

 $\Psi$ 

bearing of line of fire relative to true north

 $\psi$ 

azimuth of the longitudinal axis of the shell

$\psi_s$  azimuth of the sun.

$\Omega_{\sim}$  angular velocity of the earth, with components  
 $(\Omega_1, \Omega_2, \Omega_3)$  in range axes.

$\partial$  partial differentiation operator.

Superscripts

.

denotes differentiation with respect to time

$\wedge$  denotes an experimentally measured value of a variable

Subscripts

$o$  denotes an initial value of the variable

## REFERENCES

No.	Author	Title
1	Amery, I.O.F., Hemming, H.G.E., Lawrie, K.G.A. and Wlatnig, E.J.M.	"A Telemetry System for the Measurement of the Yaw of a Projectile Throughout the Major Part of its Trajectory" RARDE Report 1/65, March 1965.
2	Mermagen, W.B.	"Measurements of the Dynamical Behaviour of Projectiles Over Long Flight Paths" J. Spacecraft and Rockets, Vol.8, No.4, pp 380-385, April 1971.
3	Lieske, R.F. and Rieter, M.L.	"Equations of Motion for a Modified Point Mass Trajectory" BRL Report No.1314, March 1966.
4	Chapman, G.T., and Kirk, D.B.	"A Method for Extracting Aerodynamic Coefficients From Free Flight Data" AIAA Journal Vol.8, No.4, pp 753-758, April 1970.
5	Waterfall, A.P.	"A Technique for the Automatic, Digital Analysis of Flight Dynamic Response Data" Aeronautical Research Council, Reports and Memoranda, R&M 3699, 1972.
6	Whyte, R.H., and Mermagen, W.H.	"A Method for Obtaining Aerodynamic Coefficients from Yawsonde and Radar Data" J. Spacecraft and Rockets, Vol.10, No.6, pp 384-388, June 1973
7	Fitch, P.	"Derivation of Parameters From In-Flight Radar Data" Proceedings of the 4th Meeting of TTCP "Launch and Flight Dynamics" Panel W-2, November 10-18 1977.
8	Pope, R.L.	"A New Technique for Obtaining the Aerodynamics of Missiles from Flight Trials on a Gas Gun Range" WRE-TN-1719(WR&D), November 1976
9	Becker, M.	"Yawsonde and Radar Data Reduction to Obtain Aerodynamic Coefficients" Naval Weapons Laboratory Technical Report TR-3073, September 1974.
10	Shanks, D, and Walton, T.S.	"A New General Formula for Representing the Drag on a Missile Over the Entire Range of Mach number" NAVORD Report 3634, May 1957.
11	McShane, E.J., Kelly, J.L. and Reno, F.V.	"Exterior Ballistics" University of Denver Press, USA, 1953.

No.	Author	Title
12	Fletcher, R. and Powell, M.J.D.	"A Rapidly Convergent Descent Method for Minimisation" Computer Journal, Vol.6, No.3, pp 163-168, 1963.
13	-	"System/360 Scientific Subroutine Package" IBM Manual GH20-0205-4
14	Lloyd, K.H.	"Concise Method for Photogrammetry of Objects in the Sky" WRE-TN-72(WR&D), August 1971.
15	Smart, W.M.	"Spherical Astronomy" C.U.P. 4th Ed., 1956.
16	-	"The Astronomical Ephemeris" Her Majesty's Stationery Office, 1978.
17	Murphy, C.H.	"Yaw Induction by Mass Asymmetry" J. Spacecraft and Rockets, Vol.14, No.8, p.511-512, August 1977.
18	Loeb, A.A.	"Unique Aeroballistic Yaw Experiments With the 155 mm M843 Projectile" Proceedings of the TTCP Symposium on "In-Bore and Muzzle Dynamics" held at Monterey, USA, July 1976.

## APPENDIX I

## NR3634 DRAG CURVE

A brief resume of the properties of the formula, proposed in reference 10, to represent the variation of axial force over the entire Mach number range, is presented here to clarify comments on curve fitting and choice of values for parameters which are made in the main text.

The following criteria were used to construct the drag function defined below,

- (1) The function should effect some smoothing when fitted to experimental results. Hence the number of adjustable parameters, while being sufficiently large to provide adequate flexibility should be much less than the number of observations.
- (2) The function is empirical, but its behaviour should be consistent with basic characteristics of drag functions, such as asymptotic behaviour at high and low Mach numbers and transonic drag rise.
- (3) The analytic form should be simple and compact; transcendental and complex algebraic functions should be avoided.
- (4) The function should be analytic.
- (5) A simple procedure should be available for obtaining values of the parameters from experimental data.

Each of these conditions constitutes a considerable advantage over conventional methods of coefficient determination which rely on analysing only small portions of data during which the Mach number is almost constant. By repeating the analysis many times on different sections of trajectory such methods produce a table which shows variation of axial force with Mach number. Clearly an analytic representation which satisfies the above five conditions will result in greater accuracy and less computational effort in the analysis of position data for any trial.

The form for the analytic representation of the drag is

$$C_x = (1 + s)A(r) + (1-s)B(r)$$

where  $r, s$  are functions of Mach number,

$$r = (M^2 - K^2) / (M^2 + K^2)$$

$$s = r / [(1 - L^2)r^2 + L^2]^{1/2}$$

and  $A(r), B(r)$  are both polynomials in  $r$ ,

$$A(r) = \sum_{n=0}^{N_a} a_n r^n$$

$$B(r) = \sum_{n=0}^{N_b} b_n r^n$$

where  $a_n$ ,  $b_n$ ,  $K$ ,  $L$ ,  $N_a$  and  $N_b$  are constants to be determined.

The first property of the axial force coefficient function is explained by the result that  $K$  is close to 1 and  $L$  is small. Then for subsonic Mach numbers,  $M = 0$  upwards,  $r$  begins at -1 and approaches 0, somewhere in the transonic range and  $s$  is very close to -1 over the whole subsonic range, only changing appreciably when the transonic range is entered and  $r \rightarrow 0$ . Hence, subsonically

$$C_x \approx 2B(r).$$

Somewhat similar effects occur supersonically, as  $M \rightarrow \infty$ , or for  $M > 1 + \epsilon$ ,  $s \rightarrow 1$  and  $r$  progresses from 0 to 1 so that

$$C_x \approx 2A(r).$$

Hence the polynomials  $A(r)$  and  $B(r)$  represent supersonic and subsonic parts of the drag curve respectively. Relatively few terms are needed; generally, linear or quadratic forms are adequate.

With regard to the constants  $K$  and  $L$  it is instructive to look at the value at  $M=K$  and the slope at that point. When  $M=K$ ,  $r=0$ ,  $s=0$ , and

$$C_x = a_0 + b_0,$$

$$K(dC_x/dM)|_{M=K} = a_1 + b_1 + (a_0 - b_0) / L.$$

Bearing in mind that  $2a_0$  is the approximate value of  $C_x$  immediately above the transonic drag rise and  $2b_0$  is the value immediately below it, then it follows that  $K$  is the value of Mach number when the drag is midway between these two levels. If  $L \ll 1$ , then  $2L$  is the effective interval of Mach number over which the transonic drag rise,  $2(a_0 - b_0)$  would be attained if the maximum slope were maintained throughout.

Finally, consider the asymptotic behaviour of the curve. Firstly, for subsonic incompressible flow,  $M \geq 0$ , the axial force coefficient,

$$C_x = 2 \sum_{n=0}^{N_b} (-)^n b_n + O(M^2)$$

and secondly for hypersonic flow,  $M \rightarrow \infty$ , axial force coefficient,

$$C_x = 2 \sum_{n=0}^{N_a} a_n + O(M^{-2}).$$

These are the correct asymptotic forms for the axial force coefficient at both ends of the Mach number range. The properties of the transonic drag rise and the asymptotic behaviour of the curve can be used to make initial estimates for the values of each parameter. The values can then be refined by parameter estimation or nonlinear least squares curve fitting methods.

APPENDIX II  
CORIOLIS AND GRAVITY COMPONENTS

High accuracy is required in shell trajectory computation. The effects of Coriolis force and the changes to the gravity vector, occurring along the trajectory, have a significant effect on the trajectory. Therefore these changes must be included in the mathematical model. Both effects are well known and documented, but are included here so that the document is self-contained as far as the description of the mathematical model of the shell trajectory is concerned.

The Coriolis acceleration arises from the rotation of the range axes system, because the range axes system is fixed relative to a rotating earth. The acceleration vector,  $\tilde{\Lambda}$  in equation (2), is given by

$$\tilde{\Lambda} = 2 \tilde{\Omega} \times \tilde{U}$$

where  $\tilde{U}$  is the velocity of the shell and  $\tilde{\Omega}$  is the angular velocity of the earth,  $7.292115 \times 10^{-5}$  rads/s about an axis from south pole to north pole. Then at latitude  $\Theta$ , positive south, and line of fire bearing  $\Psi$  from true north

$$\begin{bmatrix} \Omega_1 \\ \Omega_2 \\ \Omega_3 \end{bmatrix} = \begin{bmatrix} 2 \cos \Theta \cos \Psi \\ 2 \cos \Theta \sin \Psi \\ 2 \sin \Theta \end{bmatrix} | \tilde{\Omega} |$$

assuming that the OX axis is along the line of fire, the OZ axis vertically downwards and the OY axis horizontal to the right, thus forming a right handed axes system.

The second part of this appendix looks at the problem of defining the components of gravity in the same axes system. The magnitude of the acceleration due to gravity at a distance  $r$  from the centre of the earth is

$$|g| = g_o r_o^2 / r^2$$

where  $g$  is the local acceleration at mean sea level and  $r_o$  is the radius of the earth. The direction of the acceleration is radially inwards. Then at a point  $(x, y, z)$  in a Cartesian coordinate system with axes as described above and origin at an altitude,  $h_o$ , above mean sea level the gravity vector can be represented by

$$\tilde{g} = -g_o r_o^2 [x \tilde{i} + y \tilde{j} - (h_o + r_o - z) \tilde{k}] / r^3$$

where  $r^2 = x^2 + y^2 + (h_o + r_o - z)^2$ . This result can be easily derived from the geometry of the situation, using the knowledge that  $x$ ,  $y$  and  $z$  are all very small compared with  $r_o$ .

## APPENDIX III

## PARTIAL DERIVATIVES WITH RESPECT TO PARAMETERS FOR SHELTRAJ

In order to implement a parameter estimation algorithm we need to know partial derivatives of the measured variables with respect to the unknown parameters. These partial derivatives are obtained by numerical solution of a set of simultaneous ordinary differential equations obtained by partial differentiation of the mathematical model equations presented in Section 3.1. By separating out the components of velocity and acceleration in equation (2) and differentiating with respect to the parameter,  $P_i$ , we obtain the following set of differential equations

$$\frac{d^2}{dt^2} \left( \frac{\partial x}{\partial P_i} \right) = \left( \frac{\rho S}{2m} \right) (C_D V_1 \frac{\partial V}{\partial P_i} + C_D \frac{\partial V_1}{\partial P_i} V + \frac{\partial C_D}{\partial P_i} V_1 V) + \frac{\partial g_1}{\partial P_i} - \frac{\partial \Lambda_1}{\partial P_i} \quad (15)$$

$$\begin{aligned} \frac{d^2}{dt^2} \left( \frac{\partial y}{\partial P_i} \right) &= \left( \frac{\rho S}{2m} \right) (C_D V_2 \frac{\partial V}{\partial P_i} + C_D \frac{\partial V_2}{\partial P_i} V + \frac{\partial C_D}{\partial P_i} V_2 V + 2C_L V \frac{\partial V}{\partial P_i} + \frac{\partial C_L}{\partial P_i} V^2) \\ &\quad + \frac{\partial g_2}{\partial P_i} - \frac{\partial \Lambda_2}{\partial P_i} \end{aligned} \quad (16)$$

$$\frac{d^2}{dt^2} \left( \frac{\partial z}{\partial P_i} \right) = \left( \frac{\rho S}{2m} \right) (C_D V_3 \frac{\partial V}{\partial P_i} + C_D \frac{\partial V_3}{\partial P_i} V + \frac{\partial C_D}{\partial P_i} V_3 V) + \frac{\partial g_3}{\partial P_i} - \frac{\partial \Lambda_3}{\partial P_i} \quad (17)$$

$$\frac{d}{dt} \left( \frac{\partial p_s}{\partial P_i} \right) = \left( \frac{\rho S d^2}{4 I_x} \right) (C_t p_s \frac{\partial V}{\partial P_i} + C_t \frac{\partial p_s}{\partial P_i} V + \frac{\partial C_t}{\partial P_i} p_s V) \quad (18)$$

if we assume that local air density,  $\rho$  and speed of sound  $a$ , are insensitive to changes in parameter values. These then are the basic differential equations which can be solved to provide values of the partial derivatives,

$$\frac{\partial x}{\partial P_i}, \frac{\partial y}{\partial P_i}, \frac{\partial z}{\partial P_i} \text{ and } \frac{\partial p_s}{\partial P_i}$$

required by the parameter estimation algorithm. However, these equations include many partial derivatives which are not available from the solution of the equations but must be obtained by partial differentiation of other relationships. The method of calculating these partial derivatives is outlined below. Using the relation

$$V^2 = V_1^2 + V_2^2 + V_3^2 .$$

we find that

$$V \frac{\partial V}{\partial P_i} = V_1 \frac{d}{dt} \left( \frac{\partial x}{\partial P_i} \right) + V_2 \frac{d}{dt} \left( \frac{\partial y}{\partial P_i} \right) + V_3 \frac{d}{dt} \left( \frac{\partial z}{\partial P_i} \right) ,$$

since it follows easily from the relation between velocity relative to range axes and true air velocity that

$$\frac{\partial}{\partial P_i} \begin{bmatrix} V_1 \\ V_2 \\ V_3 \end{bmatrix} = \frac{d}{dt} \left\{ \frac{\partial}{\partial P_i} \begin{bmatrix} x \\ y \\ z \end{bmatrix} \right\}.$$

Using the expressions given in Appendix II for the accelerations due to Coriolis and gravity effects, the following results can be derived;

$$\frac{\partial}{\partial P_i} \begin{bmatrix} \Lambda_1 \\ \Lambda_2 \\ \Lambda_3 \end{bmatrix} = 2 \begin{bmatrix} \Omega_1 \\ \Omega_2 \\ \Omega_3 \end{bmatrix} \frac{d}{dt} \left\{ \frac{\partial}{\partial P_i} \begin{bmatrix} x \\ y \\ z \end{bmatrix} \right\}$$

and

$$\frac{\partial}{\partial P_i} \begin{bmatrix} g_1 \\ g_2 \\ g_3 \end{bmatrix} \approx -g \left( r_o/r \right)^2 \frac{1}{r} \frac{\partial}{\partial P_i} \begin{bmatrix} x \\ y \\ z \end{bmatrix},$$

although the approximation in this equation is negligible. The partial derivatives of the aerodynamic force and moment coefficients can be obtained from equations (1), (3), (5), (6) and (7) which can be combined to define the coefficients in terms of the parameters,  $P_i$ . This yields the following results,

$$\frac{\partial C_D}{\partial P_i} = - \frac{\partial C_x}{\partial P_i} \cos\xi - \frac{\partial C_z}{\partial P_i} \sin\xi + C_L \frac{\partial \xi}{\partial P_i}$$

$$\frac{\partial C_L}{\partial P_i} = \frac{\partial C_x}{\partial P_i} \sin\xi - \frac{\partial C_z}{\partial P_i} \cos\xi - C_D \frac{\partial \xi}{\partial P_i}$$

From the expression for the yaw of repose it follows that

$$\begin{aligned} \frac{\partial \xi_R}{\partial P_i} &= (2I_x/\rho S d C_m \xi^5) \left\{ V_p_s V_1 \frac{\partial g_3}{\partial P_i} + V_p_s \frac{\partial V_1}{\partial P_i} g_3 \right. \\ &\quad \left. + V \frac{\partial p_s}{\partial P_i} V_1 g_3 - 4 \frac{\partial V}{\partial P_i} p_s V_1 g_3 \right\}. \end{aligned}$$

Finally, using the parametric representations of the aerodynamic coefficients, we obtain the results, for the axial force coefficient,

$$\begin{aligned}\frac{\partial C_x}{\partial P_i} = & (1+s)(\delta_{9i} + \delta_{10i}r + \delta_{11i}r^2) + (1-s)(\delta_{12i} + \delta_{13i}r + \delta_{14i}r^2) \\ & + (P_q + P_{10}r + P_{11}r^2 - P_{12} - P_{13}r - P_{14}r^2) \frac{\partial s}{\partial P_i} \\ & + [(1+s)(P_{10} + 2P_{11}r) + (1-s)(P_{13} + 2P_{14}r)] \frac{\partial r}{\partial P_i}\end{aligned}$$

where

$$\frac{\partial s}{\partial P_i} = [P_8^2 \frac{\partial r}{\partial P_i} + r(r^2 - 1) P_8 \delta_{8i}] [(1 - P_8^2) r^2 + P_8^2]^{-3/2},$$

$$\frac{\partial r}{\partial P_i} = [2MP_7^2 \frac{\partial M}{\partial P_i} - 2M^2 P_7 \delta_{7i}] [M^2 + P_7^2]^{-2}$$

and

$$\frac{\partial M}{\partial P_i} \approx \frac{1}{a} \frac{\partial V}{\partial P_i}$$

Similarly for the normal force coefficient, we obtain

$$\frac{\partial C_z}{\partial P_i} = \frac{\partial C_{z\xi}}{\partial P_i} + C_{z\xi} \frac{\partial \xi}{\partial P_i}$$

$$\begin{aligned}\frac{\partial C_{z\xi}}{\partial P_i} = & (1+f)(\delta_{17i} + \delta_{18i}g^2) + (1-f)(\delta_{20i} + \delta_{21i}g + \delta_{22i}g^2) \\ & + (P_{17} + P_{18}g + P_{19}g^2 - P_{20} - P_{21}g - P_{22}g^2) \frac{\partial f}{\partial P_i} \\ & + [(1+f)(P_{18} + 2P_{19}g) + (1-f)(P_{21} + 2P_{22}g)] \frac{\partial g}{\partial P_i}\end{aligned}$$

where

$$\frac{\partial f}{\partial P_i} = [P_{16}^2 \frac{\partial g}{\partial P_i} + g(g^2 - 1) P_{16} \delta_{16i}] [(1 - P_{16}^2) g^2 + P_{16}^2]^{-3/2}$$

$$\frac{\partial f}{\partial P_i} = [2MP_{15}^2 \frac{\partial M}{\partial P_i} - 2M^2 P_{15} \delta_{15i}] [M^2 + P_{15}^2]^{-2}$$

While the rolling moment coefficient representation yields the result,

$$\frac{\partial C_t}{\partial P_i}^P = (\delta_{23i} + \delta_{24i} M + \delta_{25i} M^2 + \delta_{26i} M^3) \\ + (P_{24} + 2P_{25}M + 3P_{26}M^2) \frac{\partial M}{\partial P_i} .$$

The equations in this appendix embody all the information necessary for calculating those partial derivatives required by the parameter estimation algorithm to estimate corrections for the initial estimates of the parameter values. If all 27 parameters are allowed to vary, the equations (15) to (18) represent 189 simultaneous, first order, ordinary, differential equations. So, including the equations (2), which define the mathematical model, we find that for each iteration of the parameter estimation algorithm 197 first order equations must be solved.

APPENDIX IV

#### LISTING OF PROGRAM SHELLS











```

      C IF(IND.EQ.1) GO TO 120
      C I=N1
      C GO TO 110
      C HAS THE NEAR DATA POINT BEEN REACHED
      C 120 IF(I.GT.NMAX) GO TO 100
      C ESTIMATE STATE VARIABLES AND PARTIAL DERIVATIVES
      C DO 130 J=1,N
      130 PI(J)=0.0
      C DO 150 I=1,27
      C IF(J.GE.PI(I).GT.0.0) GO TO 150
      C DO 160 J=2,5
      160 2*(J*J*ODER(I))+J-4)*PI(17*I+J)
      C 150 CONTINUE
      C OUTPUT RESULTS OF INTEGRATION STEP IF REQUIRED
      C 170 IF(IND.EQ.0).OR.(ITER.GE.ITERN)) AND (INPLNT.NE.0.)
      C WRITE (6,1) (PI(I),I=1,5)
      C RETURN
      1 FORMAT(1X,F7.3,F9.1,2F9.1,F11.2)
      END

      SUBROUTINE SINVIA(N,EPS,IER)
      IMPLICIT REAL *8 (A-H,O-Z)
      C ROUTINE FROM SYSTEM/360 SCIENTIFIC SUBROUTINE PACKAGE
      C FOR INVERTING A POSITIVE DEFINITE SYMMETRIC MATRIX
      C DIMENSION A(1,1)
      CALL MFSD (A,N,EPS,IER)
      IF(IER.LT.0) RETURN
      IPVANE(N+1)/2
      INPLTV
      DO 600 I=1,N
      DINPLTV=A/I*IPV
      A(I,PV)=DINPLTV
      600 CONTINUE
      L=IPV-1
      L1=L-1
      L2=L-2
      DO 500 I=L1,N
      IPV=IPV+1
      L=L-1
      500 CONTINUE
      L=L-1
      L1=L-1
      L2=L-2
      DO 400 I=L1,N
      IPV=IPV+1
      L=L-1
      400 CONTINUE
      L=L-1
      L1=L-1
      L2=L-2
      DO 300 I=L1,N
      IPV=IPV+1
      L=L-1
      300 CONTINUE
      A(I,J)=A(I,J)-IPV
      400 J=1-N
      500 IPV=IPV-IN
      600 IN=IN-1
      IPV=IPV+1
      J=IPV
      DO 800 I=1,N
      IPV=IPV+1
      800 CONTINUE
      L=L-1
      L1=L-1
      L2=L-2
      DO 700 I=L1,N
      IPV=IPV+1
      L=L-1
      700 L=L-1
      800 J=1-N
      900 J=1-N
      END

      SUBROUTINE SOLVE(INP,SIGMA,NPTS)
      IMPLICIT REAL *8 (A-H,O-Z)
      C USFS THE SCIENTIFIC SUBROUTINE PACKAGE'S 'SINV' AND 'MFSD'. TR
      C SOLVE THE NORMAL EQUATIONS
      C ASSUMES MATRIX PSI IS POSITIVE DEFINITE SYMMETRIC
      DO 100 I=1,N
      DO 200 J=1,N
      DO 300 K=1,N
      DO 400 L=1,N
      DO 500 M=1,N
      DO 600 N=1,N
      DO 700 O=1,N
      DO 800 P=1,N
      DO 900 Q=1,N
      DO 1000 R=1,N
      DO 1100 S=1,N
      DO 1200 T=1,N
      DO 1300 U=1,N
      DO 1400 V=1,N
      DO 1500 W=1,N
      DO 1600 X=1,N
      DO 1700 Y=1,N
      DO 1800 Z=1,N
      DO 1900 AA=1,N
      DO 2000 BB=1,N
      DO 2100 CC=1,N
      DO 2200 DD=1,N
      DO 2300 EE=1,N
      DO 2400 FF=1,N
      DO 2500 GG=1,N
      DO 2600 HH=1,N
      DO 2700 II=1,N
      DO 2800 JJ=1,N
      DO 2900 KK=1,N
      DO 3000 LL=1,N
      DO 3100 MM=1,N
      DO 3200 NN=1,N
      DO 3300 OO=1,N
      DO 3400 PP=1,N
      DO 3500 QQ=1,N
      DO 3600 RR=1,N
      DO 3700 SS=1,N
      DO 3800 TT=1,N
      DO 3900 UU=1,N
      DO 4000 VV=1,N
      DO 4100 WW=1,N
      DO 4200 XX=1,N
      DO 4300 YY=1,N
      DO 4400 ZZ=1,N
      DO 4500 AAA=1,N
      DO 4600 BBB=1,N
      DO 4700 CCC=1,N
      DO 4800 DDD=1,N
      DO 4900 EEE=1,N
      DO 5000 FFF=1,N
      DO 5100 GGG=1,N
      DO 5200 HHH=1,N
      DO 5300 III=1,N
      DO 5400 JJJ=1,N
      DO 5500 KKK=1,N
      DO 5600 LLL=1,N
      DO 5700 MMM=1,N
      DO 5800 NNN=1,N
      DO 5900 OOO=1,N
      DO 6000 PPP=1,N
      DO 6100 QQQ=1,N
      DO 6200 RRR=1,N
      DO 6300 SSS=1,N
      DO 6400 TTT=1,N
      DO 6500 UUU=1,N
      DO 6600 VVV=1,N
      DO 6700 WWW=1,N
      DO 6800 XXX=1,N
      DO 6900 YYY=1,N
      DO 7000 ZZZ=1,N
      DO 7100 AAAA=1,N
      DO 7200 BBBB=1,N
      DO 7300 CCCC=1,N
      DO 7400 DDDD=1,N
      DO 7500 EEEE=1,N
      DO 7600 FFFF=1,N
      DO 7700 GGGG=1,N
      DO 7800 HHHH=1,N
      DO 7900 IIII=1,N
      DO 8000 JJJJ=1,N
      DO 8100 KKKK=1,N
      DO 8200 LLLL=1,N
      DO 8300 MAAA=1,N
      DO 8400 BBBB=1,N
      DO 8500 CCCC=1,N
      DO 8600 DDDD=1,N
      DO 8700 EEEE=1,N
      DO 8800 FFFF=1,N
      DO 8900 GGGG=1,N
      DO 9000 HHHH=1,N
      DO 9100 IIII=1,N
      DO 9200 JJJJ=1,N
      DO 9300 KKKK=1,N
      DO 9400 LLLL=1,N
      DO 9500 MAAA=1,N
      DO 9600 BBBB=1,N
      DO 9700 CCCC=1,N
      DO 9800 DDDD=1,N
      DO 9900 EEEE=1,N
      DO 10000 FFFF=1,N
      DO 10100 GGGG=1,N
      DO 10200 HHHH=1,N
      DO 10300 IIII=1,N
      DO 10400 JJJJ=1,N
      DO 10500 KKKK=1,N
      DO 10600 LLLL=1,N
      DO 10700 MAAA=1,N
      DO 10800 BBBB=1,N
      DO 10900 CCCC=1,N
      DO 11000 DDDD=1,N
      DO 11100 EEEE=1,N
      DO 11200 FFFF=1,N
      DO 11300 GGGG=1,N
      DO 11400 HHHH=1,N
      DO 11500 IIII=1,N
      DO 11600 JJJJ=1,N
      DO 11700 KKKK=1,N
      DO 11800 LLLL=1,N
      DO 11900 MAAA=1,N
      DO 12000 BBBB=1,N
      DO 12100 CCCC=1,N
      DO 12200 DDDD=1,N
      DO 12300 EEEE=1,N
      DO 12400 FFFF=1,N
      DO 12500 GGGG=1,N
      DO 12600 HHHH=1,N
      DO 12700 IIII=1,N
      DO 12800 JJJJ=1,N
      DO 12900 KKKK=1,N
      DO 13000 LLLL=1,N
      DO 13100 MAAA=1,N
      DO 13200 BBBB=1,N
      DO 13300 CCCC=1,N
      DO 13400 DDDD=1,N
      DO 13500 EEEE=1,N
      DO 13600 FFFF=1,N
      DO 13700 GGGG=1,N
      DO 13800 HHHH=1,N
      DO 13900 IIII=1,N
      DO 14000 JJJJ=1,N
      DO 14100 KKKK=1,N
      DO 14200 LLLL=1,N
      DO 14300 MAAA=1,N
      DO 14400 BBBB=1,N
      DO 14500 CCCC=1,N
      DO 14600 DDDD=1,N
      DO 14700 EEEE=1,N
      DO 14800 FFFF=1,N
      DO 14900 GGGG=1,N
      DO 15000 HHHH=1,N
      DO 15100 IIII=1,N
      DO 15200 JJJJ=1,N
      DO 15300 KKKK=1,N
      DO 15400 LLLL=1,N
      DO 15500 MAAA=1,N
      DO 15600 BBBB=1,N
      DO 15700 CCCC=1,N
      DO 15800 DDDD=1,N
      DO 15900 EEEE=1,N
      DO 16000 FFFF=1,N
      DO 16100 GGGG=1,N
      DO 16200 HHHH=1,N
      DO 16300 IIII=1,N
      DO 16400 JJJJ=1,N
      DO 16500 KKKK=1,N
      DO 16600 LLLL=1,N
      DO 16700 MAAA=1,N
      DO 16800 BBBB=1,N
      DO 16900 CCCC=1,N
      DO 17000 DDDD=1,N
      DO 17100 EEEE=1,N
      DO 17200 FFFF=1,N
      DO 17300 GGGG=1,N
      DO 17400 HHHH=1,N
      DO 17500 IIII=1,N
      DO 17600 JJJJ=1,N
      DO 17700 KKKK=1,N
      DO 17800 LLLL=1,N
      DO 17900 MAAA=1,N
      DO 18000 BBBB=1,N
      DO 18100 CCCC=1,N
      DO 18200 DDDD=1,N
      DO 18300 EEEE=1,N
      DO 18400 FFFF=1,N
      DO 18500 GGGG=1,N
      DO 18600 HHHH=1,N
      DO 18700 IIII=1,N
      DO 18800 JJJJ=1,N
      DO 18900 KKKK=1,N
      DO 19000 LLLL=1,N
      DO 19100 MAAA=1,N
      DO 19200 BBBB=1,N
      DO 19300 CCCC=1,N
      DO 19400 DDDD=1,N
      DO 19500 EEEE=1,N
      DO 19600 FFFF=1,N
      DO 19700 GGGG=1,N
      DO 19800 HHHH=1,N
      DO 19900 IIII=1,N
      DO 20000 JJJJ=1,N
      DO 20100 KKKK=1,N
      DO 20200 LLLL=1,N
      DO 20300 MAAA=1,N
      DO 20400 BBBB=1,N
      DO 20500 CCCC=1,N
      DO 20600 DDDD=1,N
      DO 20700 EEEE=1,N
      DO 20800 FFFF=1,N
      DO 20900 GGGG=1,N
      DO 21000 HHHH=1,N
      DO 21100 IIII=1,N
      DO 21200 JJJJ=1,N
      DO 21300 KKKK=1,N
      DO 21400 LLLL=1,N
      DO 21500 MAAA=1,N
      DO 21600 BBBB=1,N
      DO 21700 CCCC=1,N
      DO 21800 DDDD=1,N
      DO 21900 EEEE=1,N
      DO 22000 FFFF=1,N
      DO 22100 GGGG=1,N
      DO 22200 HHHH=1,N
      DO 22300 IIII=1,N
      DO 22400 JJJJ=1,N
      DO 22500 KKKK=1,N
      DO 22600 LLLL=1,N
      DO 22700 MAAA=1,N
      DO 22800 BBBB=1,N
      DO 22900 CCCC=1,N
      DO 23000 DDDD=1,N
      DO 23100 EEEE=1,N
      DO 23200 FFFF=1,N
      DO 23300 GGGG=1,N
      DO 23400 HHHH=1,N
      DO 23500 IIII=1,N
      DO 23600 JJJJ=1,N
      DO 23700 KKKK=1,N
      DO 23800 LLLL=1,N
      DO 23900 MAAA=1,N
      DO 24000 BBBB=1,N
      DO 24100 CCCC=1,N
      DO 24200 DDDD=1,N
      DO 24300 EEEE=1,N
      DO 24400 FFFF=1,N
      DO 24500 GGGG=1,N
      DO 24600 HHHH=1,N
      DO 24700 IIII=1,N
      DO 24800 JJJJ=1,N
      DO 24900 KKKK=1,N
      DO 25000 LLLL=1,N
      DO 25100 MAAA=1,N
      DO 25200 BBBB=1,N
      DO 25300 CCCC=1,N
      DO 25400 DDDD=1,N
      DO 25500 EEEE=1,N
      DO 25600 FFFF=1,N
      DO 25700 GGGG=1,N
      DO 25800 HHHH=1,N
      DO 25900 IIII=1,N
      DO 26000 JJJJ=1,N
      DO 26100 KKKK=1,N
      DO 26200 LLLL=1,N
      DO 26300 MAAA=1,N
      DO 26400 BBBB=1,N
      DO 26500 CCCC=1,N
      DO 26600 DDDD=1,N
      DO 26700 EEEE=1,N
      DO 26800 FFFF=1,N
      DO 26900 GGGG=1,N
      DO 27000 HHHH=1,N
      DO 27100 IIII=1,N
      DO 27200 JJJJ=1,N
      DO 27300 KKKK=1,N
      DO 27400 LLLL=1,N
      DO 27500 MAAA=1,N
      DO 27600 BBBB=1,N
      DO 27700 CCCC=1,N
      DO 27800 DDDD=1,N
      DO 27900 EEEE=1,N
      DO 28000 FFFF=1,N
      DO 28100 GGGG=1,N
      DO 28200 HHHH=1,N
      DO 28300 IIII=1,N
      DO 28400 JJJJ=1,N
      DO 28500 KKKK=1,N
      DO 28600 LLLL=1,N
      DO 28700 MAAA=1,N
      DO 28800 BBBB=1,N
      DO 28900 CCCC=1,N
      DO 29000 DDDD=1,N
      DO 29100 EEEE=1,N
      DO 29200 FFFF=1,N
      DO 29300 GGGG=1,N
      DO 29400 HHHH=1,N
      DO 29500 IIII=1,N
      DO 29600 JJJJ=1,N
      DO 29700 KKKK=1,N
      DO 29800 LLLL=1,N
      DO 29900 MAAA=1,N
      DO 30000 BBBB=1,N
      DO 30100 CCCC=1,N
      DO 30200 DDDD=1,N
      DO 30300 EEEE=1,N
      DO 30400 FFFF=1,N
      DO 30500 GGGG=1,N
      DO 30600 HHHH=1,N
      DO 30700 IIII=1,N
      DO 30800 JJJJ=1,N
      DO 30900 KKKK=1,N
      DO 31000 LLLL=1,N
      DO 31100 MAAA=1,N
      DO 31200 BBBB=1,N
      DO 31300 CCCC=1,N
      DO 31400 DDDD=1,N
      DO 31500 EEEE=1,N
      DO 31600 FFFF=1,N
      DO 31700 GGGG=1,N
      DO 31800 HHHH=1,N
      DO 31900 IIII=1,N
      DO 32000 JJJJ=1,N
      DO 32100 KKKK=1,N
      DO 32200 LLLL=1,N
      DO 32300 MAAA=1,N
      DO 32400 BBBB=1,N
      DO 32500 CCCC=1,N
      DO 32600 DDDD=1,N
      DO 32700 EEEE=1,N
      DO 32800 FFFF=1,N
      DO 32900 GGGG=1,N
      DO 33000 HHHH=1,N
      DO 33100 IIII=1,N
      DO 33200 JJJJ=1,N
      DO 33300 KKKK=1,N
      DO 33400 LLLL=1,N
      DO 33500 MAAA=1,N
      DO 33600 BBBB=1,N
      DO 33700 CCCC=1,N
      DO 33800 DDDD=1,N
      DO 33900 EEEE=1,N
      DO 34000 FFFF=1,N
      DO 34100 GGGG=1,N
      DO 34200 HHHH=1,N
      DO 34300 IIII=1,N
      DO 34400 JJJJ=1,N
      DO 34500 KKKK=1,N
      DO 34600 LLLL=1,N
      DO 34700 MAAA=1,N
      DO 34800 BBBB=1,N
      DO 34900 CCCC=1,N
      DO 35000 DDDD=1,N
      DO 35100 EEEE=1,N
      DO 35200 FFFF=1,N
      DO 35300 GGGG=1,N
      DO 35400 HHHH=1,N
      DO 35500 IIII=1,N
      DO 35600 JJJJ=1,N
      DO 35700 KKKK=1,N
      DO 35800 LLLL=1,N
      DO 35900 MAAA=1,N
      DO 36000 BBBB=1,N
      DO 36100 CCCC=1,N
      DO 36200 DDDD=1,N
      DO 36300 EEEE=1,N
      DO 36400 FFFF=1,N
      DO 36500 GGGG=1,N
      DO 36600 HHHH=1,N
      DO 36700 IIII=1,N
      DO 36800 JJJJ=1,N
      DO 36900 KKKK=1,N
      DO 37000 LLLL=1,N
      DO 37100 MAAA=1,N
      DO 37200 BBBB=1,N
      DO 37300 CCCC=1,N
      DO 37400 DDDD=1,N
      DO 37500 EEEE=1,N
      DO 37600 FFFF=1,N
      DO 37700 GGGG=1,N
      DO 37800 HHHH=1,N
      DO 37900 IIII=1,N
      DO 38000 JJJJ=1,N
      DO 38100 KKKK=1,N
      DO 38200 LLLL=1,N
      DO 38300 MAAA=1,N
      DO 38400 BBBB=1,N
      DO 38500 CCCC=1,N
      DO 38600 DDDD=1,N
      DO 38700 EEEE=1,N
      DO 38800 FFFF=1,N
      DO 38900 GGGG=1,N
      DO 39000 HHHH=1,N
      DO 39100 IIII=1,N
      DO 39200 JJJJ=1,N
      DO 39300 KKKK=1,N
      DO 39400 LLLL=1,N
      DO 39500 MAAA=1,N
      DO 39600 BBBB=1,N
      DO 39700 CCCC=1,N
      DO 39800 DDDD=1,N
      DO 39900 EEEE=1,N
      DO 40000 FFFF=1,N
      DO 40100 GGGG=1,N
      DO 40200 HHHH=1,N
      DO 40300 IIII=1,N
      DO 40400 JJJJ=1,N
      DO 40500 KKKK=1,N
      DO 40600 LLLL=1,N
      DO 40700 MAAA=1,N
      DO 40800 BBBB=1,N
      DO 40900 CCCC=1,N
      DO 41000 DDDD=1,N
      DO 41100 EEEE=1,N
      DO 41200 FFFF=1,N
      DO 41300 GGGG=1,N
      DO 41400 HHHH=1,N
      DO 41500 IIII=1,N
      DO 41600 JJJJ=1,N
      DO 41700 KKKK=1,N
      DO 41800 LLLL=1,N
      DO 41900 MAAA=1,N
      DO 42000 BBBB=1,N
      DO 42100 CCCC=1,N
      DO 42200 DDDD=1,N
      DO 42300 EEEE=1,N
      DO 42400 FFFF=1,N
      DO 42500 GGGG=1,N
      DO 42600 HHHH=1,N
      DO 42700 IIII=1,N
      DO 42800 JJJJ=1,N
      DO 42900 KKKK=1,N
      DO 43000 LLLL=1,N
      DO 43100 MAAA=1,N
      DO 43200 BBBB=1,N
      DO 43300 CCCC=1,N
      DO 43400 DDDD=1,N
      DO 43500 EEEE=1,N
      DO 43600 FFFF=1,N
      DO 43700 GGGG=1,N
      DO 43800 HHHH=1,N
      DO 43900 IIII=1,N
      DO 44000 JJJJ=1,N
      DO 44100 KKKK=1,N
      DO 44200 LLLL=1,N
      DO 44300 MAAA=1,N
      DO 44400 BBBB=1,N
      DO 44500 CCCC=1,N
      DO 44600 DDDD=1,N
      DO 44700 EEEE=1,N
      DO 44800 FFFF=1,N
      DO 44900 GGGG=1,N
      DO 45000 HHHH=1,N
      DO 45100 IIII=1,N
      DO 45200 JJJJ=1,N
      DO 45300 KKKK=1,N
      DO 45400 LLLL=1,N
      DO 45500 MAAA=1,N
      DO 45600 BBBB=1,N
      DO 45700 CCCC=1,N
      DO 45800 DDDD=1,N
      DO 45900 EEEE=1,N
      DO 46000 FFFF=1,N
      DO 46100 GGGG=1,N
      DO 46200 HHHH=1,N
      DO 46300 IIII=1,N
      DO 46400 JJJJ=1,N
      DO 46500 KKKK=1,N
      DO 46600 LLLL=1,N
      DO 46700 MAAA=1,N
      DO 46800 BBBB=1,N
      DO 46900 CCCC=1,N
      DO 47000 DDDD=1,N
      DO 47100 EEEE=1,N
      DO 47200 FFFF=1,N
      DO 47300 GGGG=1,N
      DO 47400 HHHH=1,N
      DO 47500 IIII=1,N
      DO 47600 JJJJ=1,N
      DO 47700 KKKK=1,N
      DO 47800 LLLL=1,N
      DO 47900 MAAA=1,N
      DO 48000 BBBB=1,N
      DO 48100 CCCC=1,N
      DO 48200 DDDD=1,N
      DO 48300 EEEE=1,N
      DO 48400 FFFF=1,N
      DO 48500 GGGG=1,N
      DO 48600 HHHH=1,N
      DO 48700 IIII=1,N
      DO 48800 JJJJ=1,N
      DO 48900 KKKK=1,N
      DO 49000 LLLL=1,N
      DO 49100 MAAA=1,N
      DO 49200 BBBB=1,N
      DO 49300 CCCC=1,N
      DO 49400 DDDD=1,N
      DO 49500 EEEE=1,N
      DO 49600 FFFF=1,N
      DO 49700 GGGG=1,N
      DO 49800 HHHH=1,N
      DO 49900 IIII=1,N
      DO 50000 JJJJ=1,N
      DO 50100 KKKK=1,N
      DO 50200 LLLL=1,N
      DO 50300 MAAA=1,N
      DO 50400 BBBB=1,N
      DO 50500 CCCC=1,N
      DO 50600 DDDD=1,N
      DO 50700 EEEE=1,N
      DO 50800 FFFF=1,N
      DO 50900 GGGG=1,N
      DO 51000 HHHH=1,N
      DO 51100 IIII=1,N
      DO 51200 JJJJ=1,N
      DO 51300 KKKK=1,N
      DO 51400 LLLL=1,N
      DO 51500 MAAA=1,N
      DO 51600 BBBB=1,N
      DO 51700 CCCC=1,N
      DO 51800 DDDD=1,N
      DO 51900 EEEE=1,N
      DO 52000 FFFF=1,N
      DO 52100 GGGG=1,N
      DO 52200 HHHH=1,N
      DO 52300 IIII=1,N
      DO 52400 JJJJ=1,N
      DO 52500 KKKK=1,N
      DO 52600 LLLL=1,N
      DO 52700 MAAA=1,N
      DO 52800 BBBB=1,N
      DO 52900 CCCC=1,N
      DO 53000 DDDD=1,N
      DO 53100 EEEE=1,N
      DO 53200 FFFF=1,N
      DO 53300 GGGG=1,N
      DO 53400 HHHH=1,N
      DO 53500 IIII=1,N
      DO 53600 JJJJ=1,N
      DO 53700 KKKK=1,N
      DO 53800 LLLL=1,N
      DO 53900 MAAA=1,N
      DO 54000 BBBB=1,N
      DO 54100 CCCC=1,N
      DO 54200 DDDD=1,N
      DO 54300 EEEE=1,N
      DO 54400 FFFF=1,N
      DO 54500 GGGG=1,N
      DO 54600 HHHH=1,N
      DO 54700 IIII=1,N
      DO 54800 JJJJ=1,N
      DO 54900 KKKK=1,N
      DO 55000 LLLL=1,N
      DO 55100 MAAA=1,N
      DO 55200 BBBB=1,N
      DO 55300 CCCC=1,N
      DO 55400 DDDD=1,N
      DO 55500 EEEE=1,N
      DO 55600 FFFF=1,N
      DO 55700 GGGG=1,N
      DO 55800 HHHH=1,N
      DO 55900 IIII=1,N
      DO 56000 JJJJ=1,N
      DO 56100 KKKK=1,N
      DO 56200 LLLL=1,N
      DO 56300 MAAA=1,N
      DO 56400 BBBB=1,N
      DO 56500 CCCC=1,N
      DO 56600 DDDD=1,N
      DO 56700 EEEE=1,N
      DO 56800 FFFF=1,N
      DO 56900 GGGG=1,N
      DO 57000 HHHH=1,N
      DO 57100 IIII=1,N
      DO 57200 JJJJ=1,N
      DO 57300 KKKK=1,N
      DO 57400 LLLL=1,N
      DO 57500 MAAA=1,N
      DO 57600 BBBB=1,N
      DO 57700 CCCC=1,N
      DO 57800 DDDD=1,N
      DO 57900 EEEE=1,N
      DO 58000 FFFF=1,N
      DO 58100 GGGG=1,N
      DO 58200 HHHH=1,N
      DO 58300 IIII=1,N
      DO 58400 JJJJ=1,N
      DO 58500 KKKK=1,N
      DO 58600 LLLL=1,N
      DO 58700 MAAA=1,N
      DO 58800 BBBB=1,N
      DO 58900 CCCC=1,N
      DO 59000 DDDD=1,N
      DO 59100 EEEE=1,N
      DO 59200 FFFF=1,N
      DO 59300 GGGG=1,N
      DO 59400 HHHH=1,N
      DO 59500 IIII=1,N
      DO 59600 JJJJ=1,N
      DO 59700 KKKK=1,N
      DO 59800 LLLL=1,N
      DO 59900 MAAA=1,N
      DO 60000 BBBB=1,N
      DO 60100 CCCC=1,N
      DO 60200 DDDD=1,N
      DO 60300 EEEE=1,N
      DO 60400 FFFF=1,N
      DO 60500 GGGG=1,N
      DO 60600 HHHH=1,N
      DO 60700 IIII=1,N
      DO 60800 JJJJ=1,N
      DO 60900 KKKK=1,N
      DO 61000 LLLL=1,N
      DO 61100 MAAA=1,N
      DO 61200 BBBB=1,N
      DO 61300 CCCC=1,N
      DO 61400 DDDD=1,N
      DO 61500 EEEE=1,N
      DO 61600 FFFF=1,N
      DO 61700 GGGG=1,N
      DO 61800 HHHH=1,N
      DO 61900 IIII=1,N
      DO 62000 JJJJ=1,N
      DO 62100 KKKK=1,N
      DO 62200 LLLL=1,N
      DO 62300 MAAA=1,N
      DO 62400 BBBB=1,N
      DO 62500 CCCC=1,N
      DO 62600 DDDD=1,N
      DO 62700 EEEE=1,N
      DO 62800 FFFF=1,N
      DO 62900 GGGG=1,N
      DO 63000 HHHH=1,N
      DO 63100 IIII=1,N
      DO 63200 JJJJ=1,N
      DO 63300 KKKK=1,N
      DO 63400 LLLL=1,N
      DO 63500 MAAA=1,N
      DO 63600 BBBB=1,N
      DO 63700 CCCC=1,N
      DO 63800 DDDD=1,N
      DO 63900 EEEE=1,N
      DO 64000 FFFF=1,N
      DO 64100 GGGG=1,N
      DO 64200 HHHH=1,N
      DO 64300 IIII=1,N
      DO 64400 JJJJ=1,N
      DO 64500 KKKK=1,N
      DO 64600 LLLL=1,N
      DO 64700 MAAA=1,N
      DO 64800 BBBB=1,N
      DO 64900 CCCC=1,N
      DO 65000 DDDD=1,N
      DO 65100 EEEE=1,N
      DO 65200 FFFF=1,N
      DO 65300 GGGG=1,N
      DO 65400 HHHH=1,N
      DO 65500 IIII=1,N
      DO 65600 JJJJ=1,N
      DO 65700 KKKK=1,N
      DO 65800 LLLL=1,N
      DO 65900 MAAA=1,N
      DO 66000 BBBB=1,N
      DO 66100 CCCC=1,N
      DO 66200 DDDD=1,N
      DO 66300 EEEE=1,N
      DO 66400 FFFF=1,N
      DO 66500 GGGG=1,N
      DO 66600 HHHH=1,N
      DO 66700 IIII=1,N
      DO 66800 JJJJ=1,N
      DO 66900 KKKK=1,N
      DO 67000 LLLL=1,N
      DO 67100 MAAA=1,N
      DO 67200 BBBB=1,N
      DO 67300 CCCC=1,N
      DO 67400 DDDD=1,N
      DO 67500 EEEE=1,N
      DO 67600 FFFF=1,N
      DO 67700 GGGG=1,N
      DO 67800 HHHH=1,N
      DO 67900 IIII=1,N
      DO 68000 JJJJ=1,N
      DO 68100 KKKK=1,N
      DO 68200 LLLL=1,N
      DO 68300 MAAA=1,N
      DO 68400 BBBB=1,N
      DO 68500 CCCC=1,N
      DO 68600 DDDD=1,N
      DO 68700 EEEE=1,N
      DO 68800 FFFF=1,N
      DO 68900 GGGG=1,N
      DO 69000 HHHH=1,N
      DO 69100 IIII=1,N
      DO 69200 JJJJ=1,N
      DO 69300 KKKK=1,N
      DO 69400 LLLL=1,N
      DO 69500 MAAA=1,N
      DO 69600 BBBB=1,N
      DO 69700 CCCC=1,N
      DO 69800 DDDD=1,N
      DO 69900 EEEE=1,N
      DO 70000 FFFF=1,N
      DO 70100 GGGG=1,N
      DO 70200 HHHH=1,N
      DO 70300 IIII=1,N
      DO 70400 JJJJ=1,N
      DO 70500 KKKK=1,N
      DO 70600 LLLL=1,N
      DO 70700 MAAA=1,N
      DO 70800 BBBB=1,N
      DO 70900 CCCC=1,N
      DO 71000 DDDD=1,N
      DO 71100 EEEE=1,N
      DO 71200 FFFF=1,N
      DO 71300 GGGG=1,N
      DO 71400 HHHH=1,N
      DO 71500 IIII=1,N
      DO 71600 JJJJ=1,N
      DO 71700 KKKK=1,N
      DO 71800 LLLL=1,N
      DO 71900 MAAA=1,N
      DO 72000 BBBB=1,N
      DO 72100 CCCC=1,N
      DO 72200 DDDD=1,N
      DO 72300 EEEE=1,N
      DO 72400 FFFF=1,N
      DO 72500 GGGG=1,N
      DO 72600 HHHH=1,N
      DO 72700 IIII=1,N
      DO 72800 JJJJ=1,N
      DO 72900 KKKK=1,N
      DO 73000 LLLL=1,N
      DO 73100 MAAA=1,N
      DO 73200 BBBB=1,N
      DO 73300 CCCC=1,N
      DO 73400 DDDD=1,N
      DO 73500 EEEE=1,N
      DO 73600 FFFF=1,N
      DO 73700 GGGG=1,N
      DO 73800 HHHH=1,N
      DO 73900 IIII=1,N
      DO 74000 JJJJ=1,N
      DO 74100 KKKK=1,N
      DO 74200 LLLL=1,N
      DO 
```

## APPENDIX V

## YAWSONDE CALIBRATION

Consider the yawsonde depicted in figure 4. It consists of two sun slits at angles  $\gamma_1$  and  $\gamma_2$  to the longitudinal axis of the shell as shown in figure 4(c). The centres of the slits are separated by rotation about the shell longitudinal axis through an angle  $\beta$  in figure 4(b). When the shell rotates during flight a train of pulses of opposite polarity like the train in figure 4(d) with period  $T$ , the roll period, is emitted by each sensor. The relationship connecting the time,  $\tau$ , between pulses of opposite polarity and the complementary solar aspect angle,  $\sigma_N$  in figure 4(a), is the calibration curve of the yawsonde. This appendix is concerned with the derivation of that curve. It is assumed during the derivation that the shell does not pitch or yaw so that the direction of the longitudinal axis remains constant. The errors arising from this assumption will not be significant if the roll rate is much greater than the nutation and precession rates, as is generally the case.

If the sun is detected by sensor 1 of the yawsonde then it lies in the half plane defined by the relations,

$$x'' \sin \gamma_1 - y'' \cos \gamma_1 = 0, z'' > 0 \quad (19)$$

where the axes system  $Sx''y''z''$  is fixed in the shell and rotates with it;  $Sx''$  is forward along the shell axis,  $Sz''$  is outwards through the centre of sensor 1 and  $Sy''$  completes a right handed set as shown in figure 4. The sun is likewise detected by sensor 2 when it lies in the half plane defined by the relations

$$\begin{aligned} x'' \sin \gamma_2 - y'' \cos \gamma_2 \cos \beta - z'' \cos \gamma_2 \sin \beta &= 0, \\ z'' \cos \beta - y'' \sin \beta &\geq 0. \end{aligned} \quad (20)$$

If the angular velocity component about the longitudinal axis is  $p_s$ , then

$$2\pi p_s = 1/T,$$

and the direction cosines of the sun in terms of the complementary solar aspect angle are

$$(\sin \sigma_N, \cos \sigma_N \sin p_s t, \cos \sigma_N \cos p_s t) \quad (21)$$

where  $t$  is time measured from when the sun is in the  $Sx''z''$  plane. Hence using equations (19) to (21), the complementary solar aspect angle can be determined from the measured time interval,  $\tau$ , by the relation

$$\begin{aligned} \tan \sigma_N &= - \sin (2\pi\tau/T + \beta) / [\tan^2 \gamma_1 + \tan^2 \gamma_2 \\ &\quad - 2 \tan \gamma_1 \tan \gamma_2 \cos (2\pi\tau/T + \beta)]^{1/2} \end{aligned} \quad (22)$$

In order to obtain a symmetrical calibration curve and make optimum use of the yawsonde, the nominal values which are usually chosen for the parameters in equation (22) are  $\gamma_1 = -\gamma_2 = \gamma$  where  $\gamma$  is generally between  $\pi/6$  and  $\pi/4$ , and

$\beta = \pi$ . If we substitute into equation (22) for  $\gamma_1$ ,  $\gamma_2$  and  $\beta$  we find that

$$\tan \sigma_N = \cos (\pi\tau/T) / \tan \gamma. \quad (23)$$

It follows from the expression (23), since  $0 < \tau < T$ , that the range of complementary solar aspect angles which can be measured by the yawsonde is

$$- (\pi/2 - \gamma) \leq \sigma_N \leq + (\pi/2 - \gamma). \quad (24)$$

Figure 5 shows a typical yawsonde calibration curve of the type described by equation (23) with  $\gamma = \pi/4$ . The curve is approximately linear over much of its range. The extremities of the curve are not of much interest since experiments will generally be designed to avoid this area for two reasons. Firstly pulses from the two sensors will tend to interfere and the experimental record will be difficult to decipher. Secondly, the finite dimensions of the sun slits, which have been ignored in deriving the calibration curve (22), will make the calibration invalid for values of  $\tau/T$  approaching 0 or 1.

The slope of the curve at  $\tau/T = 1/2$  will be a good measure of the overall sensitivity of the yawsonde, that is,

$$d\sigma_N | d(\tau/T) |_{\tau/T=1/2} = -\pi/\tan\gamma.$$

Clearly it is necessary to compromise when choosing a value of  $\gamma$ , the angle each slit makes with the longitudinal axis of the shell. If  $\gamma$  is much greater than  $\pi/4$  the sensitivity given in this equation begins to fall away rapidly. However, the value of  $\gamma$  should be as large as possible to provide an adequate range of measurement as defined by relation (24), particularly since it is not practical to use the total range for  $\tau$ , from 0 to  $T$ .

## APPENDIX VI

## LISTING OF PROGRAM YAWCAL

THIS PAGE IS BEST QUALITY PRACTICAL  
FROM COPY BURNISHED TO DDC

APPENDIX VII  
SOLAR ASPECT ANGLE

In order to use the data on the complementary solar aspect angle which is measured with the yawsonde one must know the position of the sun. The solution for the azimuth and elevation of the sun in range axes is given in reference 14, obtained using the method given in reference 15. The derivation uses the sidereal time,  $(ST)_0$ , corresponding to the Universal or Greenwich mean time at which the position of the sun is required. The sidereal time is the Hour Angle of the first point of Aries. The right ascension, RA, and the declination,  $\delta$ , of the sun are also used. All three can be obtained from the Astronomical Ephemeris(ref.16) by interpolating between values given for each variable at 0 hours Universal Time, UT. Then, the local sidereal time,

$$LST = (ST)_0 + \frac{366.2422}{365.2422} UT - \Phi,$$

where  $\Phi$  is the longitude of the shell, and the hour angle of the sun,

$$H = LST - RA,$$

so that the azimuth,  $\psi_s$ , and elevation,  $\theta_s$ , of the sun in earth axes are given by

$$\begin{aligned}\sin \theta_s &= \sin \delta \sin \Theta + \cos \delta \cos \Theta \cos H \\ \cos \psi_s \cos \theta_s &= \sin \delta \cos \Theta - \cos \delta \sin \Theta \cos H \\ \sin \psi_s \cos \theta_s &= \sin H \cos \delta.\end{aligned}$$

It must be remembered that the azimuth,  $\psi_s$ , is measured relative to true north, so that if  $\Psi$  is the azimuth of the shell relative to true north, the complementary solar aspect angle is given by

$$\sin \sigma_N = \cos \theta_s \cos \psi_s \cos \theta \cos \Psi + \cos \theta_s \sin \psi_s \cos \theta \sin \Psi + \sin \theta_s \sin \theta$$

where  $\theta$  is the angle of elevation of the shell. The angle  $\Psi$  has two components,  $\Psi_0$ , the bearing of the line of fire of the shell and  $\psi$ , the angle of azimuth of the shell relative to the line of fire, so that  $\Psi = \Psi_0 + \psi$ . The above expression can be rearranged to give

$$\sin \sigma_N = \cos \theta_s \cos \theta \cos (\psi_s - \Psi) + \sin \theta \sin \theta_s \quad (25)$$

so that the origin used to measure the angles of azimuth is no longer relevant and the most convenient origin can be used. The expression (25) is needed both for trials planning and data analysis. For trials planning purposes, it is generally convenient to refer both azimuth angles to true north because the bearing of the line of fire is used to approximate the azimuth of the shell. However, in analysing flight data it is more convenient to refer azimuth measurements to range axes. Details of how the expression (25) is used are given in Section 4.

## APPENDIX VIII LISTING OF PROGRAM A

```

C ELEVATION AND AZIMUTH
C SINH(SIN(H))
C COS(H*COSH)
C SIN(SIN(LAMBDA))
C COS(LAMBDA)
C SIN(SIN(D))
C SIN(SIN(COS(L-COS(D*SIN(L*COSH
C SUN(SIN(COS(COS(SIN(COS(SIN(L*COSH
C SUNH(SINH(SINH(COSD(COSL(COSH
C PLASIN((SUNH(SUNL)*ODD
C AZ*AN2((SUNH(SUNL)*ODD
C ITIME(1,TIME(1)
C ITIME(11,1,TIME(1)
C ITIME(11,100,TIME(1),60,*XC15
C WRITE(16,9) ITIME(1),AZ,PL,SUNH,SUNH,SUNH
C ESTIMATE COMPLEMENTARY SOLAR ASPECT ANGLE
C DO 400 J=1,NLEVN
C COS(SIGN(J,1)*SIGNH(J)*SIGNH(J)+SIGNH(J))
C 400 SIGNH(J,1)*ACOS(COSSTG(-0.5*PI))=CON
C 400 CONTINUE
C DO 550 J=1,NLEVN
C 550 THETA(J)=THETA(J)*DOC
C WRITE(6,11) (ITIME(1),1*I,NTIMES)
C WRITE(6,12) (ITIME(1),1*I,NTIMES)
C DO 600 J=1,NLEVN
C 600 WRITE(6,13) THETA(J)*(SIGNH(J,1),I=1,NTIMES)
C DO 700 J=1,10
C 700 WRITE(J,10)
C DO 800 J=1,NTIMES
C 800 WRITE(J,10)
C DO 900 J=1,5
C 900 GLARE(J,LT1,NTIMES(J))
C GLARE(J,1)*20.
C CALL GRAPH(GLARE,XAXIS,YAXIS,YAXIS,TA,NC,CC,THETA,0.0001440
C NO 0.00 THETA(N,E,E),THETA(N,E,F),THETA(N,G),THETA,
C NH,HH,THETA(N,H),THETA(N,H,J),THETA)
C CALL ENDR
C STOP
C
C 1 FORMAT(1B4)
C 2 FORMAT(1I10 SOLAR ASPECT ANGLE FOR 1.16A4)
C 3 FORMAT(10.1C)
C 4 FORMAT(10.1C)
C *2P10.4, DEGREES/10., DEGREES/10., THE APPARENT RIGHT ASCENSIONS ARE,
C *2P10.4, DEGREES/10., DEGREES/10., AND THE APPARENT DECLINATIONS ARE,
C *2P10.4, DEGREES/10., DEGREES/10.

```

## APPENDIX IX

## PARTIAL DERIVATIVES WITH RESPECT TO PARAMETERS FOR YAWSONDE

The parameter estimation algorithm which is used to analyse the yawsonde data requires, as input, values of partial derivatives of the complementary solar aspect angle with respect to each of the parameters. These partial derivatives are obtained by partial differentiation of the expression (25) which defines the complementary solar aspect angle. Thus the partial derivatives are defined by the relation

$$\begin{aligned} \cos \sigma_N \frac{\partial \sigma_N}{\partial p_i} = & - [\cos \theta_s \sin \theta \cos(\psi_s - \psi) + \sin \theta_s \cos \theta] \frac{\partial \theta}{\partial p_i} \\ & + \cos \theta_s \cos \theta \sin(\psi_s - \psi) \frac{\partial \psi}{\partial p_i} \end{aligned} \quad (26)$$

The partial derivatives needed to evaluate equation (26) are obtained by numerical integration of a set of ordinary differential equations which are derived from the mathematical model equations (9) by partial differentiation. This results in the following equations being obtained

$$\begin{aligned} \frac{d}{dt} \left( \frac{\partial \psi}{\partial p_i} \right) &= \frac{\partial r}{\partial p_i} \sec \theta + r \sec \theta \tan \theta \frac{\partial \theta}{\partial p_i}, \\ \frac{d}{dt} \left( \frac{\partial \theta}{\partial p_i} \right) &= \frac{\partial q}{\partial p_i} \\ \frac{d}{dt} \left( \frac{\partial q}{\partial p_i} \right) &= [p - (I_x/I)p_s] \frac{\partial r}{\partial p_i} + r \frac{\partial p}{\partial p_i} + \left( \frac{QSD}{I} \right) \left\{ \left[ \frac{\partial C_m}{\partial \xi} \cos \phi \right. \right. \\ &\quad \left. \left. - \left( \frac{p_s d}{2V} \right) \frac{\partial C_{np}}{\partial \delta} \sin \phi + \frac{\partial C_m}{\partial \xi} \left( \frac{qd}{2V} \right) \right] \frac{\partial \xi}{\partial p_i} - [C_m \sin \phi \right. \\ &\quad \left. + C_m p \left( \frac{p_s d}{2V} \right) \cos \phi] \frac{\partial \phi}{\partial p_i} + C_m q \left( \frac{d}{2V} \right) \frac{\partial q}{\partial p_i} + \frac{\partial C_m}{\partial p_i} \cos \phi \right. \\ &\quad \left. - \frac{\partial C_{np}}{\partial p_i} \left( \frac{p_s d}{2V} \right) \sin \phi + \frac{\partial C_m}{\partial p_i} \left( \frac{qd}{2V} \right) \right], \\ \frac{d}{dt} \left( \frac{\partial r}{\partial p_i} \right) &= [-p + (I_x/I)p_s] \frac{\partial q}{\partial p_i} - q \frac{\partial p}{\partial p_i} + \left( \frac{QSD}{I} \right) \left\{ \left[ \frac{\partial C_m}{\partial \xi} \sin \phi + \frac{\partial C_{np}}{\partial \xi} \left( \frac{p_s d}{2V} \right) \cos \phi \right. \right. \\ &\quad \left. \left. + \frac{\partial C_{mq}}{\partial \xi} \left( \frac{rd}{2V} \right) \right] \frac{\partial \xi}{\partial p_i} + [C_m \cos \phi - C_{np} \left( \frac{p_s d}{2V} \right) \sin \phi] \frac{\partial \phi}{\partial p_i} + C_m q \left( \frac{d}{2V} \right) \frac{\partial q}{\partial p_i} \right. \\ &\quad \left. + \frac{\partial C_m}{\partial p_i} \sin \phi + \frac{\partial C_{np}}{\partial p_i} \left( \frac{p_s d}{2V} \right) \cos \phi + \frac{\partial C_{mq}}{\partial p_i} \left( \frac{rd}{2V} \right) \right]. \end{aligned} \quad (27)$$

By partial differentiation of equation (10) we obtain the relation

$$\frac{\partial p}{\partial p_i} = - \frac{\partial r}{\partial p_i} \tan \theta - r \sec^2 \theta \frac{\partial \theta}{\partial p_i}$$

Using the parametric representations of the aerodynamic coefficients defined in equation (12) we can obtain the following relations by partial differentiation

$$\begin{aligned}
 \frac{\partial C_m}{\partial \xi} &= p_5 + p_{12} M + 3p_6 \xi^2 + 5p_7 \xi^4, \\
 \frac{\partial C_{n_p}}{\partial \xi} &= p_8 + 3p_9 \xi^2 \\
 \frac{\partial C_{m_q}}{\partial \xi} &= 2p_{11} \xi, \\
 \frac{\partial C_m}{\partial p_i} &= (\delta_{5i} + \delta_{12i} M) \xi + \delta_{6i} \xi^3 + \delta_{7i} \xi^5, \\
 \frac{\partial C_{n_p}}{\partial p_i} &= \delta_{8i} \xi + \delta_{9i} \xi^3, \\
 \frac{\partial C_{m_q}}{\partial p_i} &= \delta_{10i} + \delta_{11i} \xi^2.
 \end{aligned} \tag{28}$$

Finally the partial derivatives of the magnitude and the orientation of the incidence can be obtained from the definitions given in equations (13) and (14), so that

$$\begin{aligned}
 \frac{\partial \xi}{\partial p_i} &= u (v \frac{\partial v}{\partial p_i} + w \frac{\partial w}{\partial p_i}) / V^2 (v^2 + w^2)^{\frac{1}{2}} - (v^2 + w^2)^{\frac{1}{2}} \frac{\partial u}{\partial p_i} / V^2 \\
 \frac{\partial \phi}{\partial p_i} &= (v \frac{\partial w}{\partial p_i} - w \frac{\partial v}{\partial p_i}) / (v^2 + w^2)
 \end{aligned} \tag{29}$$

where

$$\begin{aligned}
 \frac{\partial u}{\partial p_i} &= -w \frac{\partial \theta}{\partial p_i} + v \cos \theta \frac{\partial \psi}{\partial p_i} \\
 \frac{\partial v}{\partial p_i} &= - (V_1 \cos \psi + V_2 \sin \psi) \frac{\partial \psi}{\partial p_i} \\
 \frac{\partial w}{\partial p_i} &= u \frac{\partial \theta}{\partial p_i} + v \sin \theta \frac{\partial \psi}{\partial p_i}
 \end{aligned}$$

The relations (28) and (29) can be used to evaluate the terms in the differential equations (27). It then becomes possible to integrate the differential equations numerically and so find the values of the partial derivatives needed to evaluate the equations (26).

## APPENDIX X











TABLE 1. TYPICAL AERODYNAMIC DATA FOR A SHELL

M	$C_x$	$C_{y\zeta}$	$C_{z\zeta}$	$C_p$	$C_{m\zeta}$	$C_{n\zeta}$	$C_{m_q}$
0.0	-0.1299	-1.5	-1.7851	-0.0357	3.5730	0.0	-12.0
0.5	-0.1299	-1.5	-1.7851	-0.0290	3.6756	0.0	-13.0
0.55	-0.1299	-1.5	-1.7851	-0.0284	3.6931	0.0	-13.0
0.60	-0.1299	-1.5	-1.7851	-0.0279	3.7222	0.0	-13.0
0.70	-0.1281	-1.5	-1.7831	-0.0270	3.7946	0.012	-15.0
0.75	-0.1250	-1.5	-1.7738	-0.0265	3.8330	0.025	-17.0
0.80	-0.1225	-1.5	-1.7563	-0.0261	3.8762	0.038	-18.0
0.825	-0.1217	-1.5	-1.7449	-0.0259	3.9018	0.044	-19.0
0.850	-0.1214	-1.5	-1.7319	-0.0257	3.9318	0.05	-20.0
0.875	-0.1249	-1.5	-1.7206	-0.0255	3.9678	0.4	-21.0
0.90	-0.1338	-1.5	-1.7126	-0.0253	4.0124	0.75	-23.0
0.925	-0.1533	-1.5	-1.7172	-0.0252	4.0876	1.1	-24.0
0.94	-0.1769	-1.5	-1.7348	-0.0250	4.1697	1.1	-25.0
0.95	-0.1998	-1.5	-1.7551	-0.0250	4.2338	1.1	-25.0
0.96	-0.2266	-1.5	-1.7804	-0.0249	4.2916	1.05	-25.0
0.97	-0.2555	-1.5	-1.8090	-0.0248	4.3258	1.0	-24.0
0.98	-0.2849	-1.5	-1.8392	-0.0248	4.3161	0.94	-23.0
0.99	-0.3132	-1.5	-1.8695	-0.0247	4.2807	0.89	-23.0
1.00	-0.3391	-1.5	-1.8986	-0.0246	4.2341	0.85	-22.0
1.01	-0.3612	-1.5	-1.9250	-0.0245	4.1862	0.79	-21.0
1.02	-0.3784	-1.5	-1.9477	-0.0245	4.1415	0.75	-21.0
1.03	-0.3892	-1.5	-1.9651	-0.0244	4.1066	0.77	-21.0
1.04	-0.3958	-1.5	-1.9794	-0.0243	4.0749	0.65	-20.0
1.05	-0.4008	-1.5	-1.9932	-0.0243	4.0454	0.60	-20.0
1.075	-0.4085	-1.5	-2.0271	-0.0241	3.9922	0.52	-19.0
1.1	-0.4118	-1.5	-2.0620	-0.0239	3.9579	0.44	-18.0
1.125	-0.4124	-1.5	-2.0964	-0.0238	3.9369	0.37	-17.0
1.15	-0.4102	-1.5	-2.1281	-0.0236	3.9246	0.30	-16.0
1.20	-0.4007	-1.5	-2.1863	-0.0233	3.9120	0.20	-16.0
1.25	-0.3921	-1.5	-2.2422	-0.0230	3.9019	0.17	-15.0
1.30	-0.3839	-1.5	-2.3000	-0.0227	3.8920	0.13	-15.0
1.40	-0.3693	-1.5	-2.4061	-0.0221	3.8730	0.07	-14.0
1.50	-0.3566	-1.5	-2.5042	-0.0215	3.8342	0.0	-13.0
1.75	-0.3309	-1.5	-2.7107	-0.0203	3.7560	0.0	-13.0
2.00	-0.3104	-1.5	-2.8569	-0.0192	3.7232	0.0	-13.0
2.25	-0.2941	-1.5	-2.9393	-0.0182	3.6785	0.0	-13.0
2.50	-0.2841	-1.5	-2.9579	-0.0173	3.5650	0.0	-13.0

$d = 0.105 \quad S = 0.008659 \quad m = 14.9688 \quad \text{moment reference} = 0.3115$

$I_x = 0.02326 \quad I = 0.22557$

TABLE 2. FITTING ANALYTIC CURVES TO THE AXIAL FORCE COEFFICIENT

## (a) NR3634

K	L	a <sub>0</sub>	a <sub>1</sub>	a <sub>2</sub>	b <sub>0</sub>	b <sub>1</sub>	r.m.s.
0.97956	0.04979	-0.22346	0.10800	-	-0.05871	-	0.00484
0.97719	0.05633	-0.22897	0.12629	-	-0.04734	0.04665	0.00165
0.97719	0.05634	-0.22899	0.12635	-0.00005	-0.04734	0.04666	0.00167

## (b) Gavre

a	b	c	d	e	f	r.m.s.
-0.26447	0.09913	0.97206	19.963	-7.5430	-30.023	0.00903

NOTE: The Mach number range used in the nonlinear least squares fitting was 0.65 to 1.4

TABLE 3. ANALYTIC REPRESENTATIONS FOR OTHER COEFFICIENTS

## (a) Normal force derivative

K	L	a <sub>0</sub>	a <sub>1</sub>	a <sub>2</sub>	b <sub>0</sub>	b <sub>1</sub>	r.m.s.
0.97321	0.02156	-0.94111	-0.74737	-	-0.87307	-	0.0180
0.96413	0.03441	-0.93980	-0.73030	-	-0.85000	0.13116	0.0060
0.96564	0.03584	-0.94492	-0.68620	-0.10380	-0.84917	0.13321	0.0059

## (b) Roll damping derivative

a <sub>0</sub>	a <sub>1</sub>	a <sub>2</sub>	a <sub>3</sub>	a <sub>4</sub>	r.m.s.
-0.03149	0.00648	-	-	-	0.000891
-0.03485	0.01251	-0.002279	-	-	0.000243
-0.03559	0.01569	-0.005577	0.000899	-	0.000068
-0.03570	0.01702	-0.008138	0.002558	-0.000339	0.000034

TABLE 4. DESCRIPTION OF CARD INPUT TO SHELTRAJ

Card	Format	Variable	Comments																				
1	20A4	TITLE(20)	A title card to describe the job being processed, reproduced on the output.																				
2	16I5	LENTER	<p>This variable controls a facility which allows the user to begin entering data at any one of several different points in the input routine.</p> <table style="margin-left: 20px;"> <tr><td>LENTER</td><td>CARD</td></tr> <tr><td>1</td><td>3</td></tr> <tr><td>2</td><td>5</td></tr> <tr><td>3</td><td>15</td></tr> <tr><td>4</td><td>9</td></tr> <tr><td>5</td><td>13</td></tr> <tr><td>6</td><td>17</td></tr> <tr><td>7</td><td>18</td></tr> <tr><td>8</td><td>20</td></tr> <tr><td>9</td><td>return</td></tr> </table>	LENTER	CARD	1	3	2	5	3	15	4	9	5	13	6	17	7	18	8	20	9	return
LENTER	CARD																						
1	3																						
2	5																						
3	15																						
4	9																						
5	13																						
6	17																						
7	18																						
8	20																						
9	return																						
3	8F10.0	AMASS ROLLI REFS BODIAM	<p>Shell mass (kg)          Moment of inertia about the longitudinal axis (<math>\text{kg m}^2</math>)          Reference area (<math>\text{m}^2</math>)          Reference length (m)</p>																				
4	8F10.0	OMEGA  ALAT BEAR  GRAV HTASLO RO	<p>Angular velocity of the earth. Since this is added to acceleration components by the program instead of subtracted from them, as in equation (2) a negative value should be entered.  <math>(-7.292115.10^{-5} \text{ rad/s})</math></p> <p>Latitude of the shell, positive south (degrees)          Bearing of the line of fire relative to true north (degrees)          Acceleration due to gravity (<math>\text{ms}^{-2}</math>)          Height of range origin above mean sea-level (m)          Radius of the earth (m)</p>																				
5-8	8F10.0	XE(27)	The maximum changes allowed in each parameter, when testing for convergence.																				
9-12	8F10.0	X(27)	Initial estimates for values of the parameters $\Pi_i$ .																				
13-14	16I5	JORDER(27)	Order of the parameters for internal use by the program particularly when determining the first NPARAM parameters.																				
15	8F10.0	TO	Time at which integration begins.																				
16	8F10.0	XS(4)	Weighting factors proportional to the emphasis to be placed on each of the four measured quantities, range, deviation, altitude and roll rate.																				
17	8F10.0	REJECT ACCFAC  HMAX	<p>Initial data rejection level.          Scaling factor multiplying all XE. Can be used for wholesale adjustment of levels for convergence.          Maximum value allowed for integration step size.          This value will be used unless time to reach next data point is smaller.</p>																				

TABLE 4 (CONTD.).

Card	Format	Variable	Comments
18	16I5	NPARAM ITERN NPLOT	The first NPARAM parameters only, as specified in the JORDER array, will be allowed to vary. Maximum number of iterations of parameter estimation algorithm Plot every NPLOT th point of the simulated variable values. A maximum of 200 points can be plotted.
19	16I5	LENTER LCASE IFOUT	A repeat of the options allowed by card 2. Principally to avoid inputting new experimental data if none is needed. Non-zero if data for another run follows. Non-zero if a record of the experimental data points is required.
20	16I5	NPTS ISKIP	Number of data points to be used in this run. Use only every ISKIP point from the dataset containing the experimental measurements.
21	16I5	IND NWD NPT IFOUT	Control variable, describing the nature of the meteorological data, which is available = 1 none available = 2 wind table only = 3 pressure and temperature table only = 4 both wind table and pressure temperature table  NWD Number of points in wind tabulation  NPT Number of points in tabulation of temperature and pressure  IFOUT Non-zero if meteorological data should be tabulated as it is read.

TABLE 5. SAMPLE INPUT DECK FOR SHELTRAJ

## (a) Forces

```

A TEST EXERCISE FOR THE ANALYSIS OF RADAR DATA - NR3634 DRAG CURVE
1
14.9588 0.02326 0.008659 0.105
7.2722E-0535. 315. 9.807 0. 6373368.
1. 1. 1. 1. 1. 0.01 0.001
0.005 0.006 0.001 0.005 0.005 0.001 0.001
0.01 0.01 0.01 0.01 0.01 0.01 0.0001
0.00005 0.00001 1.
0. 0. 0. 280.4C 0. -363.71 0.977187 0.0563317
-0.228973 0.126289 0. -0.04734240.0466457 0. 0.964132 0.0344147
-0.939802 -0.736303 C. -0.449998 0.131162 0. -0.03559420.0156919
-0.00557720.0000000000159C.
10 11 12 7 8 9 3 6 1 4 18 2 5 19 15 22
13 16 20 14 17 21 23 24 25 26 27
0.
1. 1. 1. 0.
10. 1. 0.2
2 6 0
R 1 0
200 1
1
A TEST EXERCISE FOR THE ANALYSIS OF RADAR DATA FROM SHELL TRAJECTORIES - A
7
3 6 C
0 1 0
TEST EXERCISE FOR THE ANALYSIS OF RADAR DATA FROM SHELL TRAJECTORIES - B
7
4 6 0
0 1 C
TEST EXERCISE FOR THE ANALYSIS OF RADAR DATA FROM SHELL TRAJECTORIES - C
7
5 6 0
0 1 C
TEST EXERCISE FOR THE ANALYSIS OF RADAR DATA FROM SHELL TRAJECTORIES - D
7
6 6 0
0 1 C
TEST EXERCISE FOR THE ANALYSIS OF RADAR DATA FROM SHELL TRAJECTORIES - E
7
7 6 0
0 1 C
TEST EXERCISE FOR THE ANALYSIS OF RADAR DATA FROM SHELL TRAJECTORIES - F
7
8 6 0
0 1 C
TEST EXERCISE FOR THE ANALYSIS OF RADAR DATA FROM SHELL TRAJECTORIES - G
7
9 6 0
0 1 C
TEST EXERCISE FOR THE ANALYSIS OF RADAR DATA FROM SHELL TRAJECTORIES - H
7
10 6 0
0 1 C
TEST EXERCISE FOR THE ANALYSIS OF RADAR DATA FROM SHELL TRAJECTORIES - I
7
11 6 0
0 1 0
TEST EXERCISE FOR THE ANALYSIS OF RADAR DATA FROM SHELL TRAJECTORIES - J
7
12 6 0
0 1 0
TEST EXERCISE FOR THE ANALYSIS OF RADAR DATA FROM SHELL TRAJECTORIES - K
7
13 6 C
0 1 0
TEST EXERCISE - L
7
14 6 C
0 1 0
TEST EXERCISE - M
7
15 6 0
0 1 0
TEST EXERCISE - N
7
16 6 C
0 1 0
TEST EXERCISE - O
7
17 6 0
0 0 0

```

TABLE 5. SAMPLE INPUT DECK FOR SHELTRAJ

(b) Rolling moments

A DECK TO TEST THE ROLL FITTING CAPABILITIES OF THIS PROGRAM

1  
14.9688 0.02326 0.004659 0.1C5  
7.2722E-0535. 315. 9.467 0.  
1. 1. 1. 1. 1. 1. 0.1 0.005  
0.02 0.01 0.0001 0.005 0.005 0.0001 0.1 0.002  
0.1 0.05 0.0001 0.05 0.01 0.0001 0.005 0.001  
0.0005 0.0001 1.  
1.27 0. 1.42? 2H9. 0. -764. 0.9768 0.05731  
-0.2296 0.12H9 0. -0.04444 0.06547 0. 0.9641 0.03441  
-0.9162 -0.7303 0. -0.8307 0.1312 0. -0.034 0.016  
0. 0. 1390.  
6 7 8 9 10 11 12 13 14 15 16 17 18 19 20 21  
22 23 24 25 26 27 1 2 4 5 3  
0.  
0. 0. 0. 1.  
10. 1. 0.2  
1 20 0  
R 1 C  
200 1  
1  
ROLL TESTING - 6A  
7  
2 20 0  
9 1 0  
ROLL TESTING - 6B  
7  
3 20 0  
9 1 0  
ROLL TESTING - 6C  
7  
4 20 0  
9 1 0  
ROLL TESTING - 6D  
7  
5 20 2  
9 0 0

TABLE 6. SIMULATED EXPERIMENTAL DATA FOR SHELTRAJ

Time	Range	Drift	Altitude	Roll rate
0.0000000F+00	0.0000000E+00	0.0000000F+00	0.0000000F+00	1.3899733F+03
1.0000000F-01	2.4851295E+01	3.5840267E-04	-3.6210655E+01	1.3881710F+03
2.0000000F-01	5.7525882E+01	2.44925130F-03	-7.2103222F+01	1.3863843F+03
3.0000000F-01	1.6226647E+01	7.5528392F-03	-1.3748065F+02	1.3846191F+03
4.0000000F-01	1.1435735E+02	1.44627133F-02	-1.4295876F+02	1.3828691F+03
5.0000000F-01	1.4251963E+02	2.26587447E-02	-1.7790246F+02	1.3811360F+03
6.0000000F-01	1.7051133E+02	3.2380756E-02	-2.1255476F+02	1.3794197F+03
7.0000000F-01	1.9838276E+02	4.4712344F-02	-2.4690562E+02	1.3777200F+03
8.0000000F-01	2.2401057E+02	6.9258958F-02	-2.8097676E+02	1.3760365F+03
9.0000000F-01	2.5151827E+02	7.5050253E-02	-3.1471407E+02	1.3743692F+03
1.0000000F+00	2.8208472E+02	9.2098361F-02	-3.4817858F+02	1.3727178F+03
1.1000000F+00	3.0405951E+02	1.1297298E-01	-3.8135424F+02	1.3710820F+03
1.2000000F+00	3.3509175E+02	1.3291705E-01	-4.1424352F+02	1.3694414F+03
1.3000000F+00	3.6149352E+02	1.5291716E-01	-4.4464905F+02	1.3676568F+03
1.4000000F+00	3.9471907E+02	1.8469498E-01	-4.7917398F+02	1.3662470F+03
1.5000000F+00	4.15136651F+02	2.0492667E-01	-5.1122149E+02	1.3646920F+03
1.6000000F+00	4.4174473E+02	2.3055840E-01	-5.4994278E+02	1.3631318F+03
1.7000000F+00	4.6803949E+02	2.6854012E-01	-5.7449465E+02	1.3615861F+03
1.8000000F+00	4.9449014E+02	2.9474786E-01	-6.0572510F+02	1.3600547F+03
1.9000000F+00	5.2013998E+02	3.3085025E-01	-6.3668841F+02	1.3585174F+03
2.0000000F+00	5.4606929E+02	3.6563329E-01	-6.6739742E+02	1.3570242F+03
2.1000000F+00	5.7180011E+02	4.0222944E-01	-6.9782465F+02	1.3555544F+03
2.2000000F+00	5.9739415E+02	4.4049090E-01	-7.2800233F+02	1.3540684F+03
2.3000000F+00	6.2228532E+02	4.8143283E-01	-7.5922264E+02	1.3526066F+03
2.4000000F+00	6.4841797E+02	5.2347949E-01	-7.8758793E+02	1.3511576F+03
2.5000000F+00	6.7337266E+02	5.6685575E-01	-8.1700747E+02	1.3497214F+03
2.6000000F+00	6.9843577E+02	6.1171714E-01	-8.4416375F+02	1.3482974F+03
2.7000000F+00	7.2337006E+02	6.5834776E-01	-8.7507947F+02	1.3465542F+03
2.8000000F+00	7.4417741E+02	7.0088520E-01	-9.0375025E+02	1.3454850F+03
2.9000000F+00	7.7285977E+02	7.5719923E-01	-9.3217852E+02	1.3440078F+03
3.0000000F+00	7.9741904E+02	8.1064335E-01	-9.6166933F+02	1.3427234F+03
3.1000000F+00	8.2185949E+02	8.6226319E-01	-9.8318212F+02	1.3413629F+03
3.2000000F+00	8.4617524E+02	9.1690524E-01	-1.043515F+03	1.3400117F+03
3.3000000F+00	8.7073752E+02	9.7134097E-01	-1.065264F+03	1.3396675F+03
3.4000000F+00	8.9446045E+02	1.0311149E+00	-1.0777766E+03	1.3372484F+03
3.5000000F+00	9.1843114E+02	1.0908333E+00	-1.0978043F+03	1.3350317F+03
3.6000000F+00	9.42297C5E+02	1.1521740E+00	-1.1261612E+03	1.3343257F+03
3.7000000F+00	9.6604050E+02	1.2149494E+00	-1.1511971F+03	1.3334302F+03
3.8000000F+00	9.8962656E+02	1.2701999E+00	-1.1775633E+03	1.3320170F+03
3.9000000F+00	1.0132191E+03	1.3344624E+00	-1.2037151F+03	1.3300707F+03
4.0000000F+00	1.0366520E+03	1.4111992E+00	-1.2266533E+03	1.3296680F+03
4.1000000F+00	1.0599837E+03	1.4807074E+00	-1.2454383E+03	1.3284357F+03
4.2000000F+00	1.0843216E+03	1.5512281E+00	-1.2609056F+03	1.3271147F+03
4.3000000F+00	1.1043535E+03	1.6232554E+00	-1.302244RF+03	1.3258H11F+03
4.4000000F+00	1.1293973E+03	1.6967783E+00	-1.3313444E+03	1.3246577F+03
4.5000000F+00	1.1523515E+03	1.7717325E+00	-1.3562686E+03	1.3234456F+03
4.6000000F+00	1.1752197E+03	1.8481144E+00	-1.381001PE+03	1.3222427F+03
4.7000000F+00	1.1940058E+03	1.9259772E+00	-1.4055848E+03	1.3210480F+03
4.8000000F+00	1.2129713E+03	2.0053404E+00	-1.4299134E+03	1.3198A13F+03
4.9000000F+00	1.2433473E+03	2.0804052E+00	-1.4541015F+03	1.3186625F+03
5.0000000F+00	1.2559109E+03	2.1690262E+00	-1.4781116E+03	1.3175114F+03
5.1000000F+00	1.2884061E+03	2.2522121E+00	-1.5014934E+03	1.3173481F+03
5.2000000F+00	1.3108427E+03	2.3389848E+00	-1.5251661E+03	1.3151940F+03
5.3000000F+00	1.3332128E+03	2.4241834E+00	-1.5491687E+03	1.3140491F+03
5.4000000F+00	1.3555379E+03	2.5149367E+00	-1.5725350E+03	1.3129111F+03
5.5000000F+00	1.3776050E+03	2.6052513E+00	-1.5957848E+03	1.3117814F+03
5.6000000F+00	1.4000222E+03	2.6971344E+00	-1.6181813F+03	1.3106577F+03
5.7000000F+00	1.4221930E+03	2.7907R28E+00	-1.6417312F+03	1.3095406F+03
5.8000000F+00	1.4443192E+03	2.8860787E+00	-1.6646505F+03	1.3084301F+03
5.9000000F+00	1.4664403E+03	2.9830790E+00	-1.6871397E+03	1.3073271F+03
6.0000000F+00	1.4884848E+03	3.0817794E+00	-1.7064353F+03	1.3062319F+03
6.1000000F+00	1.5104546E+03	3.1821726E+00	-1.7311994E+03	1.3051441F+03
6.2000000F+00	1.5324250E+03	3.2842757E+00	-1.7542193F+03	1.3040823F+03
6.3000000F+00	1.5553405E+03	3.3880684E+00	-1.7733113E+03	1.3029860F+03
6.4000000F+00	1.5782624E+03	3.4936752E+00	-1.7982720F+03	1.3019151F+03
6.5000000F+00	1.6000000E+03	3.6010147E+00	-1.820102RE+03	1.3008498F+03
6.6000000F+00	1.6199706E+03	3.7102299E+00	-1.8410505F+03	1.2997708F+03
6.7000000F+00	1.6441770E+03	3.8212435E+00	-1.8633797E+03	1.2987734F+03
6.8000000F+00	1.6663557E+03	3.9414157E+00	-1.8848275F+03	1.2978604F+03
6.9000000F+00	1.68853075E+03	4.0489214E+00	-1.9061494F+03	1.2966488F+03
7.0000000F+00	1.7070791E+03	4.1655588E+00	-1.9273461E+03	1.2956141F+03
7.1000000F+00	1.7274723E+03	4.2840748E+00	-1.9484713F+03	1.2945481F+03
7.2000000F+00	1.7503901E+03	4.4044745E+00	-1.9693368F+03	1.2934615F+03
7.3000000F+00	1.7720304E+03	4.5267767E+00	-1.9901923E+03	1.2924573F+03
7.4000000F+00	1.7936657E+03	4.6509927E+00	-2.0108595F+03	1.2913539F+03
7.5000000F+00	1.8152354E+03	4.7771471E+00	-2.0317771E+03	1.2905321F+03
7.6000000F+00	1.8363001E+03	4.9052047E+00	-2.0519373F+03	1.2895325F+03
7.7000000F+00	1.8583402E+03	5.0353534E+00	-2.0722768F+03	1.2885384F+03
7.8000000F+00	1.8798561E+03	5.1674416E+00	-2.0924958F+03	1.2875849F+03
7.9000000F+00	1.9013481E+03	5.3015370E+00	-2.1125959F+03	1.2865657F+03
8.0000000F+00	1.9228116E+03	5.4376479E+00	-2.1325745F+03	1.2855572F+03
8.1000000F+00	1.9442617E+03	5.5757040E+00	-2.1523505F+03	1.2846130F+03
8.2000000F+00	1.9656406E+03	5.7151940E+00	-2.1721717E+03	1.2836655F+03
8.3000000F+00	1.9870303E+03	5.8551364E+00	-2.1918001F+03	1.2826282F+03
8.4000000F+00	2.0084616E+03	6.0023782E+00	-2.2113056F+03	1.2817240F+03
8.5000000F+00	2.0298162E+03	6.1486793E+00	-2.2306933E+03	1.2807707F+03
8.6000000F+00	2.0511494E+03	6.2970575E+00	-2.2499837E+03	1.2798222F+03
8.7000000F+00	2.0724610E+03	6.4475247E+00	-2.2611690F+03	1.2787877F+03
8.8000000F+00	2.0937510E+03	6.6001039E+00	-2.2881533F+03	1.2777940F+03
8.9000000F+00	2.1150196E+03	6.7556949E+00	-2.3070732F+03	1.2770060F+03
9.0000000F+00	2.1362676E+03	6.9116551E+00	-2.3258768F+03	1.2760768F+03
9.1000000F+00	2.1574935E+03	7.0706528E+00	-2.3445543E+03	1.2751524F+03
9.2000000F+00	2.1786992E+03	7.2318120E+00	-2.3631316F+03	1.2742326F+03
9.3000000F+00	2.1998436E+03	7.3951404E+00	-2.3815923F+03	1.2733174F+03
9.4000000F+00	2.2210489E+03	7.5506845E+00	-2.3999333E+03	1.2724048F+03
9.5000000F+00	2.2421032E+03	7.72P3310F+00	-2.4181501F+03	1.271500RF+03
9.6000000F+00	2.2633117E+03	7.89P2020F+00	-2.4362700F+03	1.2705993F+03
9.7000000F+00	2.2844211E+03	8.0624643E+00	-2.4542642F+03	1.2697023F+03
9.8000000F+00	2.3055540E+03	8.2445254E+00	-2.4721747F+03	1.2688076F+03
9.9000000F+00	2.3265546E+03	8.4207095F+00	-2.4909151F+03	1.2679216F+03
1.0000000F+01	2.3476120E+03	8.6064545F+00	-2.5075538F+03	1.2670378F+03
1.0100000F+01	2.3686337E+03	8.7806101F+00	-2.5251074F+03	1.2661584F+03
1.0200000F+01	2.3896208E+03	8.9637334F+00	-2.5425331F+03	1.2652833F+03
1.0300000F+01	2.4106273E+03	9.1492211F+00	-2.5598450F+03	1.2644125F+03
1.0400000F+01	2.4311593E+03	9.3363935E+00	-2.5770435E+03	1.2634559F+03
1.0500000F+01	2.4525539E+03	9.5249394E+00	-2.5948288F+03	1.2626835F+03
1.0600000F+01	2.4735847E+03	9.7102442F+00	-2.6111101F+03	1.2618254F+03

Time	Range	Drift	Altitude	Roll rate
1.0700000E+01	2.4943752E+03	9.9138575E+00	-2.6274605E+03	1.2609713E+03
1.0900000E+01	2.5152644E+03	1.0110747E+01	-2.6467072E+03	1.2461214E+03
1.0900000E+01	2.5361346E+03	1.0310041E+01	-2.66113413E+03	1.2592756E+03
1.1000000E+01	2.5569696E+03	1.0511624E+01	-2.6778631E+03	1.2584238E+03
1.1100000E+01	2.5778117E+03	1.0715544E+01	-2.6942726E+03	1.2575946E+03
1.1200000E+01	2.5986328E+03	1.0921809E+01	-2.7105701E+03	1.2567223E+03
1.1300000E+01	2.6194242E+03	1.1130429E+01	-2.7267559E+03	1.2558326E+03
1.1400000E+01	2.6402205E+03	1.1341413E+01	-2.7428797E+03	1.2551066E+03
1.1500000E+01	2.6609537E+03	1.1556477E+01	-2.7587921E+03	1.2562344E+03
1.1600000E+01	2.6817039E+03	1.1770527E+01	-2.7744311E+03	1.2536446E+03
1.1700000E+01	2.7024259E+03	1.1988481E+01	-2.7903524E+03	1.2526622E+03
1.1800000E+01	2.7231297E+03	1.2209251E+01	-2.8060114E+03	1.2518417E+03
1.1900000E+01	2.7438154E+03	1.2424320E+01	-2.8215293E+03	1.2511350E+03
1.2000000E+01	2.7644811E+03	1.2625768E+01	-2.8363934E+03	1.2502320E+03
1.2100000E+01	2.7851329E+03	1.2845856E+01	-2.8522329E+03	1.2494129E+03
1.2200000E+01	2.8057648E+03	1.3051543E+01	-2.8674185E+03	1.2484372E+03
1.2300000E+01	2.8263794E+03	1.3344754E+01	-2.8824940E+03	1.2474845E+03
1.2400000E+01	2.8469754E+03	1.3540454E+01	-2.8974553E+03	1.2470570E+03
1.2500000E+01	2.8675533E+03	1.3721218E+01	-2.9121345E+03	1.2462724E+03
1.2600000E+01	2.8881156E+03	1.3940212E+01	-2.9270599E+03	1.2454512E+03
1.2700000E+01	2.9096594E+03	1.4343490E+01	-2.9416954E+03	1.2447137E+03
1.2800000E+01	2.9291858E+03	1.4550201E+01	-2.9562214E+03	1.2439339E+03
1.2900000E+01	2.9496939E+03	1.4799019E+01	-2.9704379E+03	1.2431641E+03
1.3000000E+01	2.9701866E+03	1.5048366E+01	-2.9849450E+03	1.2424020E+03
1.3100000E+01	2.9906614E+03	1.5312126E+01	-2.9991430E+03	1.2416338E+03
1.3200000E+01	3.0111190E+03	1.5556711E+01	-3.0132319E+03	1.2406780E+03
1.3300000E+01	3.0315595E+03	1.5814730E+01	-3.0272119E+03	1.2401211E+03
1.3400000E+01	3.0519305E+03	1.6075330E+01	-3.0461031E+03	1.2393676E+03
1.3500000E+01	3.0723926E+03	1.6333525E+01	-3.0584545E+03	1.2385172E+03
1.3600000E+01	3.0927779E+03	1.6604326E+01	-3.0788997E+03	1.2378774E+03
1.3700000E+01	3.1131524E+03	1.6872744E+01	-3.0962454E+03	1.2371264E+03
1.3800000E+01	3.1335037E+03	1.7143796E+01	-3.109428PE+03	1.2362556E+03
1.3900000E+01	3.1538484E+03	1.7417485E+01	-3.1088121E+03	1.2356479E+03
1.4000000E+01	3.1741715E+03	1.7693625E+01	-3.1220313E+03	1.2349132E+03
1.4100000E+01	3.1944678E+03	1.7972624E+01	-3.1361546E+03	1.2341817E+03
1.4200000E+01	3.2147672E+03	1.8254491E+01	-3.1481524E+03	1.2336531E+03
1.4300000E+01	3.2350425E+03	1.8538835E+01	-3.1616050E+03	1.2332727E+03
1.4400000E+01	3.2552994E+03	1.8825666E+01	-3.1738410E+03	1.2330051E+03
1.4500000E+01	3.2756842E+03	1.9115590E+01	-3.1865242E+03	1.2321284E+03
1.4600000E+01	3.2957655E+03	1.9400196E+01	-3.1991601E+03	1.2305848E+03
1.4700000E+01	3.3156974E+03	1.9703134E+01	-3.2115689E+03	1.2294855E+03
1.4800000E+01	3.3316167E+03	2.0001036E+01	-3.2239330E+03	1.2294164E+03
1.4900000E+01	3.3516433E+03	2.0301632E+01	-3.2351145E+03	1.2288431E+03
1.5000000E+01	3.3726504E+03	2.0604490E+01	-3.2463333E+03	1.2277731E+03
1.5100000E+01	3.3926649E+03	2.0901106E+01	-3.2591373E+03	1.2270296E+03
1.5200000E+01	3.4126778E+03	2.1219904E+01	-3.2723110E+03	1.2262451E+03
1.5300000E+01	3.43268917E+03	2.15131617E+01	-3.2841398E+03	1.2255323E+03
1.5400000E+01	3.4526959E+03	2.18460467E+01	-3.2956113E+03	1.2249324E+03
1.5500000E+01	3.472707110E+03	2.2163321E+01	-3.3074773E+03	1.2242460E+03
1.5600000E+01	3.49271371E+03	2.2483396E+01	-3.3189573E+03	1.2235590E+03
1.5700000E+01	3.51271478E+03	2.2806298E+01	-3.3303915E+03	1.2229723E+03
1.5800000E+01	3.53272229E+03	2.3117204E+01	-3.3414899E+03	1.2223189E+03
1.5900000E+01	3.5527425E+03	2.3426034E+01	-3.3528823E+03	1.2215056E+03
1.6000000E+01	3.5727724E+03	2.3739209E+01	-3.3636939E+03	1.2204104E+03
1.6100000E+01	3.5927357E+03	2.4126118E+01	-3.3749509E+03	1.2201550E+03
1.6200000E+01	3.6127024E+03	2.4446329E+01	-3.3862626E+03	1.2199624E+03
1.6300000E+01	3.6327167E+03	2.4803729E+01	-3.3976977E+03	1.2191812E+03
1.6400000E+01	3.652711111E+03	2.51671311E+01	-3.4167236E+03	1.2184449E+03
1.6500000E+01	3.67270302E+03	2.5452644E+01	-3.4371240E+03	1.2178401E+03
1.6600000E+01	3.69269523E+03	2.5841474E+01	-3.4582796E+03	1.2170174E+03
1.6700000E+01	3.7126504E+03	2.61193241E+01	-3.4788305E+03	1.2161581E+03
1.6800000E+01	3.73272315E+03	2.6457944E+01	-3.4944776E+03	1.2155700E+03
1.6900000E+01	3.75266017E+03	2.6905597E+01	-3.5149019E+03	1.2148425E+03
1.7000000E+01	3.77264551E+03	2.7266216E+01	-3.5349050E+03	1.2141940E+03
1.7100000E+01	3.7926937E+03	2.7629794E+01	-3.5547957E+03	1.2135442E+03
1.7200000E+01	3.81261175E+03	2.7996363E+01	-3.5848115E+03	1.2129966E+03
1.7300000E+01	3.83263927E+03	2.8365919E+01	-3.6149839E+03	1.2122510E+03
1.7400000E+01	3.85267312E+03	2.8738442E+01	-3.6450159E+03	1.2116044E+03
1.7500000E+01	3.87266011E+03	2.9114018E+01	-3.6741759E+03	1.2109649E+03
1.7600000E+01	3.89265654E+03	2.9492665E+01	-3.70270879E+03	1.2103313E+03
1.7700000E+01	3.915150174E+03	2.9874304E+01	-3.7315329E+03	1.2094657E+03
1.7800000E+01	3.94547538E+03	3.02591600E+01	-3.7545000E+03	1.2080626E+03
1.7900000E+01	3.97544579E+03	3.06465752E+01	-3.78547019E+03	1.20884215E+03
1.8000000E+01	3.974741836E+03	3.1037575E+01	-3.81363993E+03	1.2070702PE+03
1.8100000E+01	3.993371770E+03	3.1431479E+01	-3.8427545E+03	1.2071763E+03
1.8200000E+01	4.0135562E+03	3.1829476E+01	-3.8713631E+03	1.2064552E+03
1.8300000E+01	4.0333212E+03	3.22224576E+01	-3.9013720E+03	1.2055290E+03
1.8400000E+01	4.0528720E+03	3.26211788E+01	-3.9305565E+03	1.2053099E+03
1.8500000E+01	4.0725057E+03	3.30381218E+01	-3.9607130E+03	1.2044921E+03
1.8600000E+01	4.0921314E+03	3.34347591E+01	-3.9915167E+03	1.2040766E+03
1.8700000E+01	4.1117401E+03	3.38466202E+01	-4.0223792E+03	1.2034628E+03
1.8800000E+01	4.1313348E+03	3.42275956E+01	-4.05319655E+03	1.2028513E+03
1.8900000E+01	4.1509156E+03	3.46894889E+01	-4.0840036E+03	1.202241PE+03
1.9000000E+01	4.1704252E+03	3.51164986E+01	-4.11480039E+03	1.2016343E+03
1.9100000E+01	4.1900356E+03	3.5562244E+01	-4.14558693E+03	1.2010287E+03
1.9200000E+01	4.2095749E+03	3.5970733E+01	-4.16636325E+03	1.2004251E+03
1.9300000E+01	4.2291004E+03	3.6402404E+01	-4.17219211E+03	1.1998234E+03
1.9400000E+01	4.24866125E+03	3.6853727E+01	-4.17885211E+03	1.1992235E+03
1.9500000E+01	4.26861109E+03	3.7275391E+01	-4.18610407E+03	1.1986256E+03
1.9600000E+01	4.2875958E+03	3.7716727E+01	-4.19366346E+03	1.1980294E+03
1.9700000E+01	4.3070671E+03	3.81411304E+01	-4.2001142E+03	1.1974351E+03
1.9800000E+01	4.3265250E+03	3.8549136E+01	-4.2060672E+03	1.1968424E+03
1.9900000E+01	4.3459694E+03	3.8940230E+01	-4.2151114E+03	1.1962519E+03

TABLE 7. BEGINNING AND END OF OUTPUT FROM SAMPLE INPUT FOR SHELTRAJ  
(A) FORCES

PARAMETER ESTIMATION FOR ANALYSIS OF TRAJECTORY AND ROLL DATA FROM RADAR AND YAWSONDE MEASUREMENTS MADE DURING THE FLIGHT OF A SHELL  
A TEST EXERCISE FOR THE ANALYSIS OF RADAR DATA - NR3634 DRAG CURVE

VEHICLE PHYSICAL CONSTANTS  
MASS 14.066KG MOMENT OF INERTIA IN ROLL 0.02326KG M2  
REFERENCE AREA 0.00856M2 REFERENCE LENGTH 0.1050M

FARTH MODEL - ANGULAR VELOCITY	LATITUDE	FIRING LINE	GRAVITATION	HEIGHT ABOVE	RADIUS OF
(RAD/SEC)	(DEG)	(DEG)	(M/S/S)	SEA LEVEL(M)	THE EARTH(M)
0.7272200D-04	35.000	315.000	9.80700	0.0	6373360D+02

ORDER OF PARAMETERS  
10 11 12 7 8 9 3 6 1 4 15 2 5 19 15 22 13 16 20 14 17 21 23 24 25 26 27

INITIAL TIME 0.0 (S)

SCALING OF RANGE AZIMUTH ALTITUDE ROLL RATE  
1.00 1.00 1.00 0.0

REJECTION LEVEL ON DATA 1E-00

ACCURACY FACTOR FOR PARAMETER ERROR LEVELS 1.000  
MAXIMUM INTEGRATION STEP 0.2000 NO. OF PARAMETERS VARIED 2 MAXIMUM NO. OF ITERATIONS 6  
NO PLOTS REQUESTED

	CDA0	CDB0	CDK	CDAI	CDB1	CDL	XD0TO	YD0TO
PARAM.	-0.22900+00	-0.47340-01	0.97720+00	0.12630+00	0.46650-01	0.56330-01	0.28940+03	0.0
DELTA	0.50000-02	0.50000-02	0.10000-01	0.50000-02	0.50000-02	0.10000-02	0.10000+01	0.10000+01
	ZD0TO	XD	YD	ZD	CZALFA0	CZALFR0	CZALFAK	CZALFA1
PARAM.	-0.36370+03	0.0	0.0	0.0	-0.93980+00	-0.85000+00	0.96410+00	-0.73030+00
DELTA	0.10000+01	0.10000+01	0.10000+01	0.10000+01	0.10000-01	0.10000-01	0.10000-01	0.10000-01
	CZALF01	CDA2	CDR2	CZALFA2	CZALFR2	CZALFAL	CLP0	CLP1
PARAM.	0.13120+00	0.0	0.0	0.0	0.0	0.34410-01	-0.35500-01	0.15600-01
DELTA	0.10000-01	0.10000-02	0.10000-02	0.10000-01	0.10000-01	0.10000-02	0.10000-03	0.10000-03
	CLP2	CLP3	PD					
PARAM.	-0.55770+02	0.89890-03	0.13900+04					
DELTA	0.50000-04	0.10000-04	0.10000+01					
SIGMA=	0.182070+01	DEGREES OF FREEDOM=	796					

COVARIANCE MATRIX (MATRIX IS SYMMETRIC)

1.250+08  
-1.190+08 3.680+08

CHANGES TO THE FOLLOWING PARAMETERS ALL SMALL

	CDA0	CDB0	CDK	CDAI	CDB1	CDL	XD0TO	YD0TO
PARAM.	-0.22780+00	-0.49540-01	0.97720+00	0.12630+00	0.46650-01	0.56330-01	0.28940+03	0.0
DELTA	0.11180-03	0.19180-03	0.10000-01	0.50000-02	0.50000-02	0.10000-02	0.10000+01	0.10000+01
	ZD0TO	XD	YD	ZD	CZALFA0	CZALFR0	CZALFAK	CZALFA1
PARAM.	-0.36370+03	0.0	0.0	0.0	-0.93980+00	-0.85000+00	0.96410+00	-0.73030+00
DELTA	0.10000+01	0.10000+01	0.10000+01	0.10000+01	0.10000-01	0.10000-01	0.10000-01	0.10000-01
	CZALF01	CDA2	CDR2	CZALFA2	CZALFR2	CZALFAL	CLP0	CLP1
PARAM.	0.13120+00	0.0	0.0	0.0	0.0	0.34410-01	-0.35500-01	0.15600-01
DELTA	0.10000-01	0.10000-02	0.10000-02	0.10000-01	0.10000-01	0.10000-02	0.10000-03	0.10000-03
	CLP2	CLP3	PD					
PARAM.	-0.55770+02	0.89890-03	0.13900+04					
DELTA	0.50000-04	0.10000-04	0.10000+01					

REJECTION LEVEL ON DATA 1.E0

ACCURACY FACTOR FOR PARAMETER ERROR LEVELS 1.000  
MAXIMUM INTEGRATION STEP 0.2000 NO. OF PARAMETERS VARIED 14 MAXIMUM NO. OF ITERATIONS 6  
NO PLOTS REQUESTED

	CDA0	CDB0	CDK	CDAI	CDB1	CDL	XD0TO	YD0TO
PARAM.	-0.22900+00	-0.44330-01	0.97890+00	0.12950+00	0.45740-01	0.57470-01	0.29800+03	0.69140-01
DELTA	0.50000-02	0.50000-02	0.10000-01	0.50000-02	0.50000-02	0.10000-02	0.10000+01	0.10000+01
	ZD0TO	XD	YD	ZD	CZALFA0	CZALFR0	CZALFAK	CZALFA1
PARAM.	-0.16400+03	0.13820+01	-0.74940-01	0.11080+01	-0.87270+00	-0.65000+00	0.94110+00	-0.71070+00
DELTA	0.10000+01	0.10000+01	0.10000+01	0.10000+01	0.10000-01	0.10000-01	0.10000-01	0.10000-01
	CZALF01	CDA2	CDR2	CZALFA2	CZALFR2	CZALFAL	CLP0	CLP1
PARAM.	0.13120+00	0.0	0.0	0.0	0.0	0.34410-01	-0.35500-01	0.15600-01
DELTA	0.10000-01	0.10000-02	0.10000-02	0.10000-01	0.10000-01	0.10000-02	0.10000-03	0.10000-03
	CLP2	CLP3	PD					
PARAM.	-0.55770+02	0.89890-03	0.13900+04					
DELTA	0.50000-04	0.10000-04	0.10000+01					

	CDA0	CDB0	CDK	CDAI	CDB1	CDL	XD0TO	YD0TO
PARAM.	-0.22970+00	-0.44420-01	0.97890+00	0.12900+00	0.45730-01	0.57350-01	0.29800+03	0.69140-02
DELTA	0.49720-02	0.42690-02	0.70170-02	0.44330-01	0.43720-01	0.68390-02	0.43210-01	0.79040-02

TABLE 7(A). (CONTINUED)

	ZD0TO	X0	Y0	Z0	CZALEF0	CZALEF0	CZALEFK	CZALEFA
PARAM.	-0.3640D+03 0.4340D+00	0.1320D+01 0.2027D+00	-0.5810D+02 0.1492D+00	0.1065D+01 0.2467D+00	-0.9160D+00 0.9451D+01	-0.1780D+00 0.1520D+01	0.4640D+00 0.1660D+01	-0.7030D+00 0.1000D+01
DELTA								
	CZALEF1	CDA2	CDB2	CZALEF2	CZALEF2	CZALEFL	CLP0	CLP1
PARAM.	0.1312D+00 0.1000D+01	0.0 0.1000D-02	0.0 0.1000D-02	0.0 0.1000D-01	0.0 0.1000D-01	0.1441D-01 -0.1000D-02	-0.3550D-01 0.1600D-02	0.1660D-01 -0.1000D-02
DELTA								
	CLP2	CLP3	RD					
PARAM.	-0.5577D-02 0.5000D-04	0.8969D-03 0.1000D-04	0.1390D+04 0.1000D+01					
DELTA								
SIGMAR	0.42139D+00	DEGREES OF FREEDOM: 740						

COVARIANCE MATRIX (MATRIX IS SYMMETRIC)

7.650-06  
 -1.070-05 1.800-05  
 -5.490-05 1.670-05 4.570-05  
 -7.720-04 1.370-04 2.730-04 1.860-03  
 -9.110-05 5.940-05 4.350-05 4.020-04 1.990-04  
 -5.240-05 2.770-05 3.260-05 2.360-04 8.690-05 4.580-05  
 2.980-03 -9.070-04 -2.230-03 -1.660-02 -2.530-03 -1.520-03 1.740-01  
 4.580-06 -6.230-07 -4.140-04 -2.660-05 -5.280-07 -1.750-04 3.300-04 5.480-03  
 -1.730-03 1.130-03 2.790-03 2.000-02 3.170-03 1.900-01 -2.170-01 -4.100-04 2.710-01  
 -9.390-02 2.630-04 6.950-04 5.350-03 7.190-04 4.300-04 -6.990-03 -1.350-04 8.630-02 3.830-02  
 -5.160-07 -6.190-07 1.140-06 5.200-03 -2.950-06 -3.240-07 -1.140-04 -6.930-03 1.410-04 5.710-04 2.080-02  
 1.180-03 -3.330-04 -6.740-04 -6.720-03 -4.260-04 -6.430-04 8.720-02 1.570-04 -1.090-01 -4.200-02 -6.020-05 5.660-02  
 -1.170-06 1.570-06 -2.640-07 3.940-02 6.340-06 1.470-06 -4.990-06 6.930-03 6.910-06 6.610-06 -1.670-02 -1.640-05 4.520-03  
 2.760-07 -3.690-07 6.830-08 -9.910-07 -1.630-06 -3.080-07 3.450-06 -7.170-04 -4.770-06 8.730-08 2.540-06 -1.060-02  
 2.410-04

CHANGES TO THE FOLLOWING PARAMETERS ALL SMALL

	CDA0	CDB0	CDK	CDA1	CDP1	CDL	XD0TO	YD0TO
PARAM.	-0.2296D+00 0.4749D+02	-0.6444D-01 0.4247D-02	0.9789D+00 0.6763D-02	0.1289D+00 0.4708D-01	0.6547D-01 0.1410D-01	0.5731D-01 0.6764D-02	0.2990D+03 0.4175D+00	0.5780D-02 0.7674D-01
DELTA								
	ZD0TO	X0	Y0	Z0	CZALEF0	CZALEF0	CZALEFK	CZALEFA
PARAM.	-0.3640D+03 0.5203D+00	0.1272D+01 0.1956D+00	-0.5992D+02 0.1441D+00	0.1023D+01 0.2380D+00	-0.9162D+00 0.9230D+01	-0.1830D+00 0.1554D+01	0.4641D+00 0.1000D-01	-0.7030D+00 0.1000D-01
DELTA								
	CZALEF1	CDA2	CDB2	CZALEF2	CZALEF2	CZALEFL	CLP0	CLP1
PARAM.	0.1312D+00 0.1000D+01	0.0 0.1000D-02	0.0 0.1000D-02	0.0 0.1000D-01	0.0 0.1000D-01	0.1441D-01 0.1000D-02	-0.3550D-01 0.1000D-03	0.1660D-01 0.1000D-01
DELTA								
	CLP2	CLP3	RD					
PARAM.	-0.5577D-02 0.5000D-04	0.8969D-03 0.1000D-04	0.1390D+04 0.1000D+01					
DELTA								

TABLE 7. BEGINNING AND END OF OUTPUT FROM SAMPLE INPUT FOR SHELTRAJ  
(B) ROLLING MOMENTS

PARAMETER ESTIMATION FOR ANALYSIS OF TRAJECTORY AND ROLL DATA FROM RADAR AND VARIOSONDE MEASUREMENTS MADE DURING THE FLIGHT OF A SHELL  
A DECK TO TEST THE ROLL FITTING CAPABILITIES OF THIS PROGRAM

VEHICLE PHYSICAL CONSTANTS  
MASS 14.968KG. MOMENT OF INERTIA IN ROLL 0.02324KG M2  
REFERENCE AREA 0.008659M2 REFERENCE LENGTH 0.1050M  
EARTH MODEL = ANGULAR VELOCITY LATITUDE FIRING LINE GRAVITATION HEIGHT ABOVE RADIUS OF  
(RAD/SEC) (DEG) (DEG) (M/S/S) SEA LEVEL(M) THE EARTH(M)  
0.72722000-04 35.000 315.000 9.80700 0.0 6.3733600+07

ORDER OF PARAMETERS  
A 7 8 9 10 11 12 13 14 15 16 17 18 19 20 21 22 23 24 25 26 27 1 2 4 5 3

INITIAL TIME 0.0 (ST)

SCALING OF RANGE AZIMUTH ALTITUDE ROLL RATE  
C=0 0.0 0.0 1.00

REJECTION LEVEL ON DATA 10.00

ACCURACY FACTOR FOR PARAMETER ERROR LEVELS 1.000  
MAXIMUM INTEGRATION STEP 0.2000 NO. OF PARAMETERS VARIED 1 MAXIMUM NO. OF ITERATIONS 20  
NO PLOTS REQUESTED

	CLP0	CLP1	P0	CLP2	CLP3	X0	Y0	Z0
PARAM. DELT A	-0.36000-01 0.45000-02	0.11000-01 0.10000-02	0.13900+04 0.10000+01	0.0 0.50000-03	0.0 0.10000-03	0.12700+01 0.10000+01	0.0 0.10000+01	0.10200+01 0.10000+01
PARAM. DELT A	0.24900+C3 0.10000+01	0.0 0.10000+01	-0.36400+C3 0.10000+01	0.97400+00 0.10000+00	0.97310-01 0.50000-02	-0.22960+00 0.20000-01	0.12800+00 0.10000-01	0.0 0.10000-03
PARAM. DELT A	-0.44440-01 0.50000-02	0.65470-01 0.50000-02	C0 0.10000-02	0.96410+00 0.10000+00	0.96410-01 0.20000-02	-0.91620+00 0.10000+00	-0.73030+00 0.50000-01	0.0 0.10000-03
PARAM. DELT A	-0.83070+00 0.50000-01	0.13120+00 0.10000-01	0.C 0.10000-03					
ST. MAX	0.78947D-01	DEGREES OF FREEDOM= 76						
	CLP0	CLP1	P0	CLP2	CLP3	X0	Y0	Z0
PARAM. DELT A	-0.41490-01 0.21420-04	0.11000-01 0.10000-02	0.13900+04 0.10000+01	0.0 0.50000-03	0.0 0.10000-03	0.12700+01 0.10000+01	0.0 0.10000+01	0.10200+01 0.10000+01
PARAM. DELT A	0.21900+03 0.10000+01	0.0 0.10000+01	-0.36400+C3 0.10000+01	0.97400+00 0.10000+00	0.97310-01 0.50000-02	-0.22960+00 0.20000-01	0.12800+00 0.10000-01	0.0 0.10000-03
PARAM. DELT A	-0.41440-01 0.50000-02	0.65470-01 0.50000-02	C0 0.10000-02	0.96410+00 0.10000+00	0.96410-01 0.20000-02	-0.91620+00 0.10000+00	-0.73030+00 0.50000-01	0.0 0.10000-03
PARAM. DELT A	-0.83070+00 0.50000-01	0.13120+00 0.10000-01	0.C 0.10000-03					

	CZALFR0	CZALFR1	CZALFR2
PARAM. DELT A	-0.83070+00 0.50000-01	0.13120+00 0.10000-01	0.0 0.10000-03
SIGMAR	0.890540+00	DEGREES OF FREEDOM= 448	

COVARIANCE MATRIX (MATRIX IS SYMMETRIC)

	CLP0	CLP1	P0	CLP2	CLP3	X0	Y0	Z0
PARAM. DELT A	-0.41490-01 0.24900-04	0.11000-01 0.10000-02	0.13900+04 0.10000+01	0.0 0.50000-03	0.0 0.10000-03	0.12700+01 0.10000+01	0.0 0.10000+01	0.10200+01 0.10000+01
PARAM. DELT A	0.24900+03 0.10000+01	0.0 0.10000+01	-0.36400+C3 0.10000+01	0.97400+00 0.10000+00	0.97310-01 0.50000-02	-0.22960+00 0.20000-01	0.12800+00 0.10000-01	0.0 0.10000-03
PARAM. DELT A	-0.44440-01 0.50000-02	0.65470-01 0.50000-02	C0 0.10000-03	0.96410+00 0.10000+00	0.96410-01 0.20000-02	-0.91620+00 0.10000+00	-0.73030+00 0.50000-01	0.0 0.10000-03
PARAM. DELT A	-0.83070+00 0.50000-01	0.13120+00 0.10000-01	0.C 0.10000-03					

TABLE 7(B). (CONTINUED)

ROLLTESTING = AC

REJECTION LEVEL ON DATA 0.18

ACCURACY FACTOR FOR PARAMETER ERROR LEVELS 1.000  
 MAXIMUM INTEGRATION STEP 0.2000 NO. OF PARAMETERS VARIED 4 MAXIMUM NO. OF ITERATIONS 20  
 NO PLOTS REQUESTED

	CLP0	CLP1	P0	CLP2	CLP3	X0	Y0	Z0
PARAM.	-0.3192D-01	0.7277D-02	0.1390D+04	0.0	0.0	0.1270D+01	0.0	0.1020D+01
DELTA	0.4000D-02	0.1000D-02	0.1000D+01	0.5000D-03	0.1000D-03	0.1000D+01	0.1000D+01	0.1000D+01

	X0D0	Y0D0	Z0D0	C0K	C0L	C0A0	C0A1	C0A2
PARAM.	0.2890D+03	0.0	-0.3640D+03	0.9760D+00	0.5721D-01	-0.2296D+00	0.1289D+00	0.0
DELTA	0.1000D+01	0.1000D+01	0.1000D+01	0.1000D+00	0.5000D-02	0.2000D-01	0.1000D-01	0.1000D-02

	C0B0	C0A1	C0A2	CZALFAK	CZALFAL	CZALFA0	CZALFA1	CZALFA2
PARAM.	-0.4444D-01	0.6547D-01	0.0	0.9641D+00	0.3441D-01	-0.9162D+00	-0.7303D+00	0.0
DELTA	0.5000D-02	0.5000D-02	0.1000D-03	0.1000D+00	0.2000D-02	0.1000D+00	0.5000D-01	0.1000D-02

	CZALFB0	CZALFB1	CZALFB2					
PARAM.	-0.4307D+00	0.1312D+00	0.0					
DELTA	0.5000D-01	0.1000D-01	0.1000D-03					

SIGMA= 0.60572D-02 DEGREES OF FREEDOM= 798

	CLP0	CLP1	P0	CLP2	CLP3	X0	Y0	Z0
PARAM.	-0.3442D-01	0.1270D-01	0.1390D+04	-0.2867D-02	0.0	0.1270D+01	0.0	0.1020D+01
DELTA	0.1689D-04	0.3684D-04	0.3081D-02	0.1945D-04	0.1000D-03	0.1000D+01	0.1000D+01	0.1000D+01

	X0D0	Y0D0	Z0D0	C0K	C0L	C0A0	C0A1	C0A2
--	------	------	------	-----	-----	------	------	------

	PARAM.	0.2890D+03	0.0	-0.3640D+03	0.9760D+00	0.5721D-01	-0.2296D+00	0.1289D+00	0.0
DELTA	0.1000D+01	0.1000D+01	0.1000D+01	0.1000D+00	0.5000D-02	0.2000D-01	0.1000D-01	0.1000D-02	

	C0B0	C0A1	C0A2	CZALFAK	CZALFAL	CZALFA0	CZALFA1	CZALFA2
PARAM.	-0.4444D-01	0.6547D-01	0.0	0.9641D+00	0.3441D-01	-0.9162D+00	-0.7303D+00	0.0
DELTA	0.5000D-02	0.5000D-02	0.1000D-03	0.1000D+00	0.2000D-02	0.1000D+00	0.5000D-01	0.1000D-02

	CZALFB0	CZALFB1	CZALFB2					
--	---------	---------	---------	--	--	--	--	--

	PARAM.	-0.4307D+00	0.1312D+00	0.0				
--	--------	-------------	------------	-----	--	--	--	--

	DELTA	0.5000D-01	0.1000D-01	0.1000D-03				
--	-------	------------	------------	------------	--	--	--	--

SIGMA= 0.63861D-02 DEGREES OF FREEDOM= 796

COVARIANCE MATRIX (MATRIX IS SYMMETRIC)

2.72D-10  
 -4.47D-10 1.27D-09  
 -2.43D-09 6.44D-08 7.34D-08  
 3.08D-10 -6.71D-10 -3.63D-08 3.55D-10

CHANGES TO THE FOLLOWING PARAMETERS ALL SMALL

	CLP0	CLP1	P0	CLP2	CLP3	X0	Y0	Z0
PARAM.	-0.3436D-01	0.1258D-01	0.1390D+04	-0.2861D-02	0.0	0.1270D+01	0.0	0.1020D+01
DELTA	0.1649D-04	0.3567D-04	0.2710D-02	0.1884D-04	0.1000D-03	0.1000D+01	0.1000D+01	0.1000D+01

	X0D0	Y0D0	Z0D0	C0K	C0L	C0A0	C0A1	C0A2
PARAM.	0.2890D+03	0.0	-0.3640D+03	0.9760D+00	0.5721D-01	-0.2296D+00	0.1289D+00	0.0
DELTA	0.1000D+01	0.1000D+01	0.1000D+01	0.1000D+00	0.5000D-02	0.2000D-01	0.1000D-01	0.1000D-02

	C0B0	C0A1	C0A2	CZALFAK	CZALFAL	CZALFA0	CZALFA1	CZALFA2
PARAM.	-0.4444D-01	0.6547D-01	0.0	0.9641D+00	0.3441D-01	-0.9162D+00	-0.7303D+00	0.0
DELTA	0.5000D-02	0.5000D-02	0.1000D-03	0.1000D+00	0.2000D-02	0.1000D+00	0.5000D-01	0.1000D-02

	CZALFB0	CZALFB1	CZALFB2					
--	---------	---------	---------	--	--	--	--	--

	PARAM.	-0.4307D+00	0.1312D+00	0.0				
--	--------	-------------	------------	-----	--	--	--	--

	DELTA	0.5000D-01	0.1000D-01	0.1000D-03				
--	-------	------------	------------	------------	--	--	--	--

TABLE 8. DESCRIPTION OF CARD INPUT TO YAWCAL

Card	Format	Variable	Description
1	18A4	TITLE(18)	A 72 character description of the job.
2	6F10.0	X(3)	<p>Initial estimates of the three parameters describing the calibration curve, equation (22)</p> $\tan \sigma_N = -[\sin a / X(1)] (1 + X(2)^2 - 2X(2) \cos a)^{-\frac{1}{2}}$ <p>where</p> $a = 2(\tau/T + X(3))$ <p>X(3) is in radians. The three parameters are defined by <math>X(1) = \tan \gamma_1</math>, <math>X(2) = \tan \gamma_2 / \tan \gamma_1</math>, and <math>X(3) = \beta</math>, where <math>\gamma_1</math>, <math>\gamma_2</math> and <math>\beta</math> are shown in figure 4.</p>
3	16I5	NPTS	Number of measured points on calibration curve.

NOTE: The three cards are followed by NPTS records on unit 4, each in 2F10.0 format, and each containing simultaneous values of time ratio,  $\tau/T$ , and complementary solar aspect angle,  $\sigma_N$ , in degrees.

TABLE 9. DESCRIPTION OF CARD INPUT TO ASPECT

Card	Format	Variable	Description
1	18A4	TITLE(18)	A 72 character description of the current job.
2	6F10.0	HA(I,J)	The hours, minutes and seconds, J=1, 2 and 3, of the hour angle of the first point of Aries at 0 hours Universal Time for the date being considered and the following day, I = 1, 2.
3	6F10.0	RA(I,J)	The hours, minutes and seconds, J=1, 2 and 3, of the right ascension of the sun at 0 hours Universal Time for the day in question and the following day, I = 1, 2.
4	6F10.0	DE(I,J)	The degrees, minutes and seconds, J=1, 2 and 3, of the declination of the sun at 0 hours Universal Time for the day in question and the following day, I=1,2.
5	18A4	DATES(5)	A 20 character description of the date for which the complementary solar aspect angle is estimated.
6	6F10.0	LAT(3), LONG(3)	Degrees, minutes and seconds for latitude and longitude of shell. Latitude is positive north and longitude is positive west.
7	12I5	NTIMES	Number of local times (local South Australian time) for which results are required. The local times used are corrected to Universal or Greenwich Mean Time in the program by subtracting nine and a half hours.
8	6F10.0	TO,DT	The local times should begin at TO hours and increment regularly by DT hours.
9	6F10.0	BEAR(3)	The degrees, minutes and seconds of the line of fire relative to true north.
10	12I5	NELEVN	The number of elevation angles for which results are required.
11	6F10.0	ELO, DEL	The elevation angles should begin with ELO degrees and increment regularly by DEL degrees.

TABLE 10. DESCRIPTION OF CARD INPUT TO YAWSONDE

Read	Format	Variable	Description
1	20A4	TITLE(20)	An 80 character job description which is reproduced on the output.
2	16I5	LENTER	A control variable which can be used to begin entering data at any one of the following points in the input stream.  LENTER   READ 1   3 2   6 3   7 4   8 5   9 6   10 7   11 8   12 9   14 10    return
3	16I5	NCOS	Number of entries in a table which provides direction cosines of the sun in range axes as a function of time along the trajectory.
4	5E16.7	TIME(I), COSL(I), COSM(I), COSN(I)	Entries in the table for I=1, NCOS with one set per card.
5	16I5	NTRAJ, IFOUT, ISKIP	Controls for the entry of trajectory data from a dataset constructed from the results of SHELTRAJ, further details of trajectory data are given in Section 4.2.1. This run uses every ISKIP th point up to a total of NTRAJ points and the points used are recorded on the printed output if IFOUT is non-zero.
6	8F10.0	XE(12)	Maximum changes in each parameter value, which are used in testing for convergence.
7	8F10.0	REFS BODIAM PITCHI ROLLI	Reference area for aerodynamic coefficients. Reference length for aerodynamic coefficients. Moment of inertia of shell in pitch and yaw Moment of inertia of shell in roll.
8	8F10.0	X(12)	Initial estimates for the values of the parameters $P_i$ .
9	16I5	JORDER(12)	Order of the parameters for internal use by the program particularly when determining values for the first NPARAM parameters.
10	8F10.0	TO	Time at which integration begins.
11	8F10.0	REJECT ACCFAC	Initial value for data rejection level. Scaling factor for all the XE. Can be used for wholesale adjustment of the convergence levels.

TABLE 10 (CONTINUED)

Read	Format	Variable	Description
		HMAX	Maximum value for integration step. This value is used unless time to next data point is smaller.
12	16I5	NPARAM ITERN NPLOT	The first NPARAM parameters only are allowed to vary. Maximum number of iterations. Plot every NPLOT th point of the simulated measurement values. A maximum of 500 points can be plotted.
13	16I5	LENTER LCASE IFOUT	A repeat of the options allowed in read 2. Principally to avoid inputting new experimental data if none is required. Non-zero if data for another run follows. Non-zero if a record of the experimental data points is required in the print out.
14	16I5	NPTS ISKIP	Number of experimentally measured data points to be used in this run. Uses every ISKIP th point from the dataset containing the experimental measurements.
15	16I5	IND  NWD NPT  IFOUT	Control variable, describing the nature of the meteorological data which is available. =1 none available. =2 wind table only, =3 pressure and temperature table only, =4 both wind table and pressure and temperature table. Number of points in wind table. Number of points in pressure and temperature table. NON-zero if meteorological data should be recorded on printed output.

TABLE 11. SAMPLE INPUT DECK FOR YAWSONDE

TEST DECK FOR YAWSONDE DATA ANALYSIS PROGRAMME

```

1
2
0.          -0.690534      0.011401      -0.723210
40.          -0.690534      0.011401      -0.723210
   10      1      1
0.001      0.001      0.01      0.01      0.1      0.1      1.        0.1
1.          1.          1.          0.01
0.008569    0.105      0.22557     0.02326
0.1        0.427431    0.        0.        3.76      0.        0.        0.
0.          -14.        0.        0.
   2      1      3      4      5      R      10      7      11      9      12      6
1R.
1.          1.          0.01
   1      2C      C
   9      1      1
  100      1
   1
PART II
  R
   2      20      0
   10      1
PART III
  R
   3      20      0
   10      1
PART IV
  R
   4      2C      C
   10      1
PART V
  R
   5      20      0
   10      1
PART VI
  R
   6      20      0
   10      1
PART VII
  R
   7      20      0
   10      1
PART VIII
  R
   8      2C      0
   10      1
PART IX
  R
   9      2C      0
   10      1
PART X
  R
   10      20      0
   1
PART XI
  R
   11      20      0
   10      1
PART XII
  R
   12      20      1
   10      C

```

TABLE 12. SIMULATED EXPERIMENTAL DATA FOR YAWSONDE

(A) TRAJECTORY MEASUREMENTS

18.000000	196.94579	9.71028	-89.705223566.139161207.80000
18.100000	196.79242	9.79641	-88.676693575.070691207.17249
18.200000	196.64590	9.88202	-87.635533583.898771206.54720
18.300000	196.50600	9.96349	-86.582633592.622201205.92411
18.400000	196.37213	10.03762	-85.519623601.239851205.30319
18.500000	196.24341	10.10182	-84.448733609.750841204.68442
18.600000	196.11874	10.15421	-83.372633618.154511204.06778
18.700000	195.99688	10.19369	-82.294233626.450471203.45325
18.800000	195.87654	10.21999	-81.216543634.638661202.84079
18.900000	195.75645	10.23362	-80.142433642.719291202.23040
19.000000	195.63549	10.23578	-79.074563650.692851201.62198
19.100000	195.51265	10.22829	-78.015163658.560091201.01551
19.200000	195.38711	10.21342	-76.965943666.321951200.41097
19.300000	195.25824	10.19376	-75.928033673.979491199.80833
19.400000	195.12568	10.17204	-74.901963681.533891199.20757
19.500000	194.98932	10.15102	-73.887643688.986331198.60868
19.600000	194.84927	10.13328	-72.884413696.337941198.01163
19.700000	194.70586	10.12116	-71.891093703.589791197.41640
19.800000	194.55960	10.11659	-70.906083710.742781196.82298
19.900000	194.41113	10.12105	-69.927453717.797651196.23134
20.000000	194.26120	10.13549	-68.953063724.754931195.64148

TABLE 12. SIMULATED EXPERIMENTAL DATA FOR YAWSONDE

## (B) YAWSONDE MEASUREMENTS

1.800000E+01	-3.3041852E-01	1.8265000E+01	-3.5929316E-01
1.8005000E+01	-3.3044029E-01	1.8270000E+01	-3.5955638E-01
1.8010000E+01	-3.3063585E-01	1.8275000E+01	-3.6012715E-01
1.8015000E+01	-3.3114431E-01	1.8280000E+01	-3.6097965E-01
1.8020000E+01	-3.3199186E-01	1.8285000E+01	-3.6198605E-01
1.8025000E+01	-3.3308270E-01	1.8290000E+01	-3.6296266E-01
1.8030000E+01	-3.3423385E-01	1.8295000E+01	-3.6373594E-01
1.8035000E+01	-3.3524110E-01	1.8300000E+01	-3.6420481E-01
1.8040000E+01	-3.3595251E-01	1.8305000E+01	-3.6437677E-01
1.8045000E+01	-3.3632292E-01	1.8310000E+01	-3.6436477E-01
1.8050000E+01	-3.3642983E-01	1.8315000E+01	-3.6434621E-01
1.8055000E+01	-3.3644504E-01	1.8320000E+01	-3.6449900E-01
1.8060000E+01	-3.3657236E-01	1.8325000E+01	-3.6493775E-01
1.8065000E+01	-3.3697433E-01	1.8330000E+01	-3.6567298E-01
1.8070000E+01	-3.3771395E-01	1.8335000E+01	-3.6660771E-01
1.8075000E+01	-3.3873251E-01	1.8340000E+01	-3.6757249E-01
1.8080000E+01	-3.3987099E-01	1.8345000E+01	-3.6838643E-01
1.8085000E+01	-3.4092745E-01	1.8350000E+01	-3.6892209E-01
1.8090000E+01	-3.4172973E-01	1.8355000E+01	-3.6915110E-01
1.8095000E+01	-3.4219726E-01	1.8360000E+01	-3.6915405E-01
1.8100000E+01	-3.4236978E-01	1.8365000E+01	-3.6909107E-01
1.8105000E+01	-3.4239251E-01	1.8370000E+01	-3.6914402E-01
1.8110000E+01	-3.4246355E-01	1.8375000E+01	-3.6945122E-01
1.8115000E+01	-3.4276237E-01	1.8380000E+01	-3.7005806E-01
1.8120000E+01	-3.4338553E-01	1.8385000E+01	-3.7090111E-01
1.8125000E+01	-3.4431235E-01	1.8390000E+01	-3.7183115E-01
1.8130000E+01	-3.4541267E-01	1.8395000E+01	-3.7266689E-01
1.8135000E+01	-3.4649392E-01	1.8400000E+01	-3.7326010E-01
1.8140000E+01	-3.4737044E-01	1.8405000E+01	-3.7354870E-01
1.8145000E+01	-3.4793015E-01	1.8410000E+01	-3.7357878E-01
1.8150000F+01	-3.4817470E-01	1.8415000E+01	-3.7348765E-01
1.8155000E+01	-3.4821840E-01	1.8420000E+01	-3.7345417E-01
1.8160000E+01	-3.4824668E-01	1.8425000E+01	-3.7363445E-01
1.8165000E+01	-3.4844911E-01	1.8430000E+01	-3.7410604E-01
1.8170000E+01	-3.4895135E-01	1.8435000E+01	-3.7484046E-01
1.8175000E+01	-3.4977035E-01	1.8440000E+01	-3.7571377E-01
1.8180000E+01	-3.5080864E-01	1.8445000E+01	-3.7655119E-01
1.8185000E+01	-3.5188960E-01	1.8450000E+01	-3.7718995E-01
1.8190000E+01	-3.5282113E-01	1.8455000E+01	-3.7753757E-01
1.8195000E+01	-3.5346462E-01	1.8460000E+01	-3.7760493E-01
1.8200000E+01	-3.5378470E-01	1.8465000E+01	-3.7750192E-01
1.8205000E+01	-3.5386154E-01	1.8470000E+01	-3.7739764E-01
1.8210000E+01	-3.5386160E-01	1.8475000E+01	-3.7745953E-01
1.8215000E+01	-3.5397740E-01	1.8480000E+01	-3.7779339E-01
1.8220000F+01	-3.5435834E-01	1.8485000E+01	-3.7840581E-01
1.8225000E+01	-3.5505729E-01	1.8490000E+01	-3.7920209E-01
1.8230000E+01	-3.5601197E-01	1.8495000E+01	-3.8002052E-01
1.8235000E+01	-3.5706769E-01		
1.8240000E+01	-3.5803301E-01		
1.8245000E+01	-3.5874866E-01		
1.8250000E+01	-3.5914460E-01		
1.8255000E+01	-3.5926495E-01		
1.8260000E+01	-3.5925168E-01		

TABLE 13. BEGINNING AND END OF OUTPUT FROM SAMPLE INPUT TO YAWSONDE

PARAMETER ESTIMATION FOR ANALYSIS OF YAWSONDE DATA FROM RADAR AND YAWSONDE MEASUREMENTS MADE DURING THE FLIGHT OF A SHELL  
TEST DECK FOR YAWSONDE DATA ANALYSIS PROGRAMME

DIRECTION COSINES FOR THE SUN IN RANGE AXES AS A FUNCTION OF TIME ALONG THE TRAJECTORY  
TIME(S)    L    M    N  
0.00 -0.690534 0.011401 -0.723210  
40.00 -0.690534 0.011401 -0.723210

## TABULATED TRAJECTORY DATA

TIME (SEC)	XDOT (METERS/SECOND)	YDOT (METERS/SECOND)	ZDOT (METERS/SECOND)	ALT (M)	ROLL (RAD/SEC)
18.0	196.05	0.71	-89.71	3566.14	1207.80
18.1	196.79	0.40	-88.66	3575.07	1207.17
18.2	196.45	0.48	-87.66	3583.99	1206.55
18.3	196.51	0.94	-86.55	3592.66	1205.92
18.4	196.37	10.04	-85.52	3601.25	1205.30
18.5	196.24	10.10	-84.45	3609.75	1204.68
18.6	196.12	10.15	-83.37	3618.15	1204.07
18.7	196.00	10.19	-82.29	3626.45	1203.45
18.8	195.88	10.22	-81.22	3634.61	1202.83
18.9	195.76	10.23	-80.15	3642.72	1202.23
19.0	195.64	10.24	-79.07	3650.89	1201.62
19.1	195.51	10.23	-78.02	3658.56	1201.02
19.2	195.39	10.21	-76.97	3666.32	1200.41
19.3	195.26	10.19	-75.93	3673.98	1199.81
19.4	195.13	10.17	-74.90	3681.53	1199.21
19.5	195.00	10.15	-73.89	3689.99	1198.61
19.6	194.85	10.13	-72.88	3696.34	1198.01
19.7	194.71	10.12	-71.89	3703.59	1197.42
19.8	194.56	10.12	-70.91	3710.74	1196.82

## VEHICLE PHYSICAL CONSTANTS

REFERENCE AREA= 0.008569(M\*\*2)  
PITCH INERTIA= 0.225570(KG M\*\*2)

BODY DIAMETER= 0.1050(M)  
ROLL INERTIA= 0.0232600(KG M\*\*2)

ORDER OF PARAMETERS  
2 1 3 4 5 8 10 7 11 9 12 6

STARTING TIME= 18.000(S)

INITIAL REJECTION LEVEL ON DATA = .00  
ACCURACY FACTOR FOR PARAMETER ERROR LEVELS = 1.000  
MAXIMUM INTEGRATION STEP = 0.0100  
NUMBER OF PARAMETERS VARIED = 1  
MAXIMUM NUMBER OF ITERATIONS = 20

NO PLOTS REQUESTED

TIME (SEC)	COMPLEMENTARY SOLAR ASPECT ANGLE(DEG)
18.0000	-0.33041452
18.0050	-0.33044029
18.0100	-0.33063585
18.0150	-0.33114431
18.0200	-0.33199186
18.0250	-0.33364970
18.0300	-0.33421385
18.0350	-0.33524110
18.0400	-0.33595251
18.0450	-0.33632292
18.0500	-0.33642983
18.0550	-0.33646504
18.0600	-0.33657236
18.0650	-0.33697433
18.0700	-0.33771395
18.0750	-0.33873251
18.0800	-0.33987699
18.0850	-0.34092745
18.0900	-0.34172973
18.0950	-0.34219726
18.1000	-0.34236978
18.1050	-0.34239251
18.1100	-0.34246355
18.1150	-0.34276237
18.1200	-0.34338553
18.1250	-0.34431235
18.1300	-0.34541267
18.1350	-0.34649392
18.1400	-0.34737044
18.1450	-0.34792015
18.1500	-0.34817470
18.1550	-0.34821940
18.1600	-0.34824668
18.1650	-0.34844911
18.1700	-0.34895135
18.1750	-0.34977635
18.1800	-0.35080894
18.1850	-0.35181996
18.1900	-0.35282113
18.1950	-0.35364642
18.2000	-0.35378470
18.2050	-0.35386154
18.2100	-0.35386160
18.2150	-0.35397740
18.2200	-0.35435834
18.2250	-0.35505729
18.2300	-0.35601197
18.2350	-0.35766769
18.2400	-0.35803301
18.2450	-0.35874866
18.2500	-0.35914460
18.2550	-0.35926495
18.2600	-0.35925148
18.2650	-0.35920316
18.2700	-0.35955638
18.2750	-0.36012715
18.2800	-0.36097065
18.2850	-0.36191606
18.2900	-0.36208766

TABLE 13. (CONTINUED)

18.2950	-0.36373594						
18.3000	-0.36420481						
18.3050	-0.36437677						
18.3100	-0.36436477						
18.3150	-0.36436421						
18.3200	-0.36449900						
18.3250	-0.36491775						
18.3300	-0.36561720						
18.3350	-0.36666771						
18.3400	-0.36757249						
18.3450	-0.36836643						
18.3500	-0.36892209						
18.3550	-0.36915110						
18.3600	-0.36915405						
18.3650	-0.36909107						
18.3700	-0.36914402						
18.3750	-0.36945122						
18.3800	-0.37005866						
18.3850	-0.37090111						
18.3900	-0.37183115						
18.3950	-0.37266689						
18.4000	-0.37326010						
18.4050	-0.37356470						
18.4100	-0.37357478						
18.4150	-0.37344765						
18.4200	-0.37345417						
18.4250	-0.37363445						
18.4300	-0.37410604						
18.4350	-0.37484046						
18.4400	-0.37571377						
18.4450	-0.37655119						
18.4500	-0.37714995						
18.4550	-0.37753757						
18.4600	-0.37766493						
18.4650	-0.37750192						
18.4700	-0.37739764						
18.4750	-0.37745553						
18.4800	-0.37779339						
18.4850	-0.37746581						
18.4900	-0.37926209						
18.4950	-0.38002652						
THE TAO	PSIO	OO	RD	CMI	CMMACH	CNP1	CM3
PARAM.	0.42740+00	0.10000+00	0.0	0.0	0.27600+01	0.0	0.0
DELTA	0.10000-02	0.10000-02	0.10000-01	0.10000-01	0.10000-01	0.10000+00	0.10000+00
CM00	CM5	CNP3	CM02				
PARAM.	-0.14000+02	0.0	0.0	0.0			
DELTA	0.10000+01	0.10000+01	0.10000+01	0.10000+01			
SIGMA=	0.180100-03	DEGREES OF FREEDOM=	99				

COVARIANCE MATRIX (MATRIX IS SYMMETRIC)

4.55D-10							
CHANGES TO THE FOLLOWING PARAMETERS ALL SMALL							
THE TAO	PSIO	OO	RD	CMI	CMMACH	CNP1	CM3
PARAM.	0.42710+00	0.10000+00	0.0	0.0	0.27600+01	0.0	0.0
DELTA	0.21330-04	0.10000-02	0.10000-01	0.10000-01	0.10000+00	0.10000-01	0.10000+00
CM00	CM5	CNP3	CM02				
PARAM.	-0.14000+02	0.0	0.0	0.0			
DELTA	0.10000+01	0.10000+01	0.10000+01	0.10000+01			

## PART XI

INITIAL REJECTION LEVEL ON DATA 0.00  
 ACCURACY FACTOR FOR PARAMETER ERROR LEVELS 1.000  
 MAXIMUM INTEGRATION STEP 0.0100  
 NUMBER OF PARAMETERS VARIED 12  
 MAXIMUM NUMBER OF ITERATIONS 20

PLOTS REQUESTED EVERY 1 POINTS

THE TAO	PSIO	OO	RD	CMI	CMMACH	CNP1	CM3
PARAM.	0.42740+00	0.10010+00	0.45100-05	-0.10670-03	0.27100+01	0.13450+00	0.16840-01
DELTA	0.10000-02	0.10000-02	0.10000-01	0.10000-01	0.10000+00	0.10000-01	0.10000+00
CM00	CM5	CNP3	CM02				
PARAM.	-0.14340+02	0.17720+04	-0.13230+01	0.0			
DELTA	0.10000+01	0.10000+01	0.10000+01	0.10000+01			
SIGMA=	0.786100-07	DEGREES OF FREEDOM=	99				
THE TAO	PSIO	OO	RD	CMI	CMMACH	CNP1	CM3
PARAM.	0.42740+00	0.10000+00	0.42940-05	-0.19760-04	0.35900+01	0.34110+00	0.70430-03
DELTA	0.44740-05	0.58120-04	0.43560-05	0.50780-04	0.19410+00	0.30330+00	0.19400-01
CM00	CM5	CNP3	CM02				
PARAM.	-0.14160+02	0.20460+04	0.47210+01	-0.12640+03			
DELTA	0.26700+00	0.78110+03	0.72480+01	0.14460+03			
SIGMA=	0.786100-07	DEGREES OF FREEDOM=	99				

TABLE 13. (CONTINUED)

COVARIANCE MATRIX (MATRIX IS SYMMETRIC)

1.990-11	3.350-09
-5.380-12	6.910-11 1.890-11
2.120-10	-2.760-09 -5.730-11 2.570-09
-7.530-07	9.810-06 2.100-07 -9.580-06 3.730-02
1.200-06	-1.560-05 -3.340-07 1.510-05 -5.830-02 9.120-02
-4.610-08	1.120-06 2.280-08 -8.960-07 3.170-03 -5.060-03 3.760-04
-1.440-05	1.850-04 3.860-06 -1.130-04 2.890-01 -4.960-01 6.340-02 1.930-01
4.340-07	-1.080-05 6.480-09 9.000-06 -3.240-02 5.140-02 -3.640-03 -5.590-01 4.280-02
1.530-03	-1.960-02 -4.110-04 7.210-03 9.500-01 6.900-00 -6.650-00 -3.210-03 5.370-01 6.130-05
3.160-05	-4.100-04 -8.280-06 3.100-04 -1.060+00 1.710+00 -1.390-01 -2.590-01 1.340+00 3.100+03 5.290+01
-6.060-04	7.870-03 3.760-05 -6.120-03 2.130+01 -3.410+01 2.670+00 4.670+02 -2.940+01 -5.290+04 -1.010+02 2.100+04

CHANGES TO THE FOLLOWING PARAMETERS ALL SMALL

PARAM.	THETAO	PSID	R0	CMS	CMMACH	CNP1	CMS3
PARAM.	0.42740+00	0.10000+00	0.43070-05	-0.49900-04	0.35910+01	0.34030+00	0.72200-03 -0.77530+01
DELTA	0.44570-05	0.57880-04	0.43520-05	0.50650-04	0.19220+00	0.30200+00	0.19390-01 0.42970+01
	CMD0	CMS	CNP3	CMD2			
PARAM.	-0.14160+02	0.20460+04	0.67300+01	-0.12650+03			
DELTA	0.20640+00	0.73000+03	0.72710+01	0.14500+03			

TIME(S)	COMPLEMENTARY SOLAR SOLAR ASPECT ANGLE RESIDUE	(RADIAN)					
1R.005	-0.3304404	6.84600-08	1R.300	-0.3642049	4.79200-08		
1R.010	-0.3304350	4.91690-08	1R.305	-0.3643768	3.21160-08		
1R.015	-0.3311143	3.44230-08	1R.310	-0.3643648	8.43910-09		
1R.020	-0.3310919	8.09630-08	1R.315	-0.3643662	-2.09090-08		
1R.025	-0.3330297	-1.10512-08	1R.320	-0.3644089	-5.85310-08		
1R.030	-0.3342733	-2.44830-08	1R.325	-0.3640377	-9.08140-08		
1R.035	-0.3352411	-3.24600-08	1R.330	-0.3656729	-1.13610-07		
1R.040	-0.3350525	-4.15600-08	1R.335	-0.3666676	-1.31270-07		
1R.045	-0.3363224	-5.41200-08	1R.340	-0.3675724	-1.15060-07		
1R.050	-0.3366298	-6.35000-08	1R.345	-0.3683663	-9.00360-08		
1R.055	-0.3366450	-8.93450-08	1R.350	-0.3689220	-6.04690-08		
1R.060	-0.3365723	-9.09600-08	1R.355	-0.3691511	-1.42710-08		
1R.065	-0.3366742	-8.31100-08	1R.360	-0.3691541	2.05670-08		
1R.070	-0.3377139	-4.82450-08	1R.365	-0.3690911	6.62480-08		
1R.075	-0.3377325	-7.01790-09	1R.370	-0.3691441	1.03760-07		
1R.080	-0.3398710	3.47500-08	1R.375	-0.3694514	1.34000-07		
1R.085	-0.3409275	7.45920-08	1R.380	-0.3705852	1.57490-07		
1R.090	-0.3417298	9.76500-08	1R.385	-0.3709013	1.40330-07		
1R.095	-0.3421197	1.07050-07	1R.390	-0.3718313	1.45720-07		
1R.100	-0.3423699	9.16100-08	1R.395	-0.3726670	1.2970-07		
1R.105	-0.3423926	8.66400-08	1R.400	-0.3732602	8.55740-08		
1R.110	-0.3424636	6.43420-08	1R.405	-0.3735487	4.01560-08		
1R.115	-0.3427624	4.61500-08	1R.410	-0.3735788	-7.54890-09		
1R.120	-0.3433356	3.03430-08	1R.415	-0.3734976	-5.67460-08		
1R.125	-0.3443124	5.70590-08	1R.420	-0.3734541	-9.00990-08		
1R.130	-0.3454126	-2.25100-08	1R.425	-0.3736343	-1.24990-07		
1R.135	-0.3464939	-3.63500-08	1R.430	-0.3741059	-1.32280-07		
1R.140	-0.3473764	-6.17470-08	1R.435	-0.3746003	-1.15120-07		
1R.145	-0.3479301	-6.82500-08	1R.440	-0.3757117	-9.05120-08		
1R.150	-0.3481746	-7.07010-08	1R.445	-0.3765511	-5.09060-08		
1R.155	-0.3482183	-5.97300-08	1R.450	-0.3771109	-3.07770-08		
1R.160	-0.3482466	-4.74500-08	1R.455	-0.3775376	-7.93390-09		
1R.165	-0.3484491	-2.69100-08	1R.460	-0.3776049	-1.33100-09		
1R.170	-0.3489514	8.45530-08	1R.465	-0.3775019	3.44930-09		
1R.175	-0.3497704	4.59640-08	1R.470	-0.3773977	1.81500-08		
1R.180	-0.3508087	8.83210-08	1R.475	-0.3774506	3.24720-08		
1R.185	-0.3511897	8.92610-08	1R.480	-0.3777934	5.21320-08		
1R.190	-0.3528212	8.27800-08	1R.485	-0.3784059	4.69840-08		
1R.195	-0.3534647	7.57800-08	1R.490	-0.3792021	3.21430-08		
1R.200	-0.3537848	6.12530-08	1R.495	-0.3800265	-1.68390-08		
1R.205	-0.3538616	5.41910-08					
1R.210	-0.3538616	3.37160-08					
1R.215	-0.3539774	7.47030-09					
1R.220	-0.3543583	-2.59540-08					
1R.225	-0.3550572	-6.68040-08					
1R.230	-0.3560119	-9.31720-08					
1R.235	-0.3570676	-1.22900-07					
1R.240	-0.3580329	-1.23510-07					
1R.245	-0.3587845	-1.18140-07					
1R.250	-0.3591445	-9.45870-08					
1R.255	-0.3592660	-5.99120-08					
1R.260	-0.3592517	-2.57310-08					
1R.265	-0.3592932	1.34210-08					
1R.270	-0.3594564	5.06770-08					
1R.275	-0.3601272	7.44490-08					
1R.280	-0.3600970	8.50790-08					
1R.285	-0.3619861	9.27990-08					
1R.290	-0.3629627	8.15930-08					
1R.295	-0.3637360	8.10310-08					

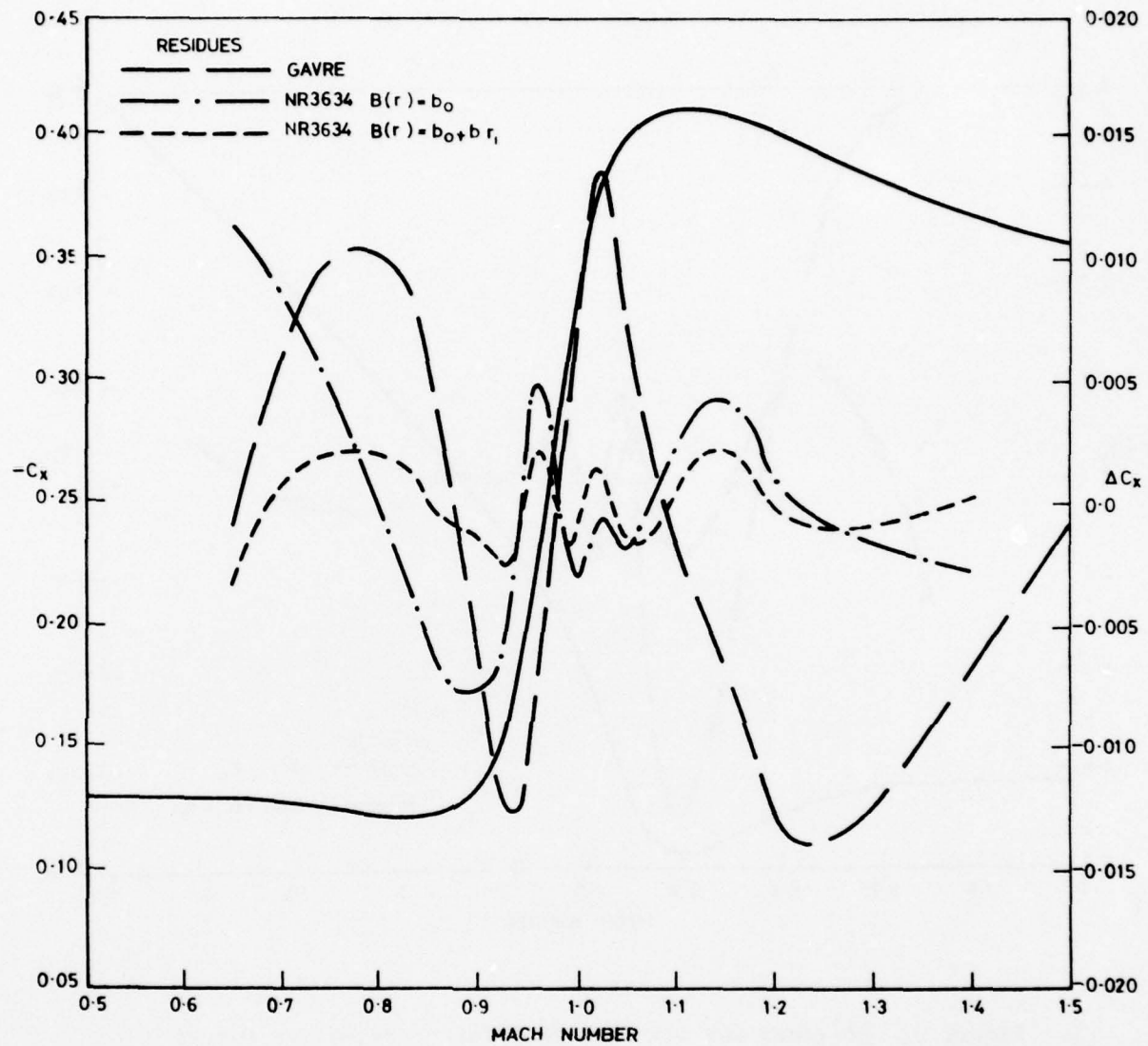


Figure 1. Residues for fitted axial force curves

Figure 2

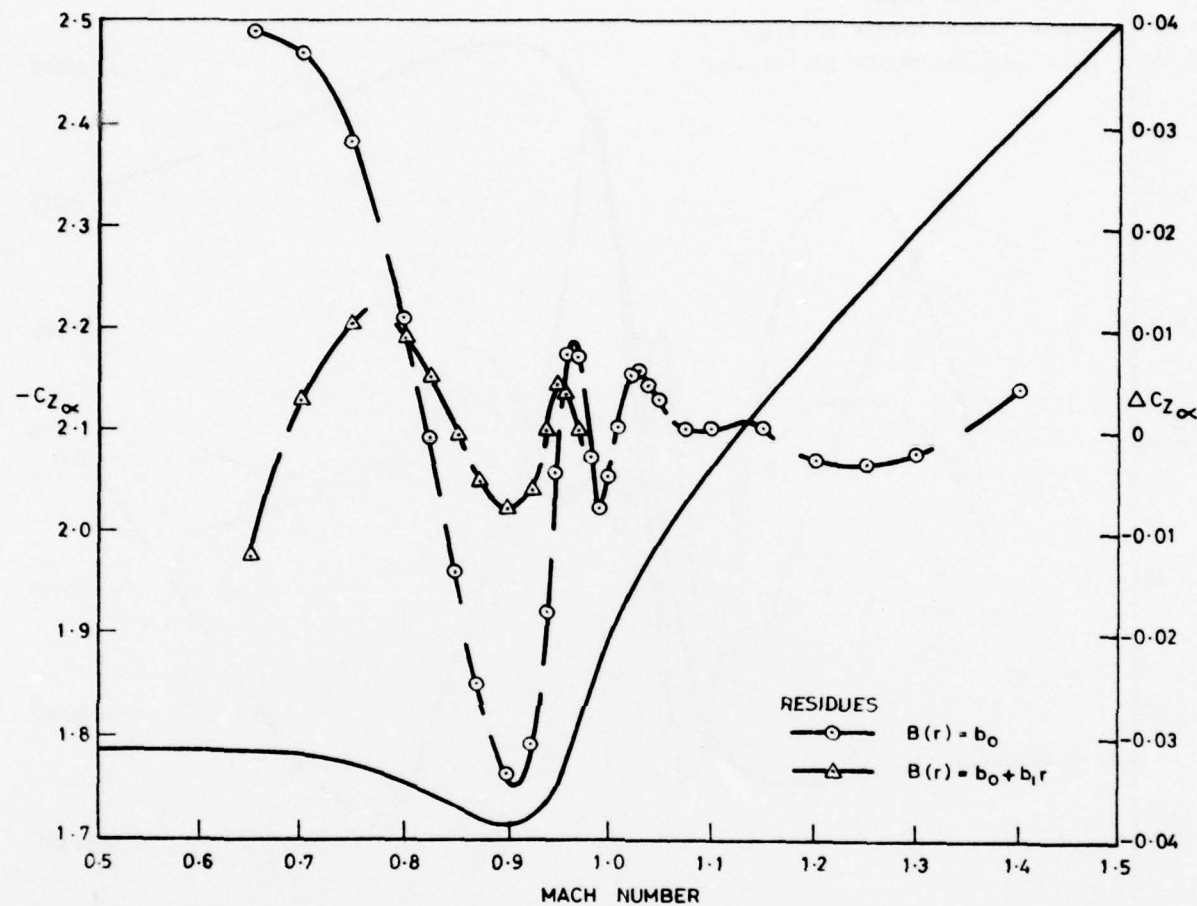


Figure 2. Residues for fitted normal force derivative curves

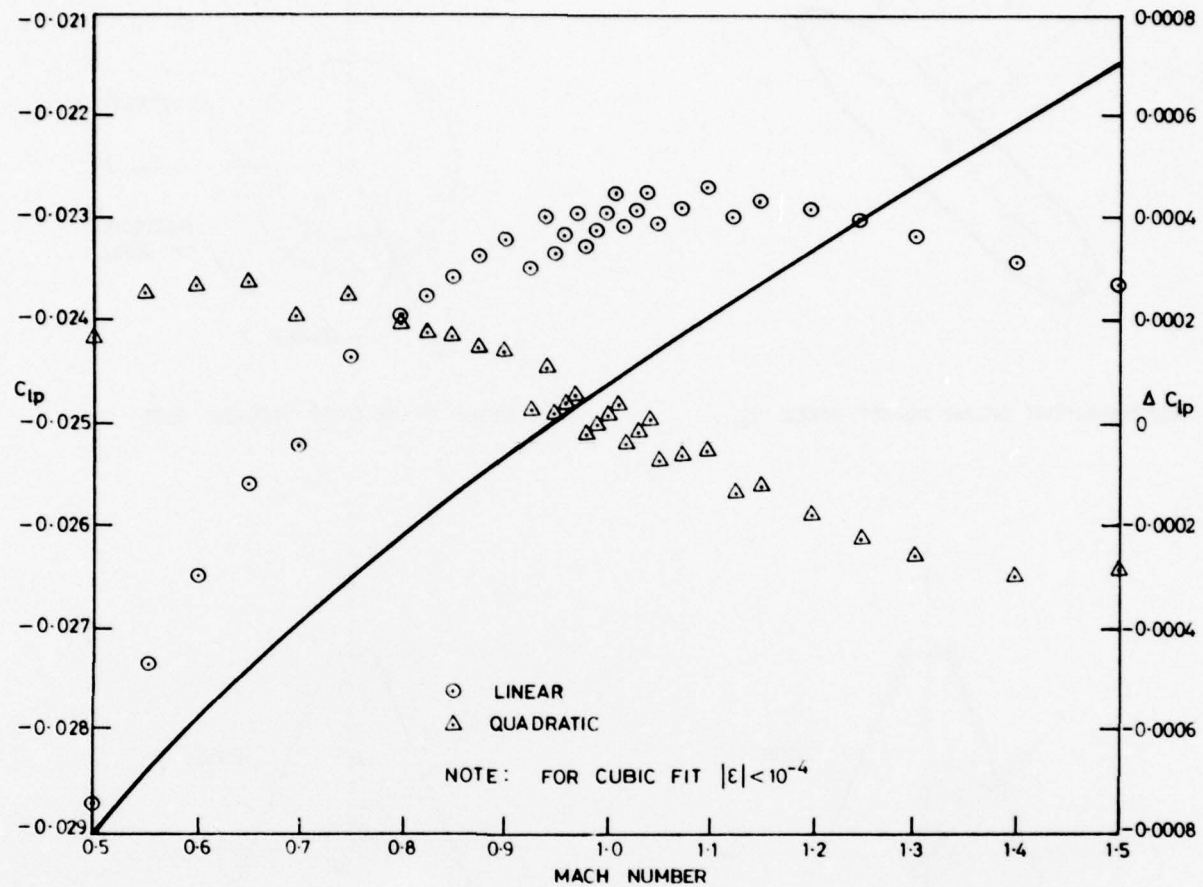
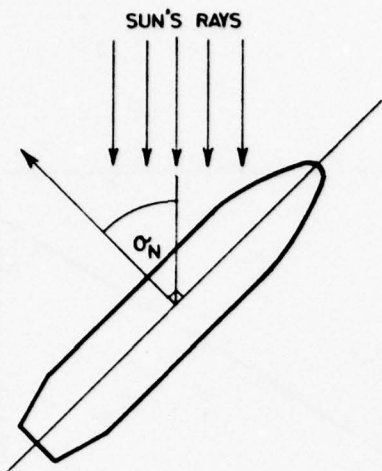
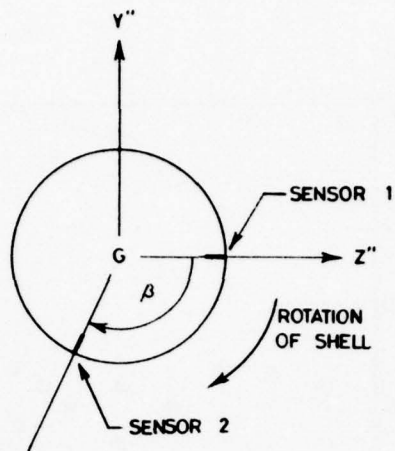
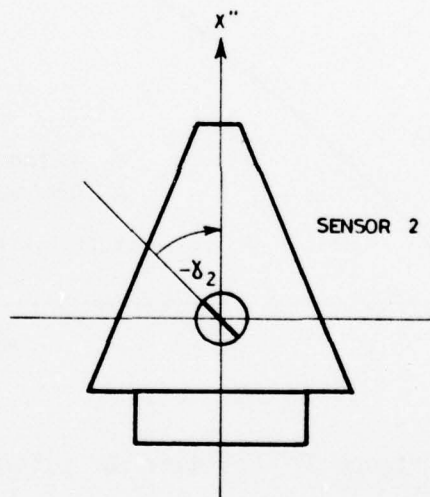
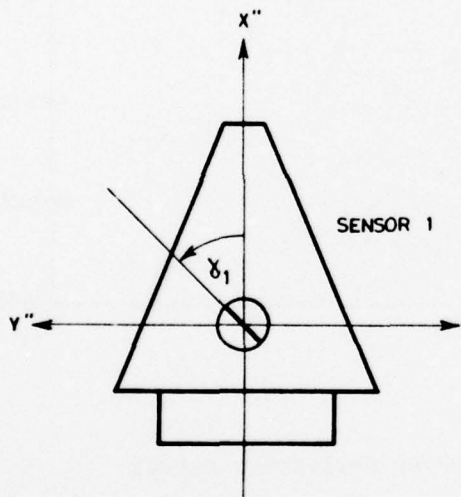


Figure 3. Residues for fitted roll damping derivative curves

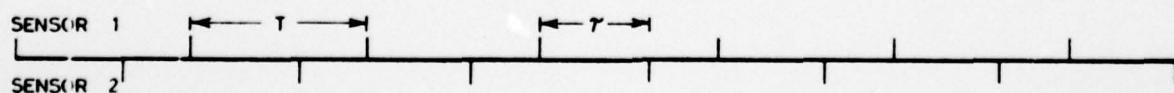
Figure 4

(a) COMPLEMENTARY SOLAR ASPECT ANGLE  $\alpha'_N$ 

(b) ANGLE OF ROTATION BETWEEN SLITS



(c) ORIENTATION OF SLITS RELATIVE TO THE LONGITUDINAL AXIS OF THE SHELL



(d) PULSE TRAIN FROM YAWSONDE

Figure 4. Schematic representation of a yawsonde

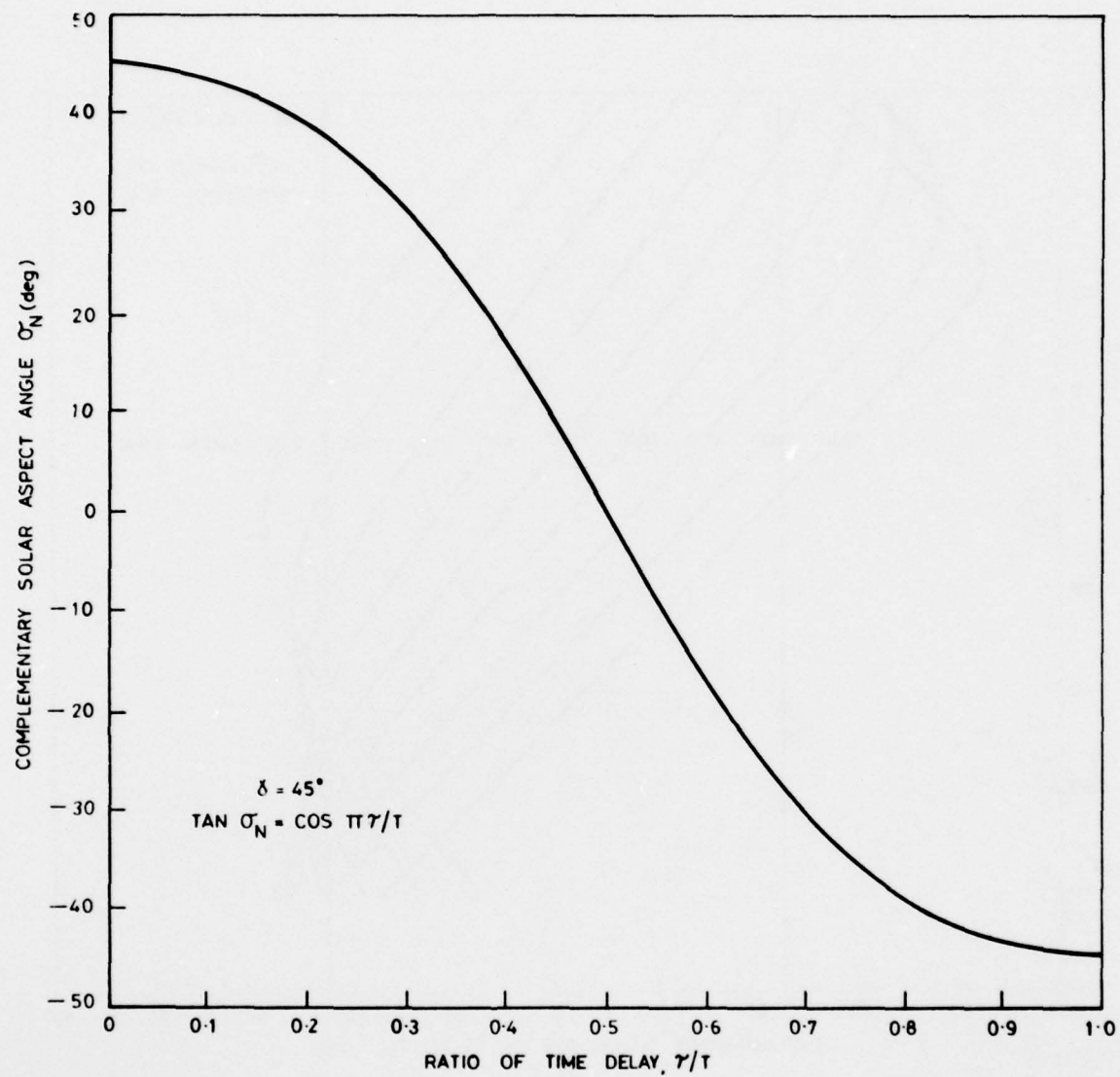
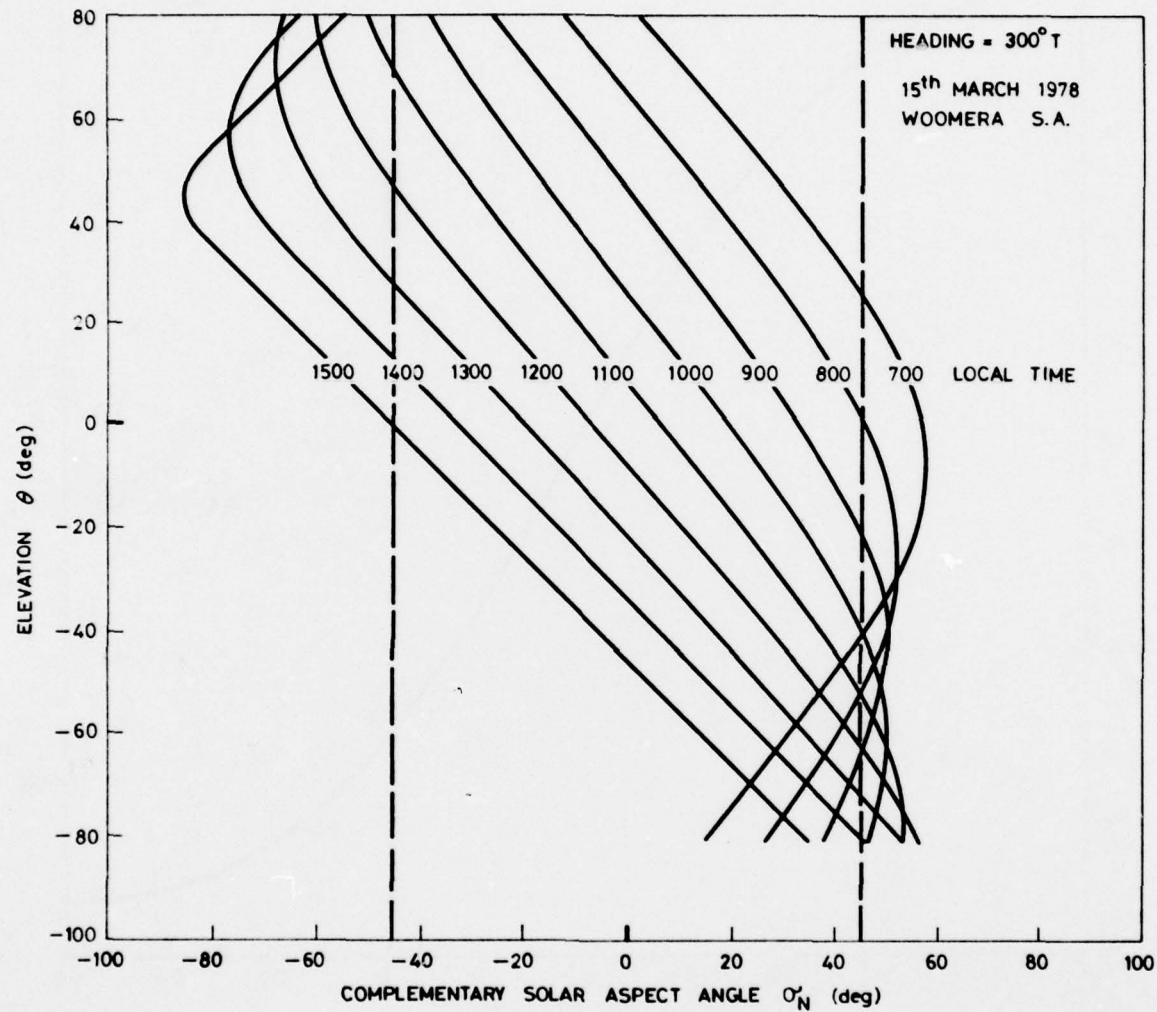


Figure 5. Typical yawsonde calibration curve

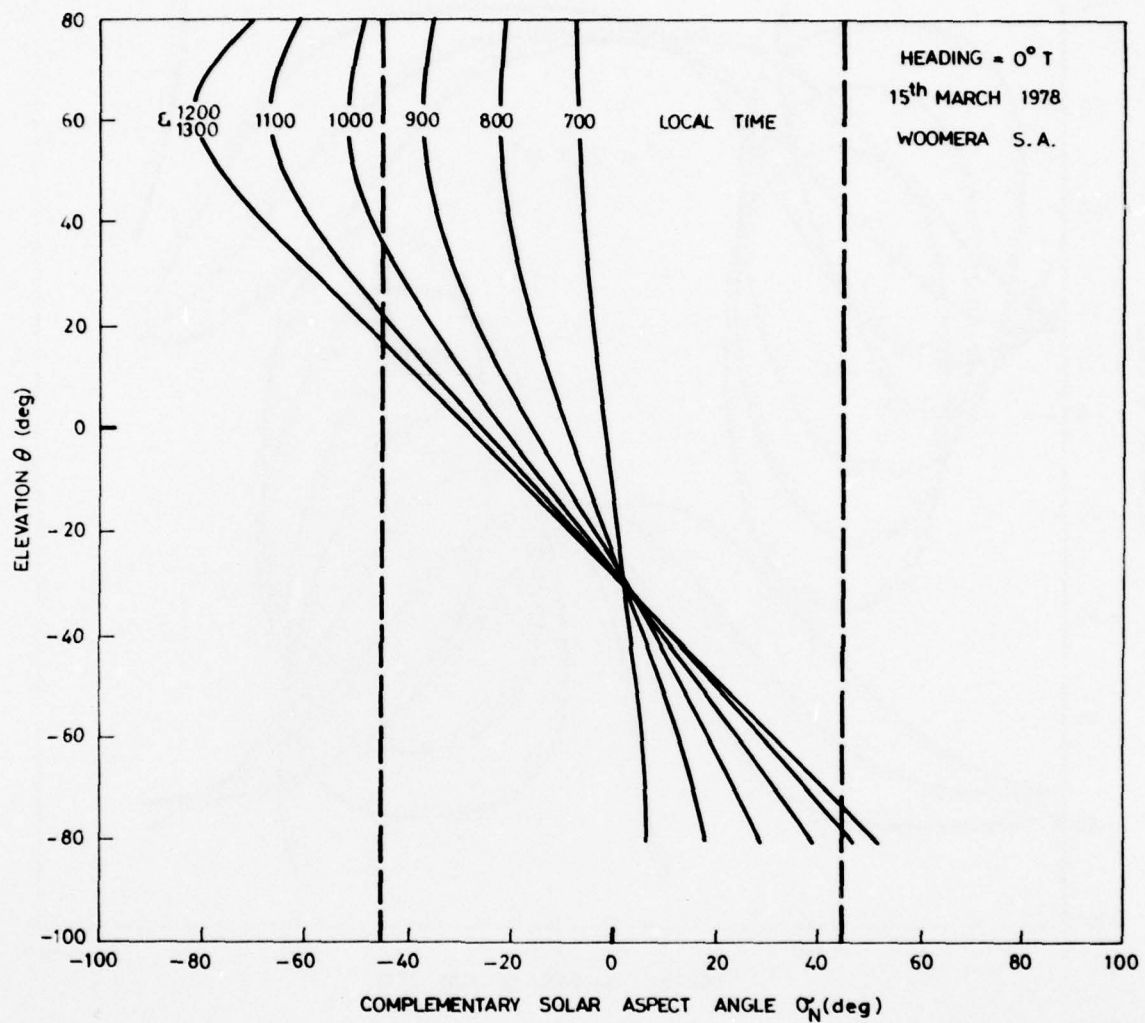
WSRL-0039-TR

Figure 6(a)



(a) heading 300 degrees T

Figure 6. Variation of complementary solar aspect angle with shell elevation



(b) heading due north

Figure 6. Variation of complementary solar aspect angle with shell elevation

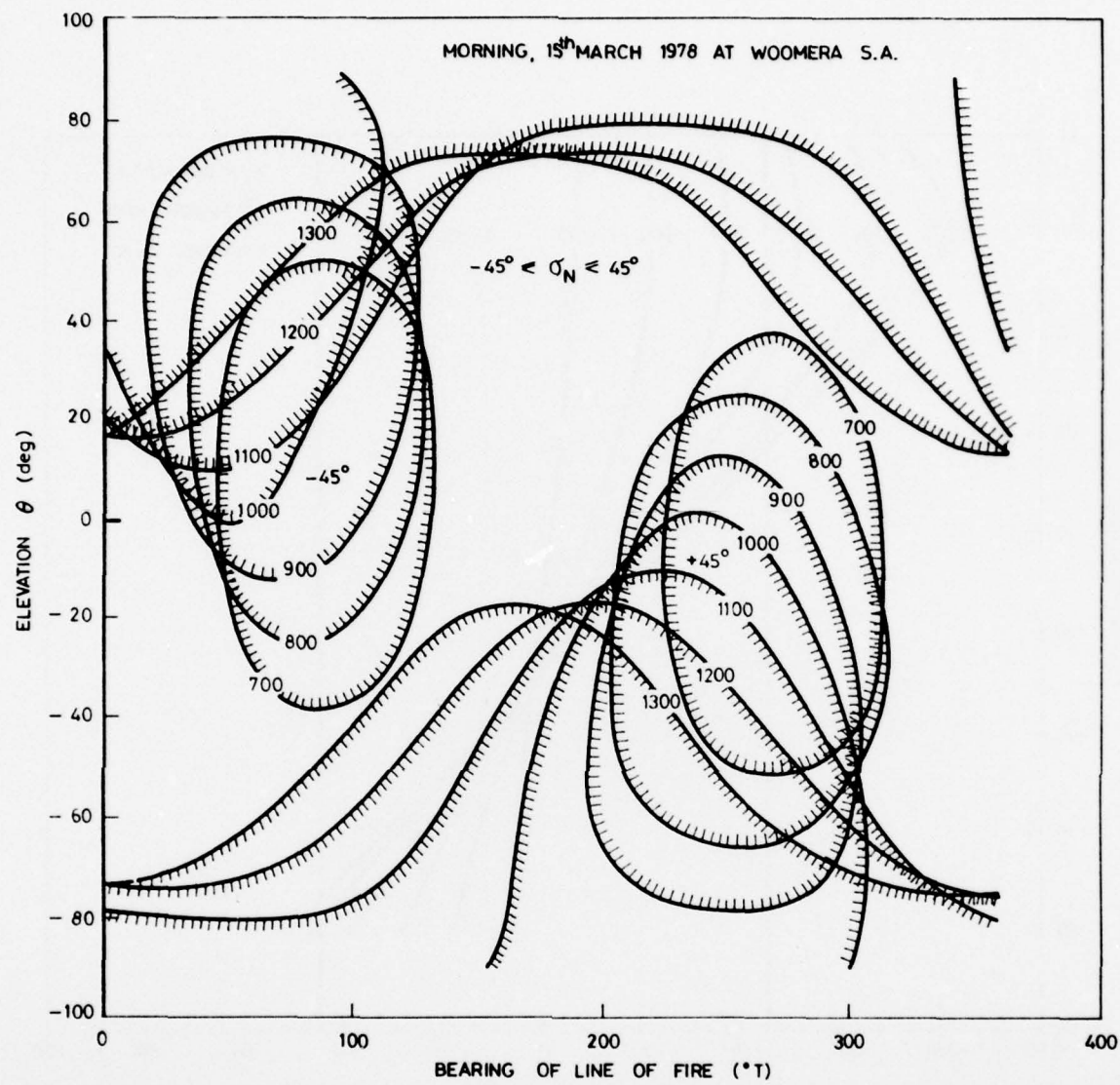
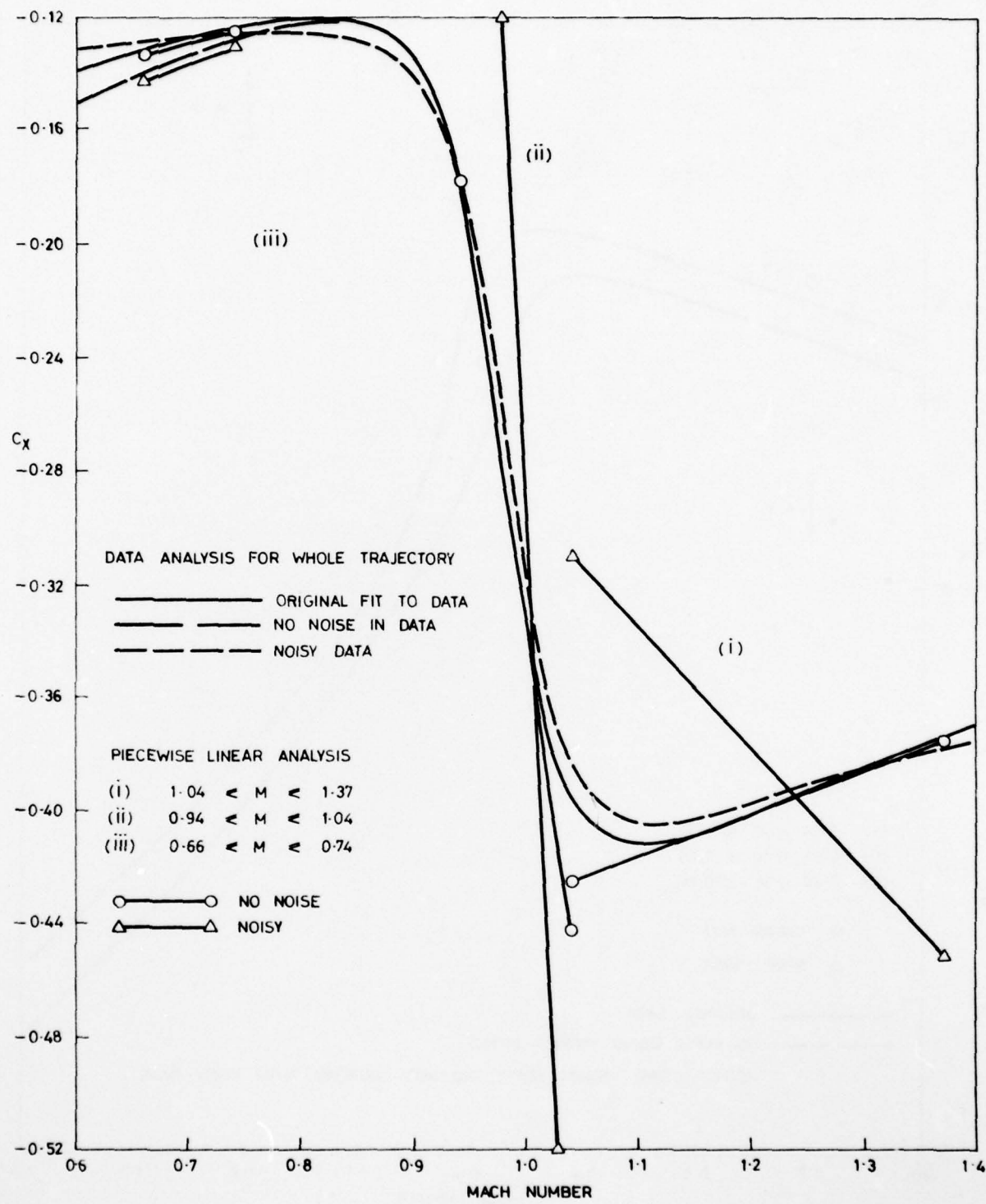
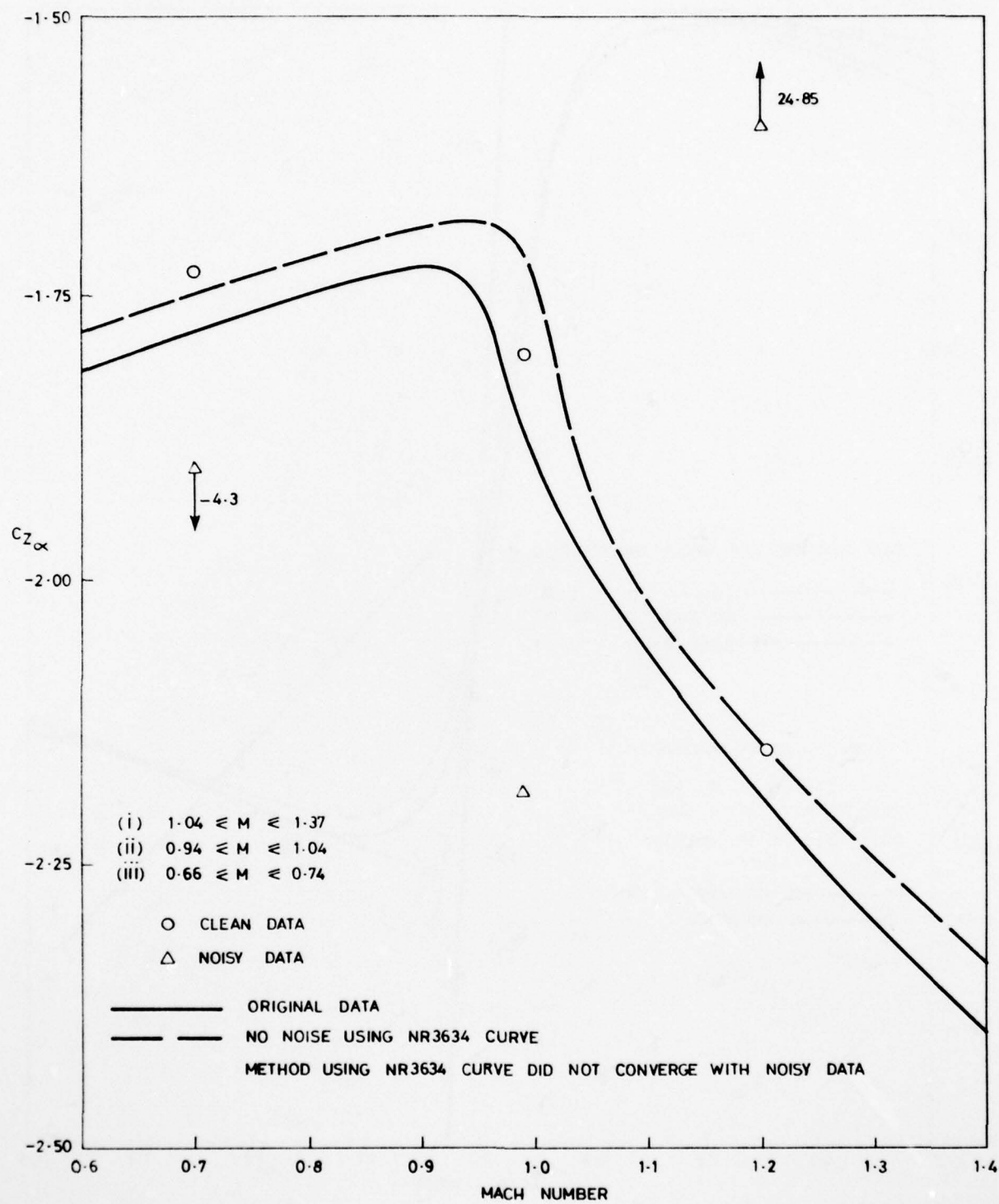


Figure 7. Conditions for detecting the sun



(a) axial force

Figure 8. Comparison of methods for estimating aerodynamic force coefficients



(b) normal force derivative

Figure 8. Comparison of methods for estimating aerodynamic force coefficients

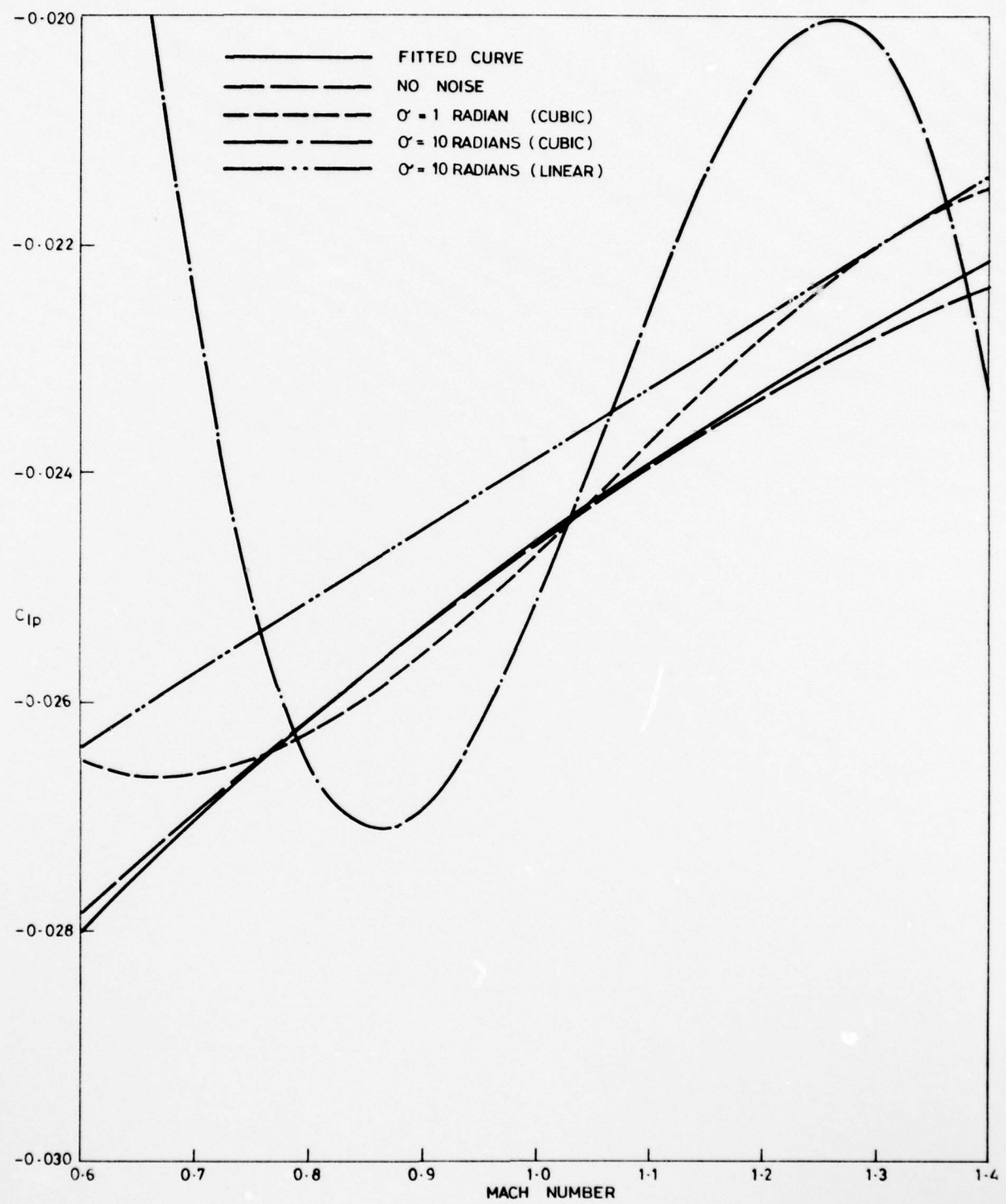


Figure 9. Effects of noise on estimation of roll damping moments

## DISTRIBUTION

EXTERNAL	COPY NO.
In United Kingdom	
Defence Scientific and Technical Representative, London	1
Royal Aircraft Establishment	
Aero Department	2
Library	3
R.A.R.D.E.	
Mr F.J. Tanner	4 - 5
Library	6
TTCP, UK National Leader Panel W-2	7 - 10
In United States of America	
Counsellor, Defence Science, Washington	11
Defence Research and Development Attaché, Washington	12
Air Force Armament Testing Laboratory	13
Ballistics Research Laboratories	
(Attention: W.H. Mermagen)	14 - 15
Edgewood Arsenal	16
Naval Surface Weapons Center	
Dahlgren	17
White Oak	18
Naval Weapons Center	19
Picatinny Arsenal	20
Redstone Arsenal	21
US National Leader Panel W-2, TTCP	22 - 25
Sandia Corporation, Library	26
In Canada	
Defence Research Establishment, Valcartier	27
N.A.E., Ottawa	28
Canadian National Leader Panel W-2, TTCP	29 - 32
In Australia	
Chief Defence Scientist	33
Deputy Chief Defence Scientist	34
Superintendent, Science and Technology Programmes	35
Army Scientific Adviser	36
Navy Scientific Adviser	37
Air Force Scientific Adviser	38
Central Studies Establishment	39
Director, Joint Intelligence Organisation (DDSTI)	40

AD-A074 420

WEAPONS SYSTEMS RESEARCH LAB ADELAIDE (AUSTRALIA)  
THE ANALYSIS OF TRAJECTORY AND SOLAR ASPECT ANGLE RECORDS OF SH--ETC(U)

F/G 19/4

SEP 78 R L POPE

UNCLASSIFIED

WSRL-0039-TR

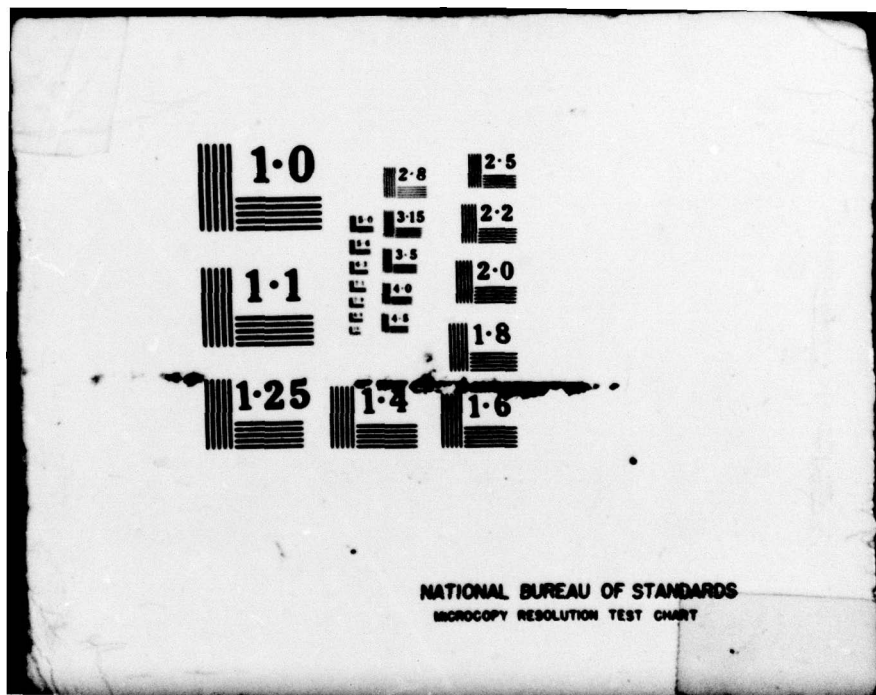
NL

2 OF 2  
AD-  
A074420



END  
DATE  
FILMED

11-79  
DOC



NATIONAL BUREAU OF STANDARDS  
MICROCOPY RESOLUTION TEST CHART

## Copy No.

<b>Aeronautical Research Laboratories</b>	
Chief Superintendent	41
Superintendent, Aerodynamics Division	42
D.A. Secomb, for data exchange agreement	43
<b>Defence Information Services Branch for:</b>	
United Kingdom, Ministry of Defence, Defence Research Information Centre (DRIC)	44
United States, Department of Defense, Defense Documentation Center	45 - 56
Canada, Department of National Defence, Defence Science Information Service	57
New Zealand, Department of Defence	58
Australian National Library	59
Defence Information Services Branch (for microfilming)	60
Defence Library, Campbell Park	61
Library, Aeronautical Research Laboratories	62
Library, Materials Research Laboratories	63
<b>WITHIN DRCS</b>	
Chief Superintendent, Weapons Systems Research Laboratory	64
Superintendent, Aeroballistics Division	65
Head, Ballistics Composite	66
Principal Officer, Dynamics Group	67
Principal Officer, Aerodynamic Research Group	68
Principal Officer, Ballistic Studies Group	69
Principal Officer, Field Experiments Group	70
Principal Officer, Flight Research Group	71
Author	72
DRCS Library	73 - 74
AD Library	75 - 80
Spares	81 - 87